Photon Counting CT: Technology and Clinical Applications

Marc Kachelrieß

German Cancer Research Center (DKFZ)

Heidelberg, Germany

www.dkfz.de/ct

Canon Aquilion ONE Vision

GE Revolution CT

Philips IQon Spectral CT

Siemens Somatom Force

Diagnostic CT

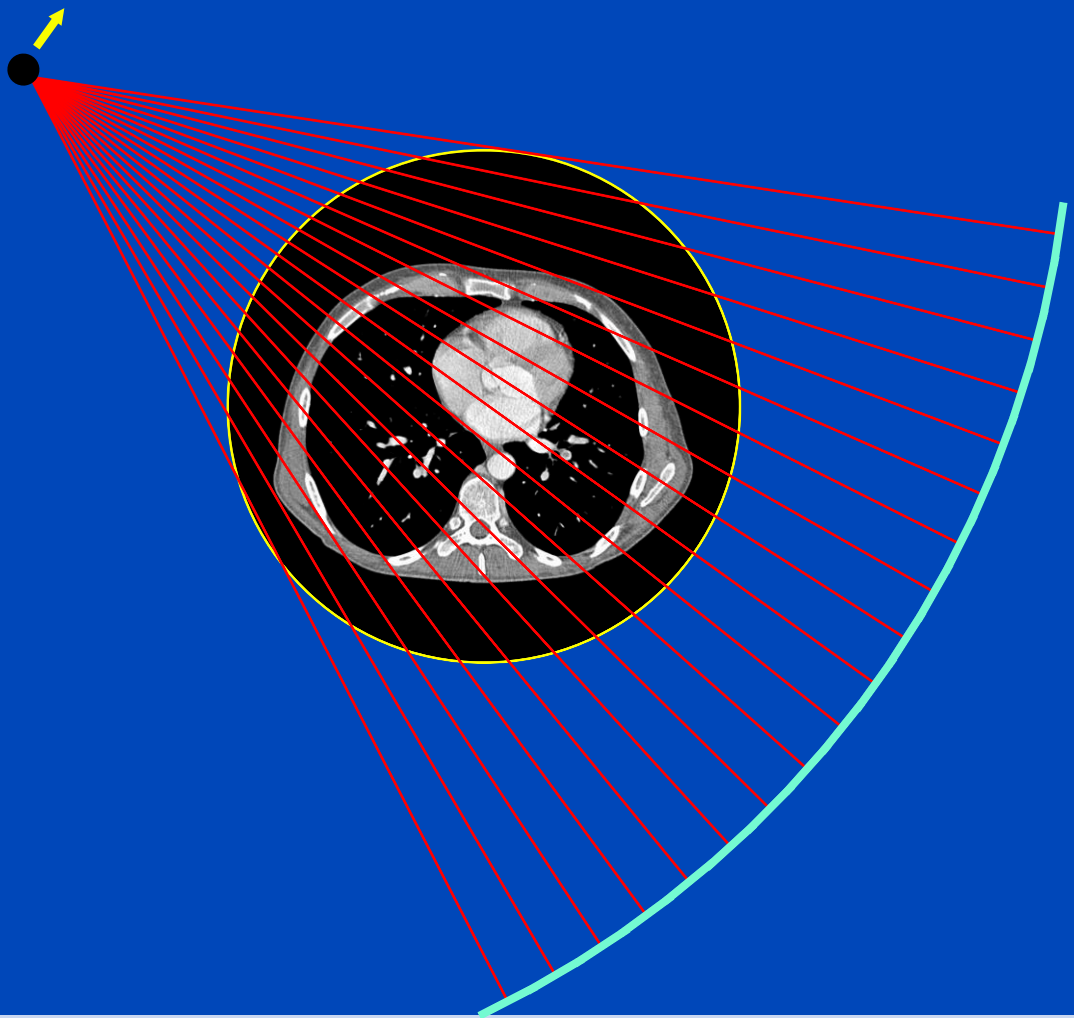

dkfz.

What does CT Measure?

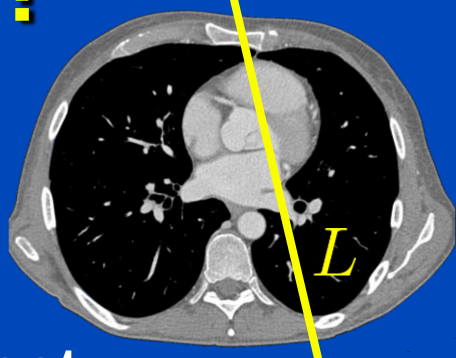

- X-rays are generated in an x-ray tube.
- The polychromatic radiation is attenuated in the patient. X-ray photon attenuation is dominated by the photo and the Compton effect.
- Detectors measure the x-ray intensity after the rays have passed through the patient along several lines *L*.
- The log intensity is the so-called x-ray transform:

$$q(L) = -\ln \frac{I(L)}{I_0} = -\ln \int dE\, w(E) e^{-\int dL \mu(\boldsymbol{r}, E)}$$

- Often, the follwing monochromatic approximation is used:

$$q(L) \approx p(L) = \int dL \mu(\boldsymbol{r}, E_{\text{eff}})$$

What is Displayed?

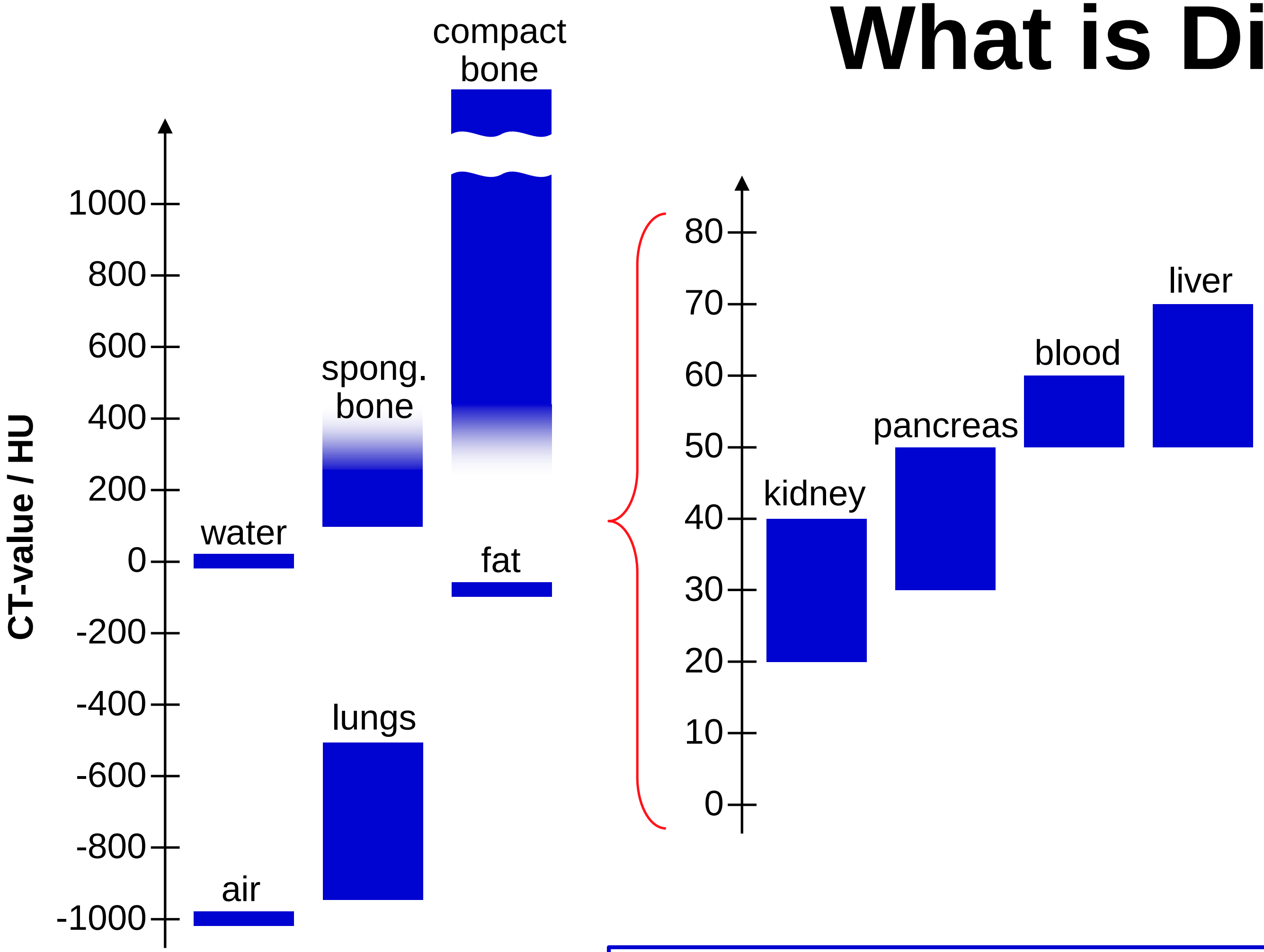

$$CT(\boldsymbol{r}) = \frac{\mu(\boldsymbol{r}) - \mu_{\text{Water}}}{\mu_{\text{Water}}} \cdot 1000 \text{ HU}$$

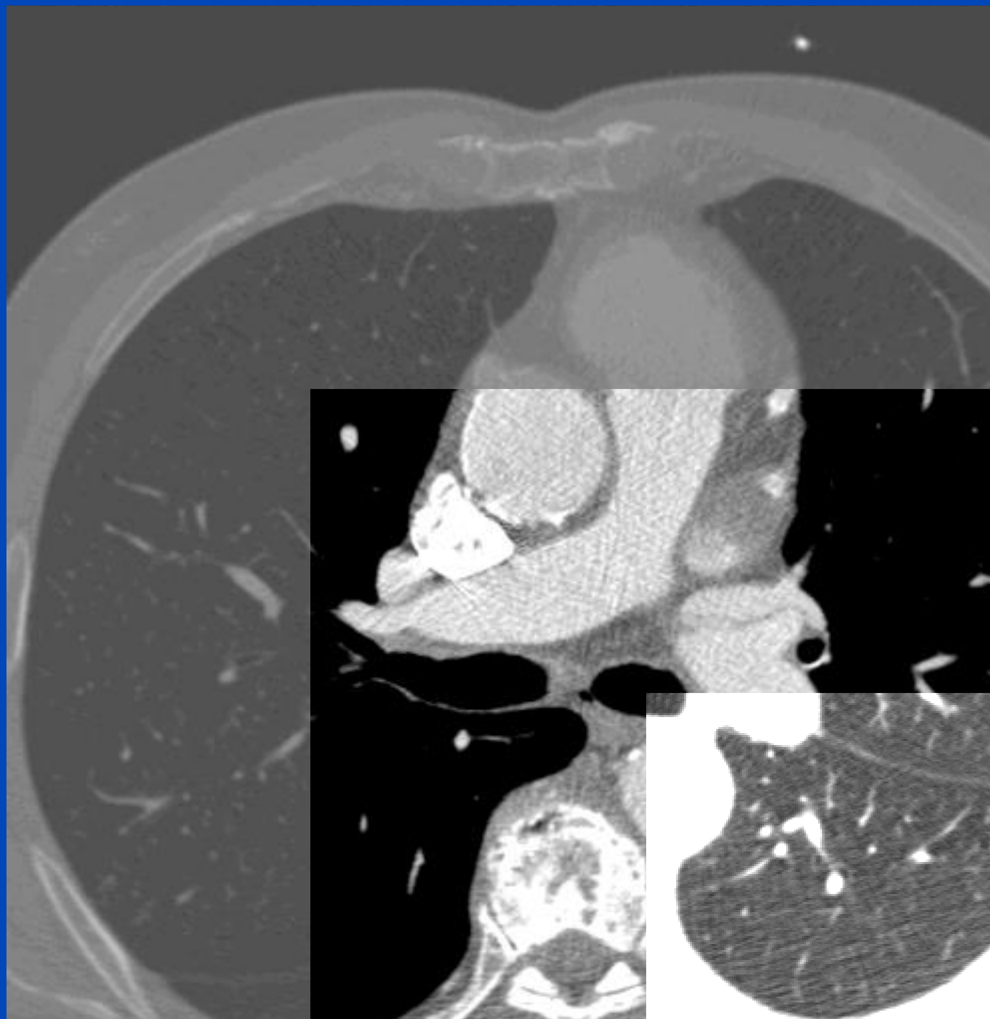

C = 0 HU, *W* = 5000 HU   *C* = 0 HU, *W* = 1000 HU   *C* = -750 HU, *W* = 1000 HU

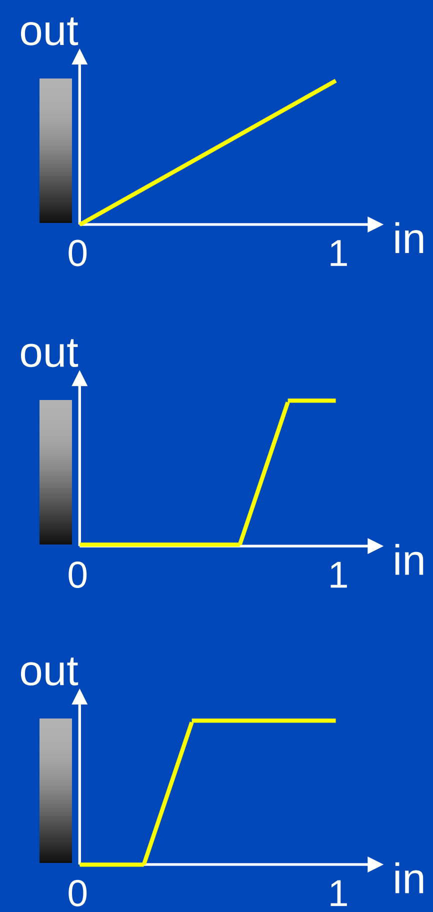

$$\mu(\boldsymbol{r}, E) = f_1(\boldsymbol{r})\psi_1(E) + f_2(\boldsymbol{r})\psi_2(E)$$

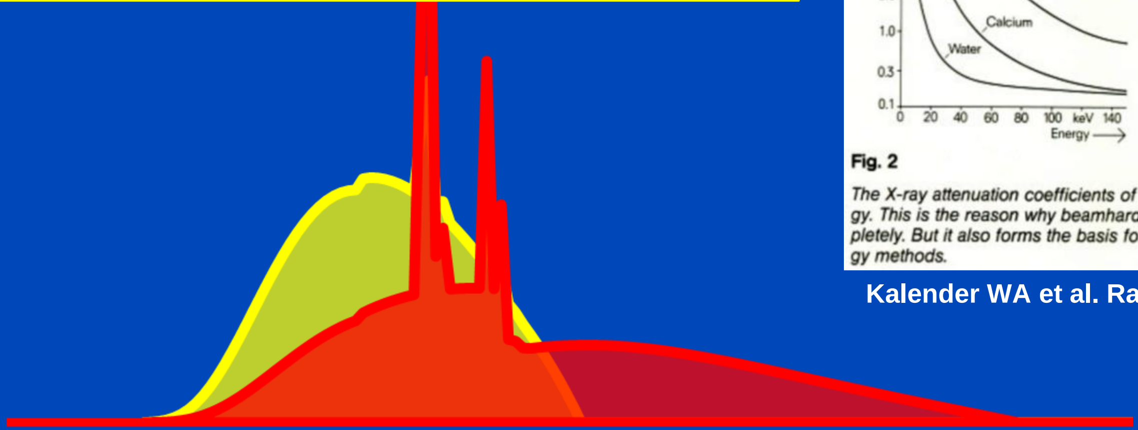

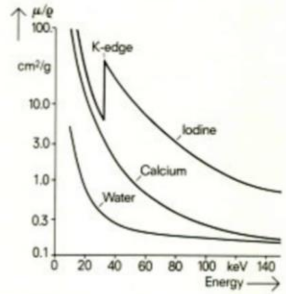

Energy keV	Linear attenuation coefficient cm⁻¹		
	Water	Calcium	Iodine
30	0.371	3.971	8.45
40	0.267	1.804	22.10
60	0.205	0.651	7.55
80	0.183	0.361	3.49
100	0.171	0.254	1.94

Energy Dependence
of the Photon Mass Attenuation Coefficient

Fig. 2

The X-ray attenuation coefficients of different materials vary widely with energy. This is the reason why beamhardening effects cannot be controlled completely. But it also forms the basis for material-selective imaging by dual energy methods.

Kalender WA et al. Radiology 164:419-423, 1987

80 kV

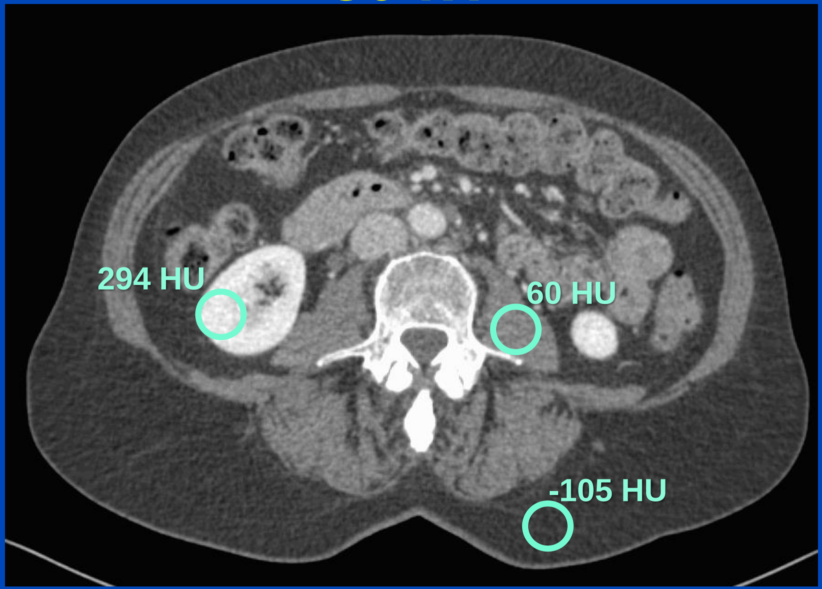

140 kV Sn

***C* = 50 HU, *W* = 600 HU**

1980ies: The First Clinical DECT Product Implementation


Standard CT image

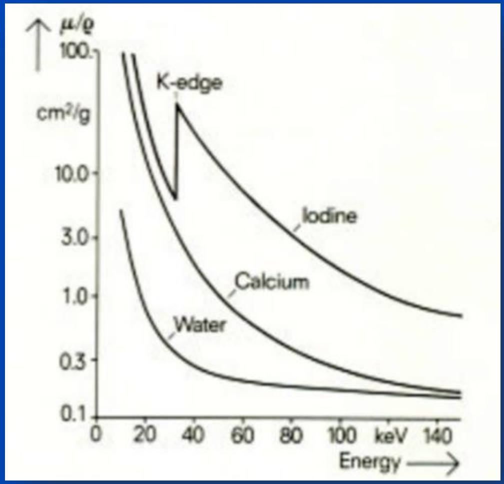

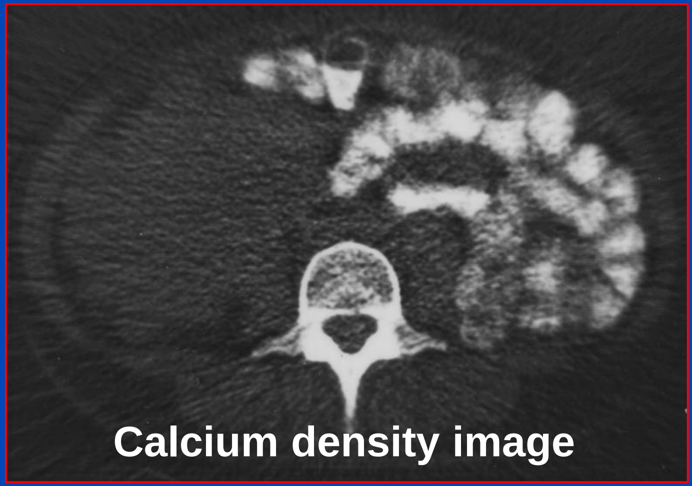
Calcium density image

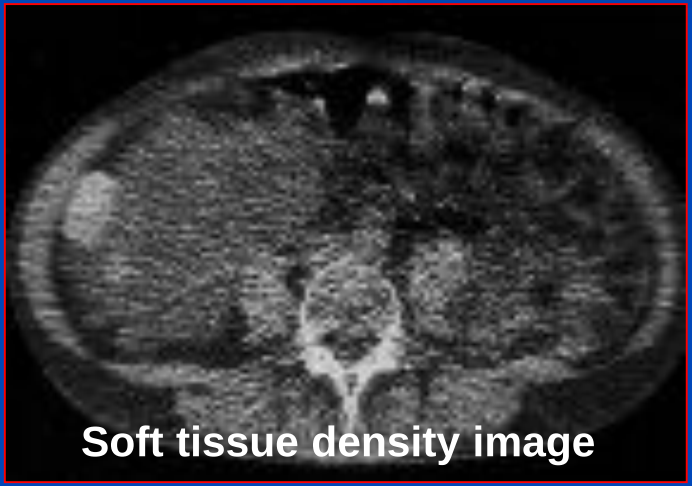
Soft tissue density image

Kalender et al. Radiology 164:419-423, 1987

Dual-Source-CT (since 2005)

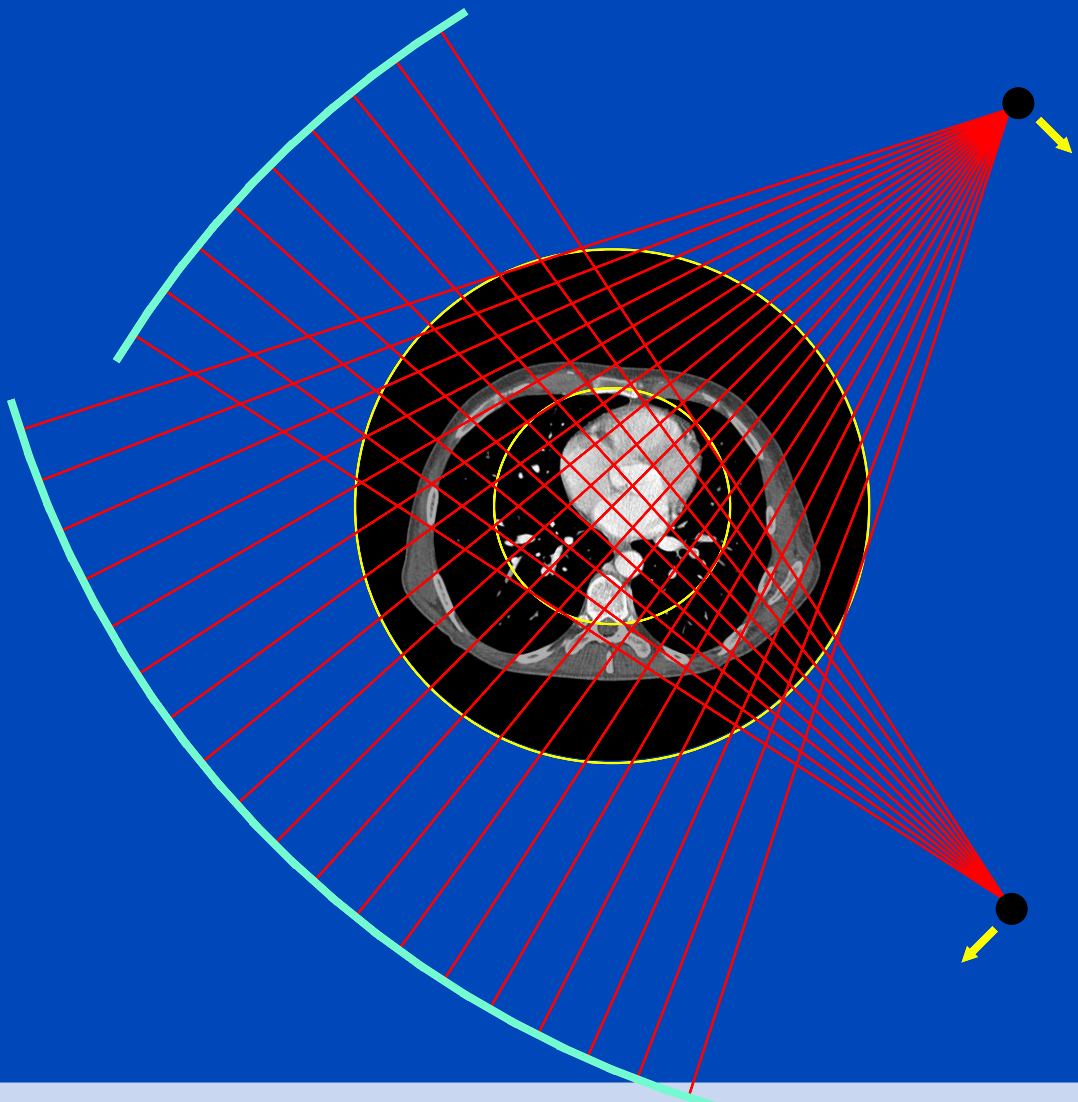

Siemens SOMATOM Force
3rd generation
dual source cone-beam spiral CT

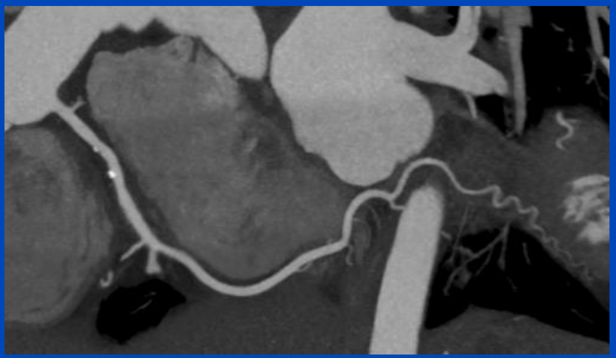

Turbo Flash, 70 kV, 0.55 mSv
63 ms temporal resolution
143 ms scan time


SIEMENS
300.0
-2000.0
SOMATOM Force

dkfz.

Examples

(Slide Courtesy of Siemens Healthcare)

DE bone removal

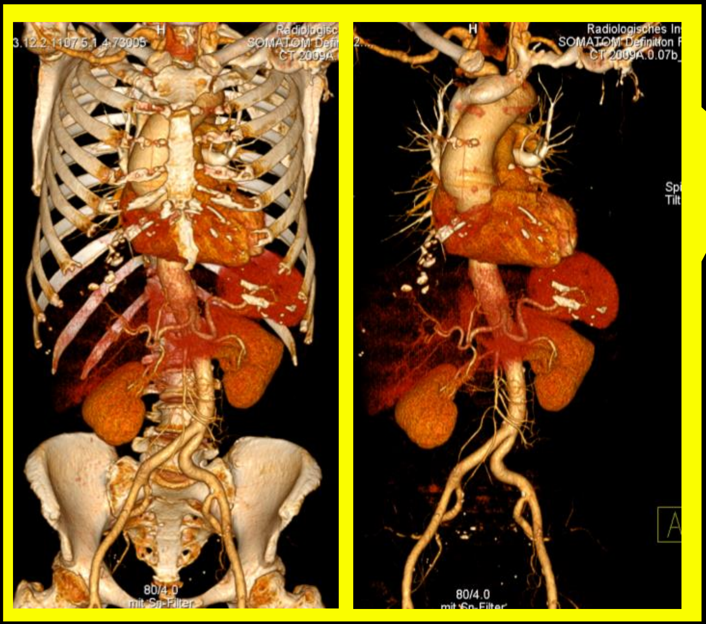

Single DECT scan

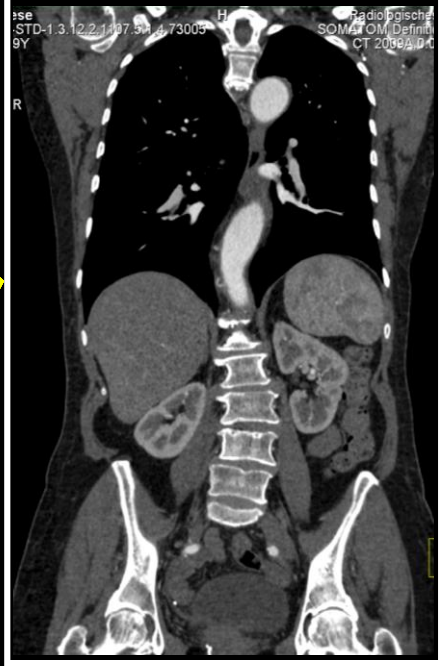

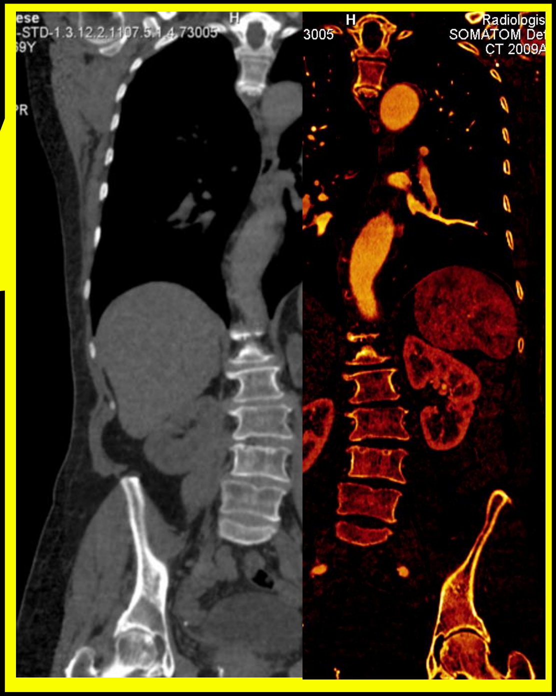

Virtual non-contrast and iodine image

Dual Energy whole body CTA: 100/140 Sn kV @ 0.6 mm

Courtesy of Friedrich-Alexander University Erlangen-Nürnberg

DECT Today: Widely Available via DSCT

(Slide Courtesy of Siemens Healthcare)

- **“Spectroscopy“: more specific tissue characterization**
  → Detection and visualization of calcium, iron, uric acid, …..

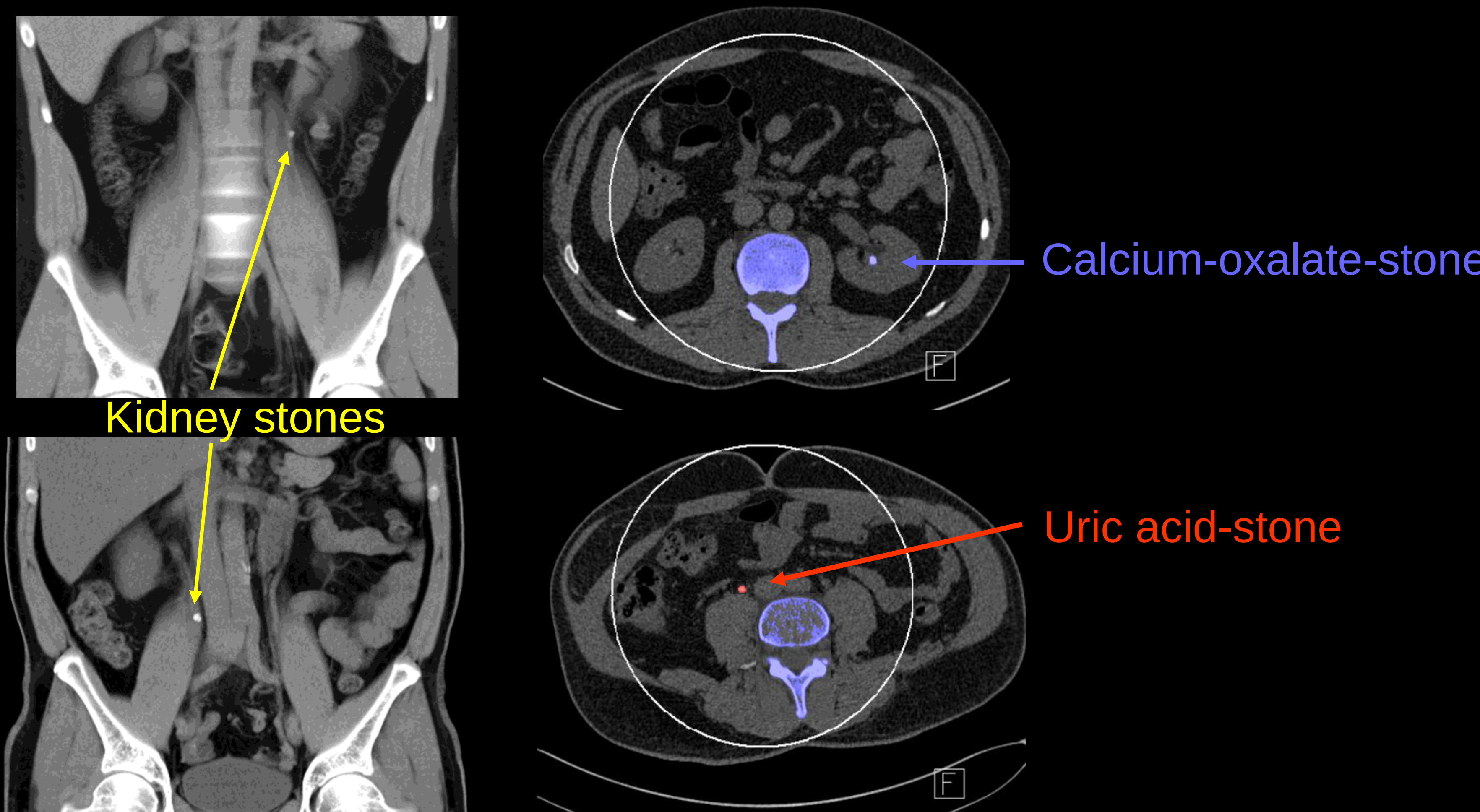

Courtesy of Klinikum Großhadern, LMU München

DECT Today: Widely Available via DSCT

(Slide Courtesy of Siemens Healthcare)

- **“Spectroscopy“: more specific tissue characterization**
  → Detection and visualization of calcium, iron, uric acid, …..

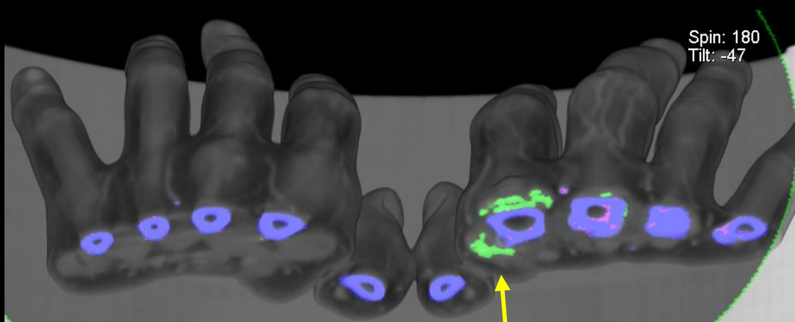

Uric acid-crystals

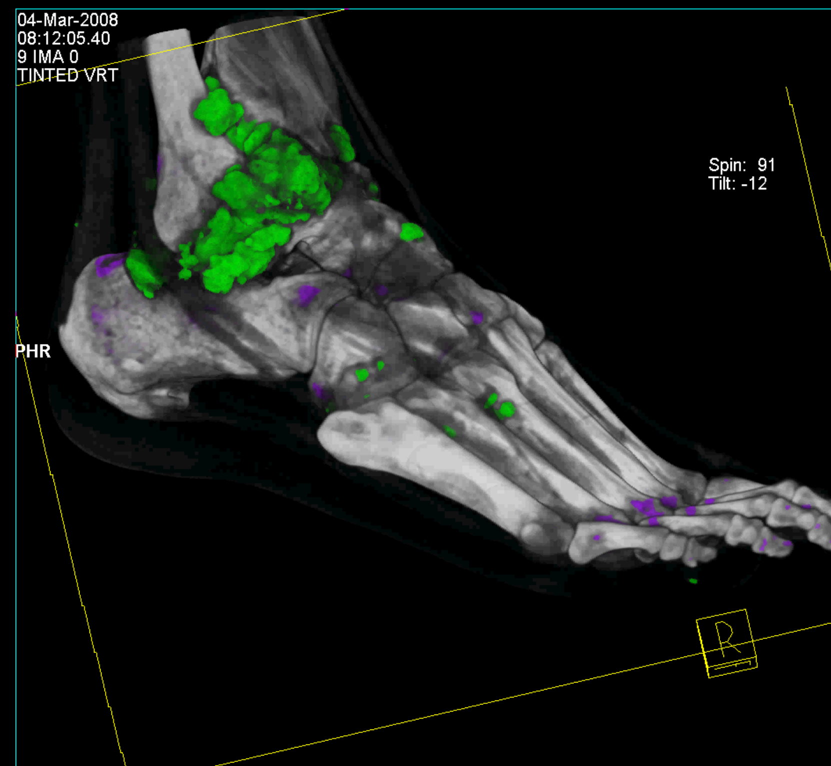

Courtesy of Klinikum Großhadern, LMU München, and CIC, Mayo Clinic Rochester, MN, USA

DECT Today: Widely Available via DSCT

(Slide Courtesy of Siemens Healthcare)

- **New approach: Detection, visualization and quantification of iodine**
  → Fully-automated bone removal in CT angiographic studies
  → Significant improvement of clinical workflow

Dual energy CT plaque-removal

Digital subtraction angiography

Courtesy of University Hospital Krakau, Polen and PUMC, Beijing, China

DECT Today: Widely Available via DSCT

(Slide Courtesy of Siemens Healthcare)

- **New approach: Detection, visualization and quantification of iodine**
  → Characterization of perfusion defects in the myocardium
  → Hemodynamic relevance of coronary artery stenosis:
  Coronary CTA = morphology, local blood volume = function

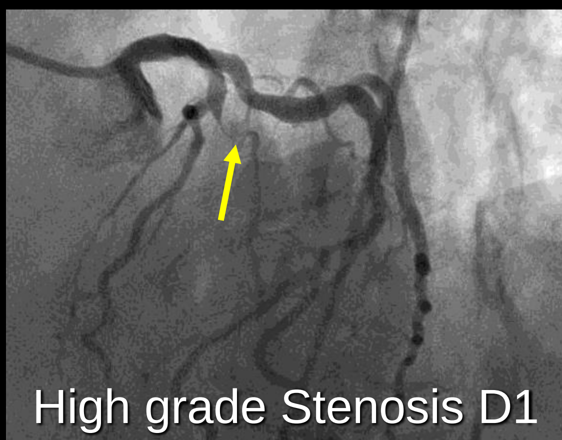

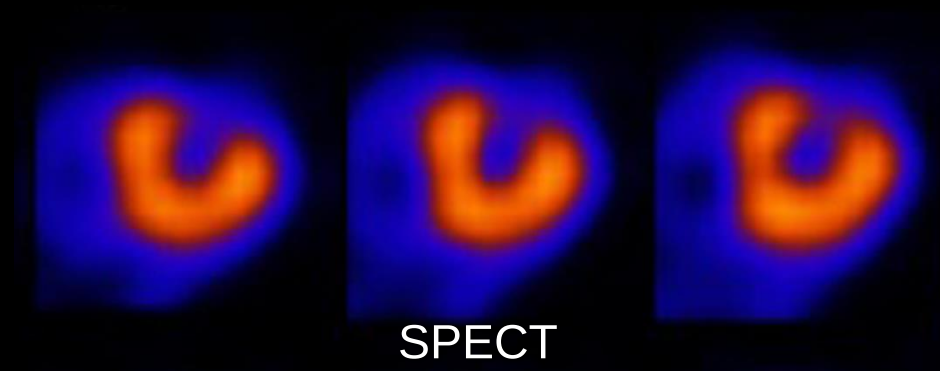

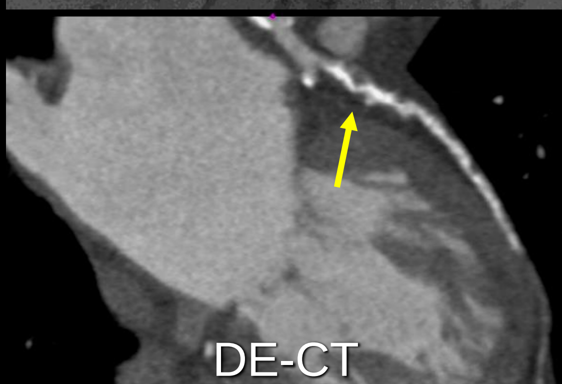

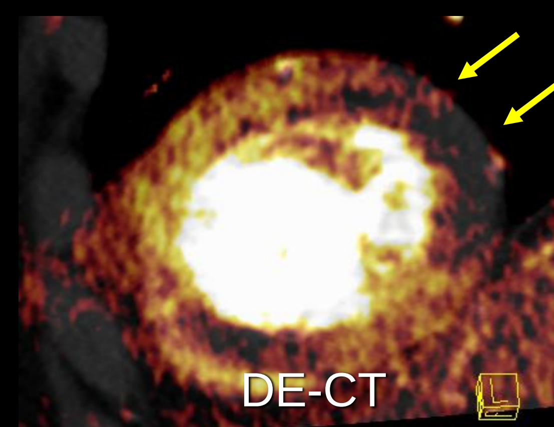

Courtesy of MUSC, Charleston, USA

Monoenergetic Imaging
(mono+ = noise reduction with frequency split)

Courtesy of Prof. Michael Lell, Friedrich-Alexander University Erlangen-Nürnberg

DECT
and Pseudo Monochromatic Imaging

Pseudo monochromatic imaging is a linear combination of DECT f_L and f_H: $$f_\alpha = (1-\alpha)\, f_\mathrm{L} + \alpha\, f_\mathrm{H}$$

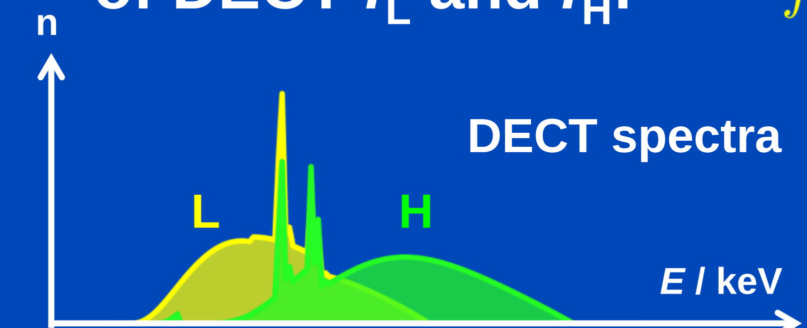

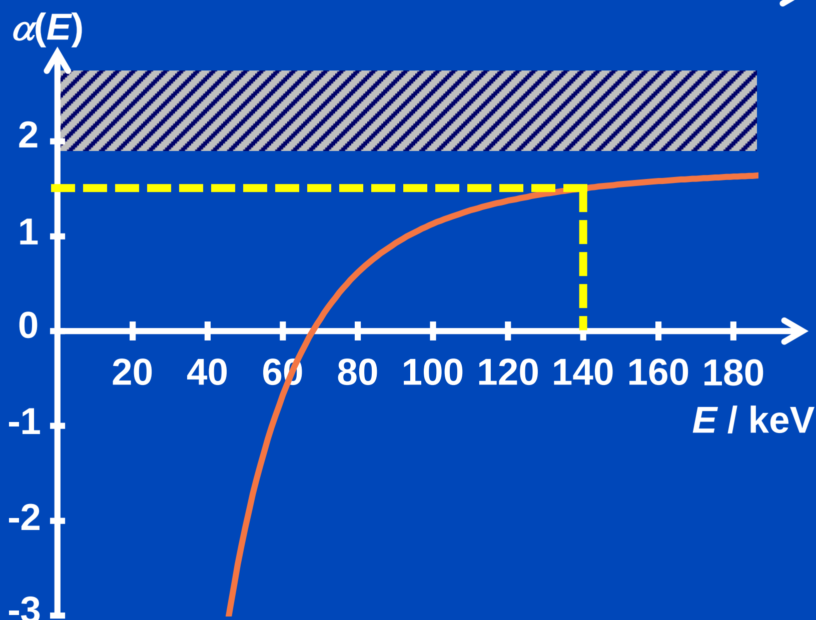

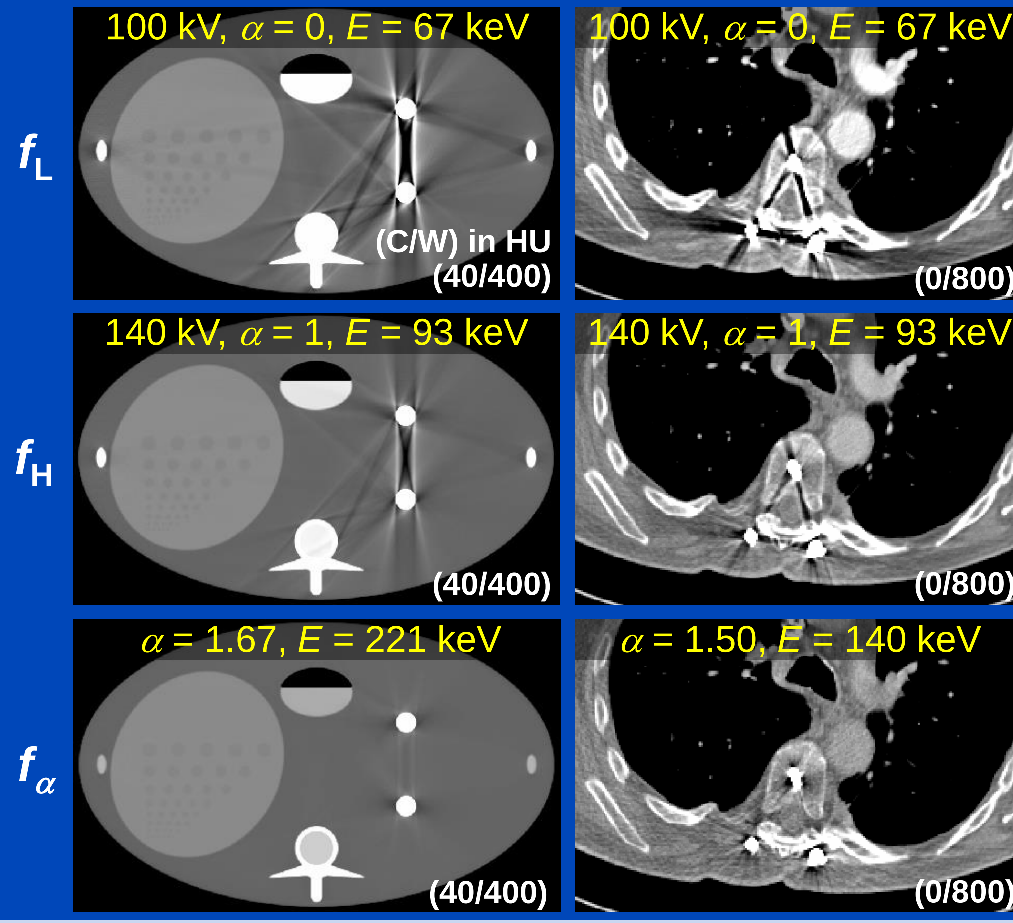

Kuchenbecker, Faby, Sawall, Lell, Kachelrieß. Dual energy CT: How well can pseudo-monochromatic imaging reduce metal artifacts? Med. Phys. 42(2), 2015

Dual Energy Metal Artifact Reduction
(linear combination plus noise reduction with mono+)

50 keV **80 keV** **160 keV**

Courtesy of Prof. Michael Lell, Friedrich-Alexander University Erlangen-Nürnberg


Gout

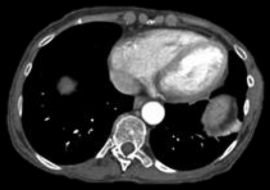
Optimum Contrast

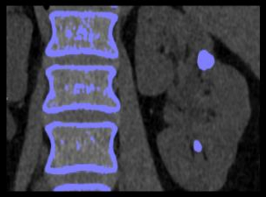
Calculi Characterization

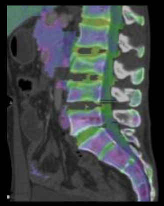
Bone Marrow

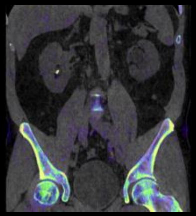
Rho/Z


Monoenergetic

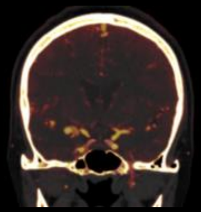
Brain Hemorrhage


Musculoskeletal*


Xenon*

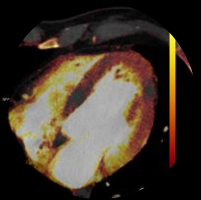
Heart PBV


Direct Angio

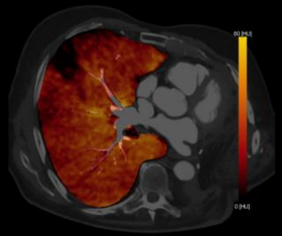
Lung Analysis


Monoenergetic Plus

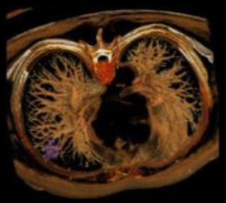
Lung Nodules*

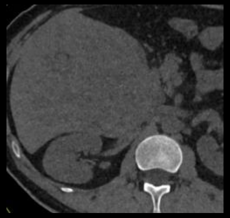
Virtual Unenhanced

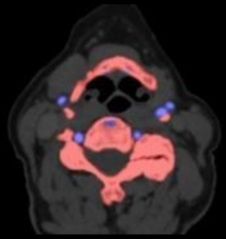
Hardplaque Display

Syngo.CT DECT application examples. Virtual unenhanced contains liver VNC, lung analysis contains lung PBV.
Courtesy of Siemens Healthineers, Forchheim, Germany

DECT Technology

- In the clinic:
  - Multiple scans at different spectra — mid-range
  - Dual source CT (DSCT), generations 2, and 3 — high-end
  - Fast tube voltage switching — high-end
  - Dual layer sandwich detectors — high-end
  - Split filter — mid-range
- First prototypes:
  - Photon counting detectors (two or more energy bins) — high-end?

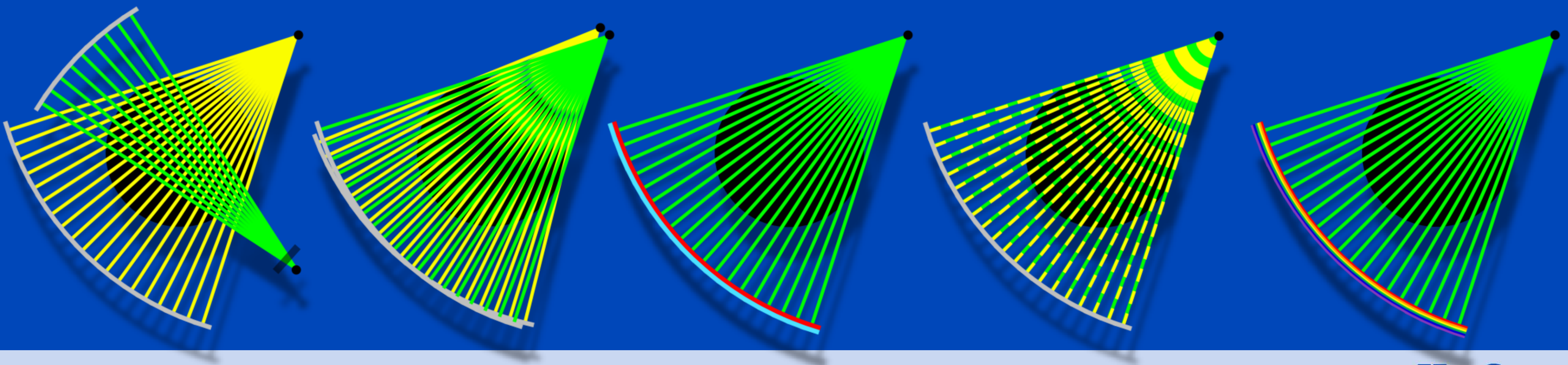

Questions?

80 kV / 140 kV

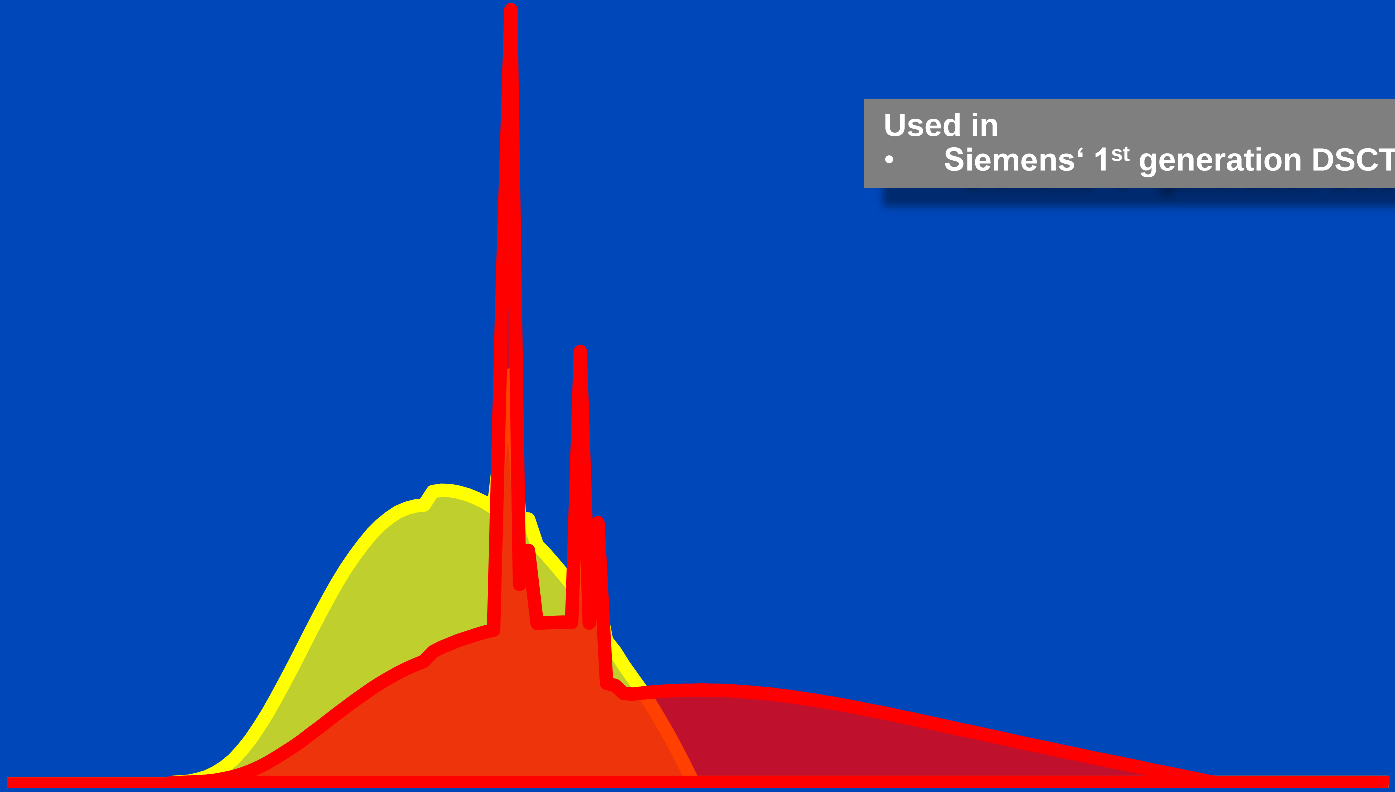

Used in
- Siemens‘ 1st generation DSCT

80 kV / 140 kV

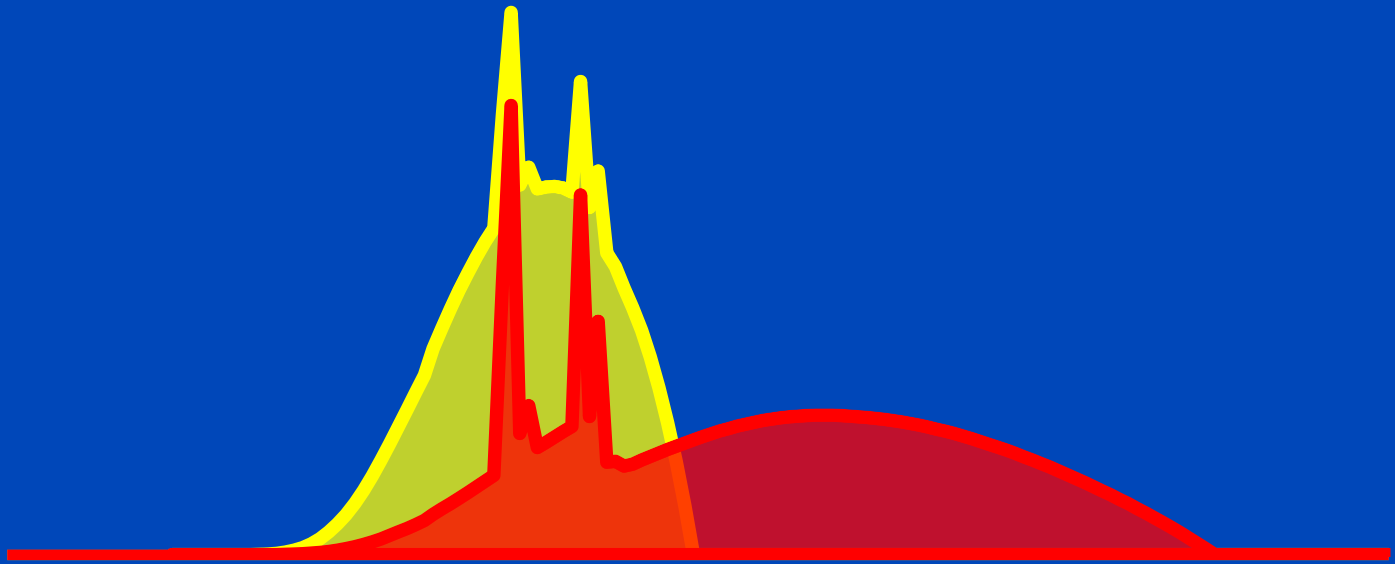

Used in
- Siemens‘ 1st generation DSCT

Spectra as seen after having passed a 32 cm water layer.

80 kV / 140 kV Sinrect kV-Switching

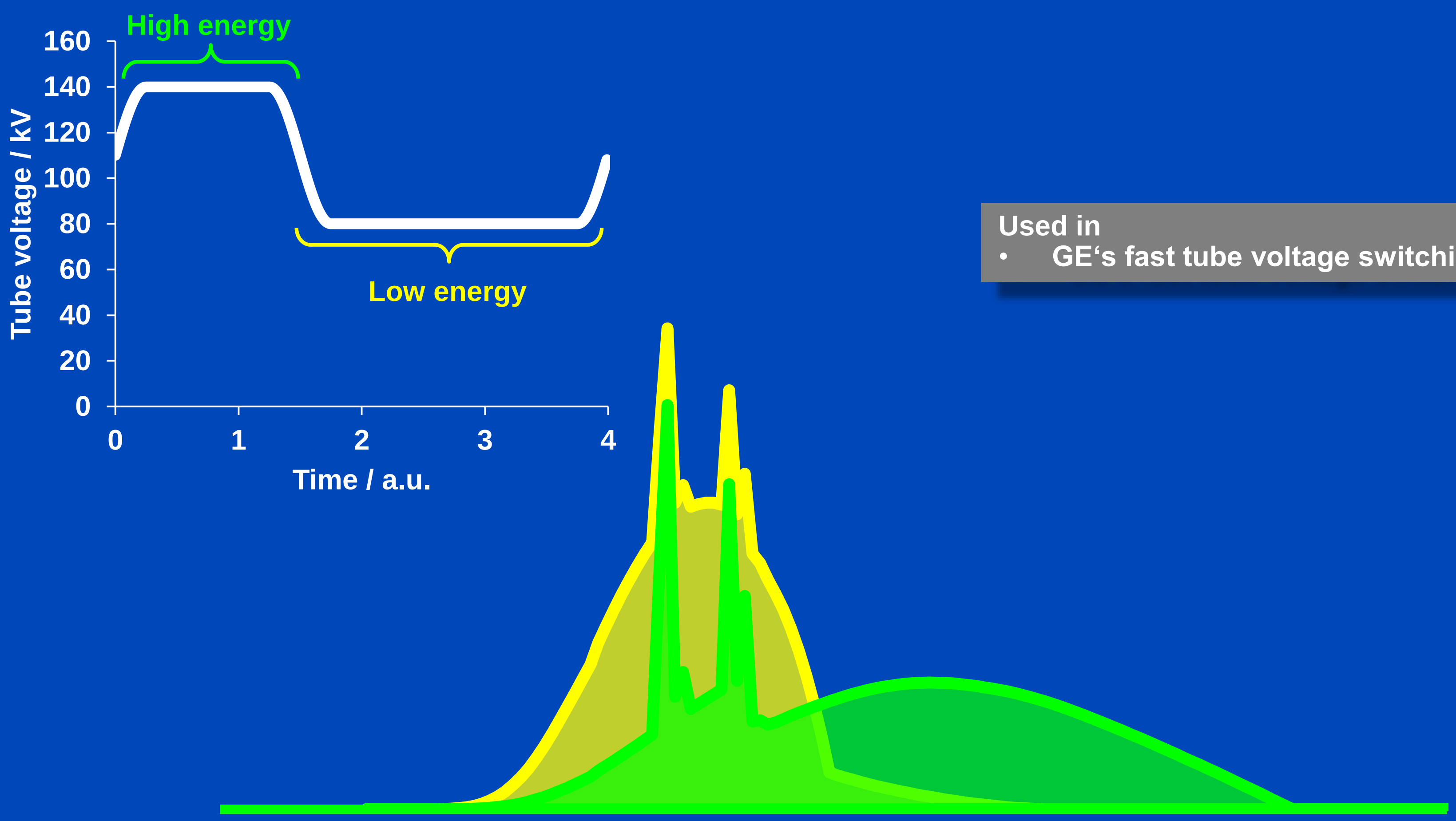

Used in
- GE‘s fast tube voltage switching CT

Spectra as seen after having passed a 32 cm water layer.

80 kV / 140 kV $Sn_{0.4\ mm}$

Used in
- Siemens' 2nd generation DSCT

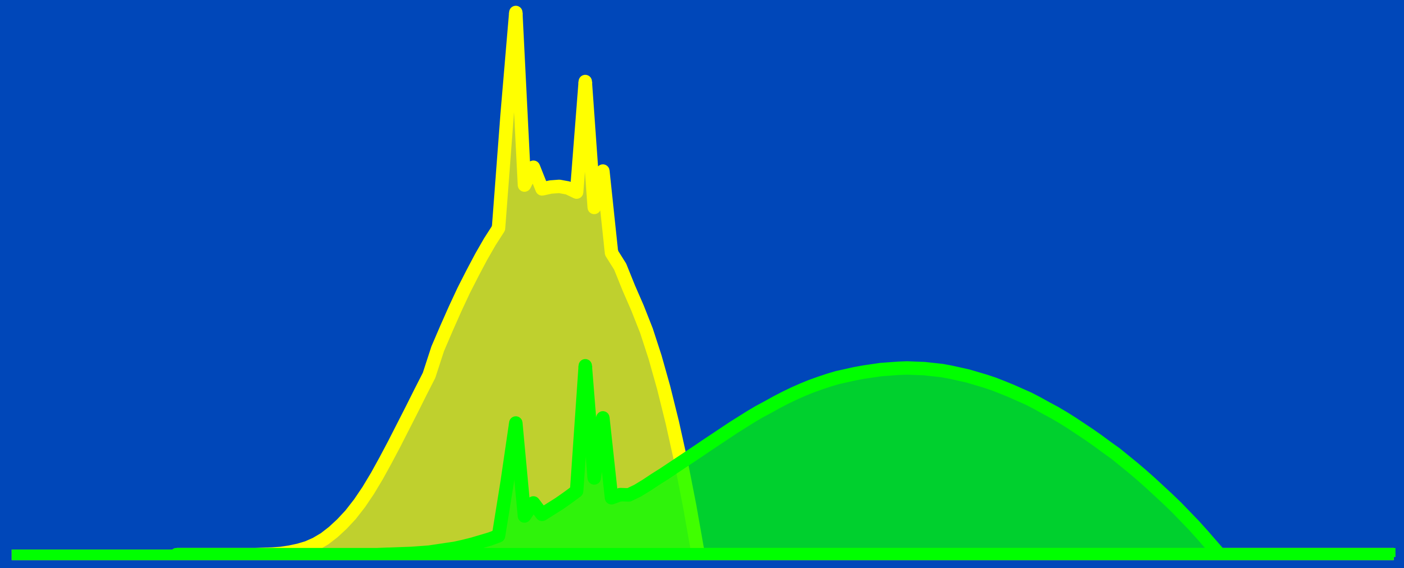

Spectra as seen after having passed a 32 cm water layer.

100 kV / 140 kV $Sn_{0.4\ mm}$

Used in
- Siemens‘ 2nd generation DSCT

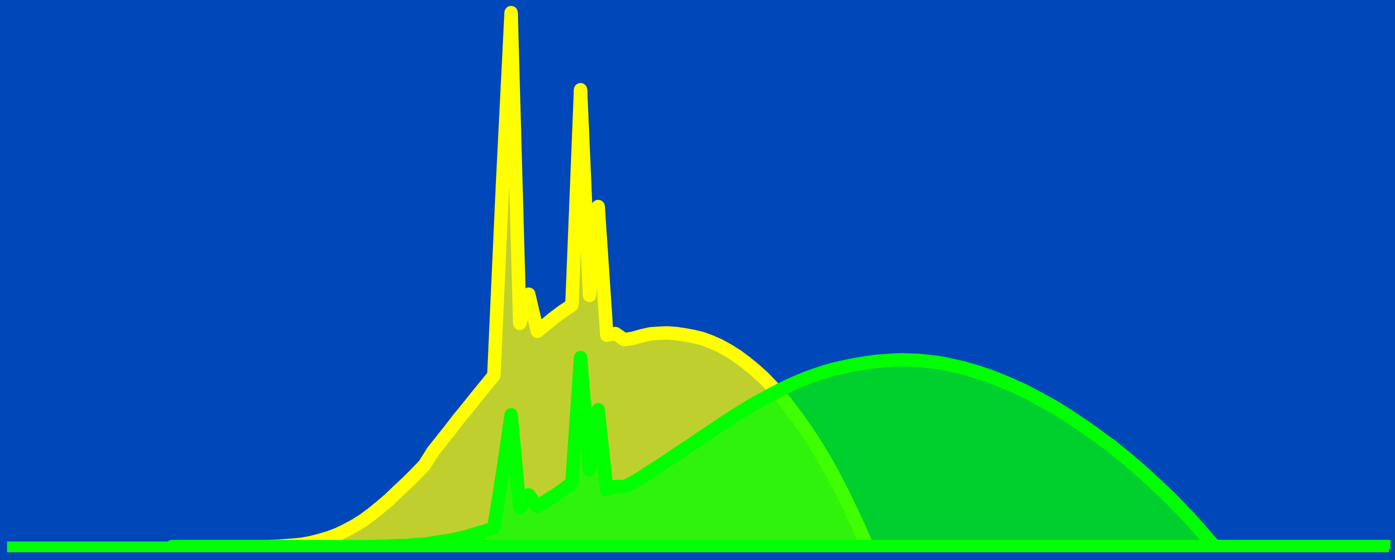

Spectra as seen after having passed a 32 cm water layer.

90 kV / 150 kV $Sn_{0.6\ mm}$

Used in
- Siemens‘ 3[rd] generation DSCT

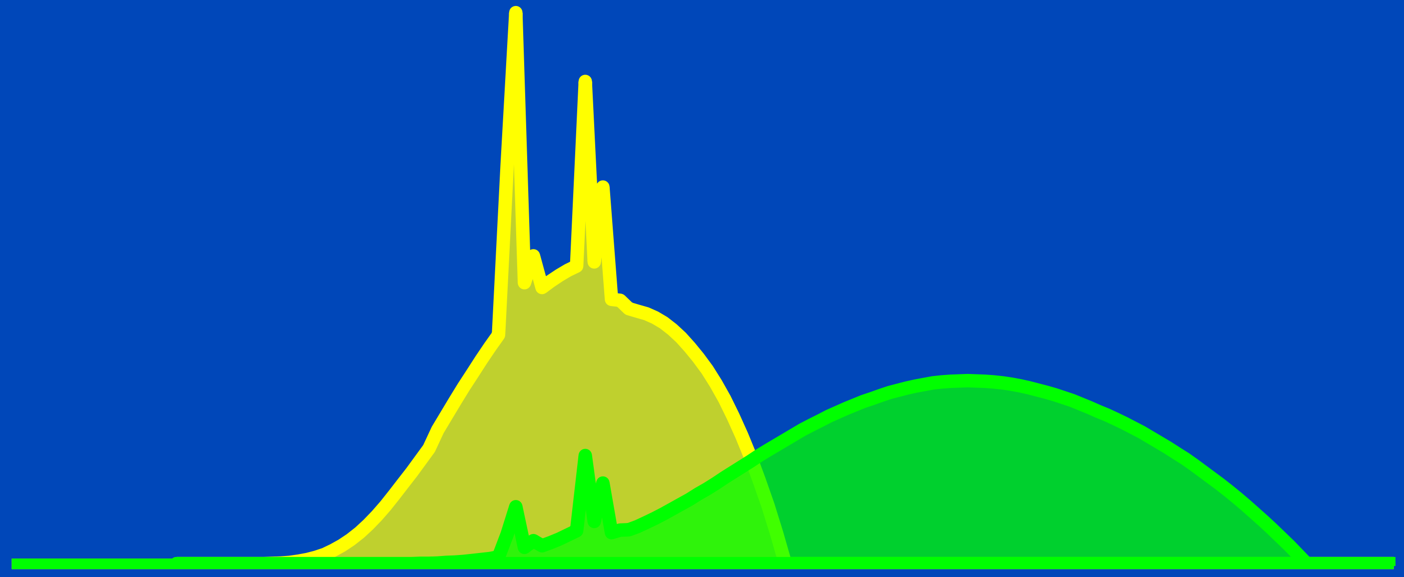

Spectra as seen after having passed a 32 cm water layer.

140 kV YAG / GOS

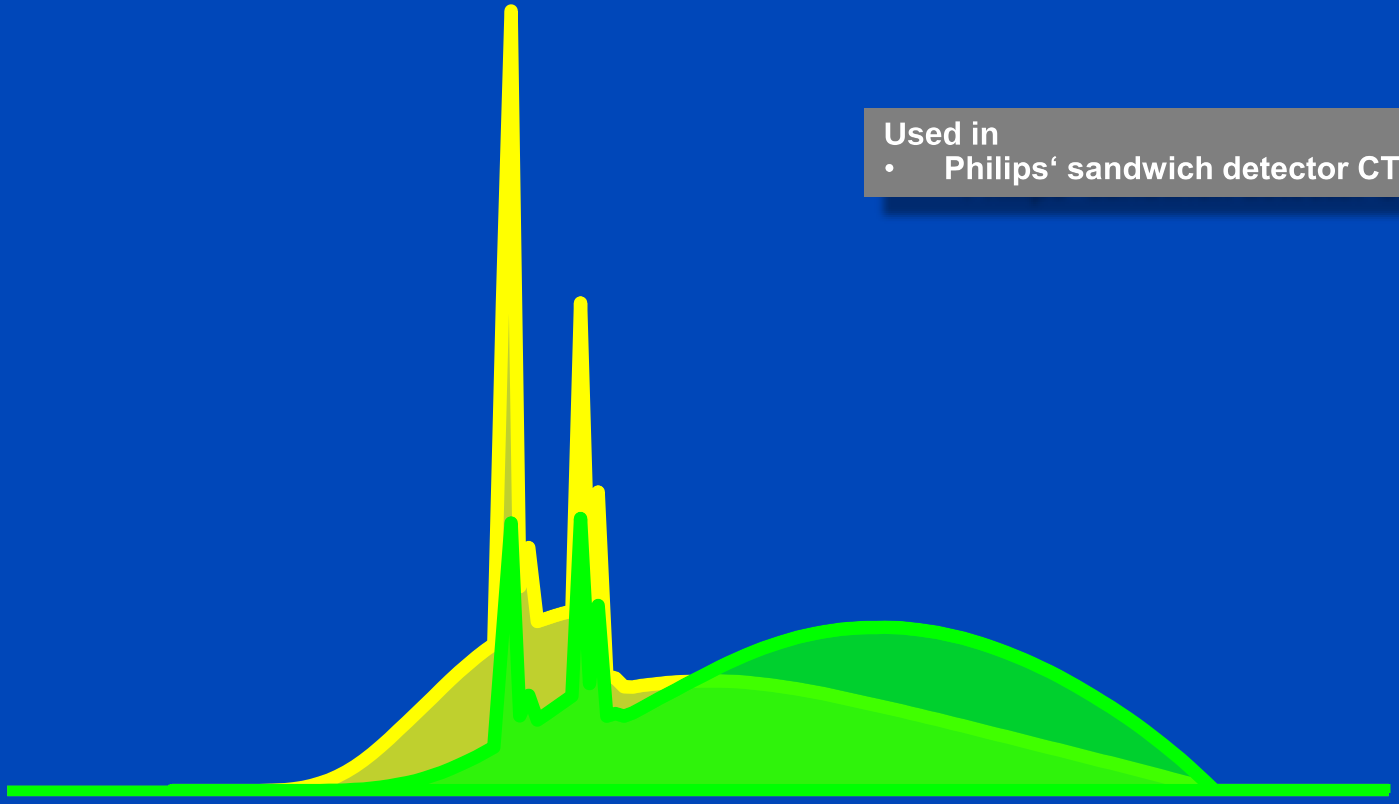

Used in
- Philips‘ sandwich detector CT

Spectra as seen after having passed a 32 cm water layer.

Split filter 120 kV (Au+Sn)

Used in
- Siemens‘ split filter DSCT

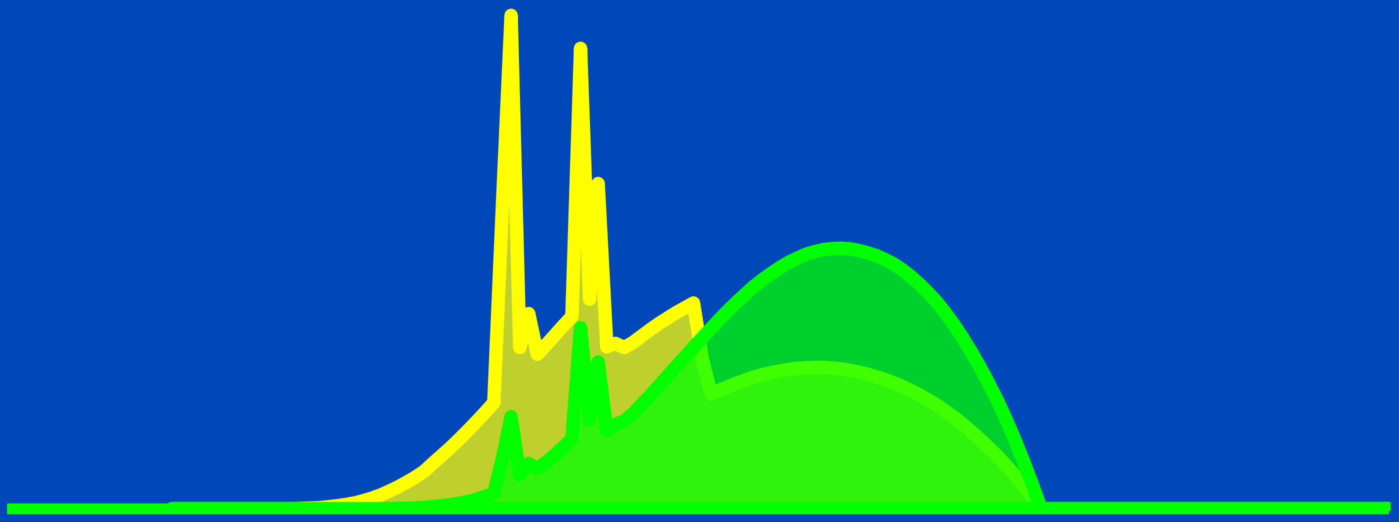

Spectra as seen after having passed a 32 cm water layer.

Photon Counting 140 kV
2 Bins Perfect

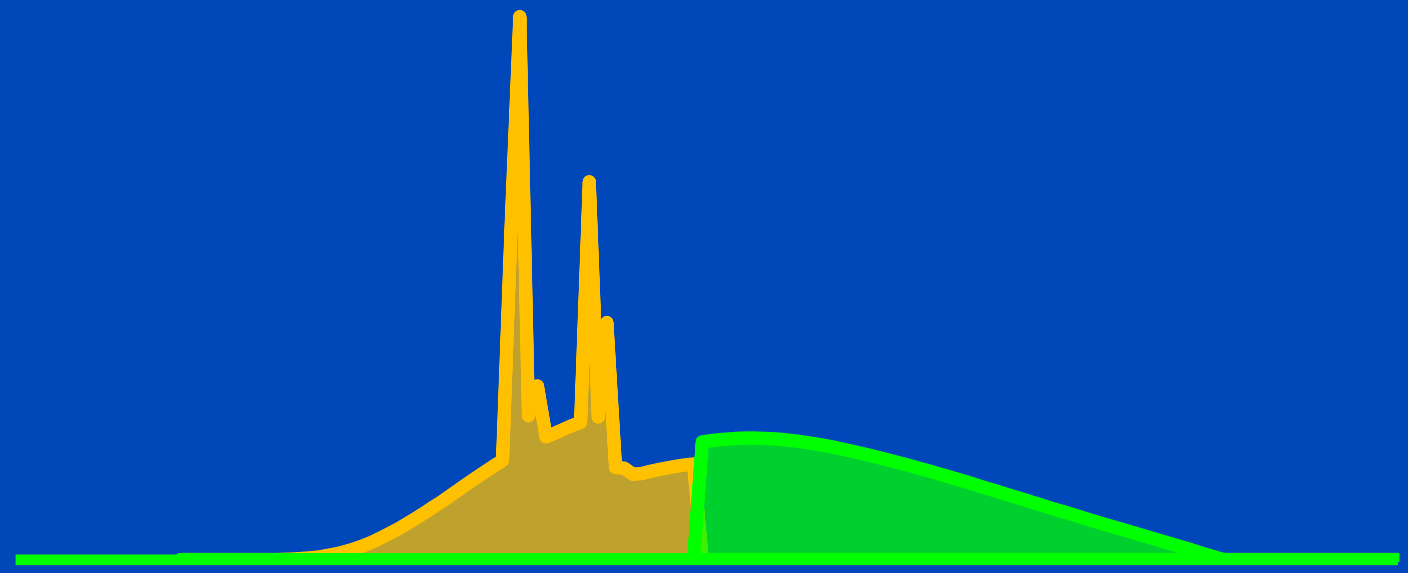

Spectra as seen after having passed a 32 cm water layer.

Photon Counting 140 kV
2 Bins Realistic

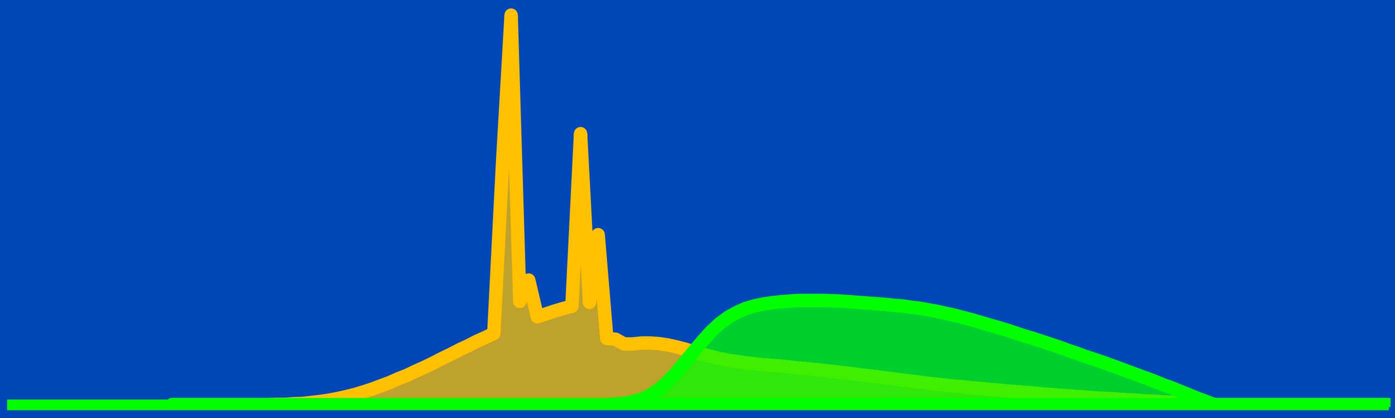

Spectra as seen after having passed a 32 cm water layer.

Photon Counting 140 kV
4 Bins Realistic

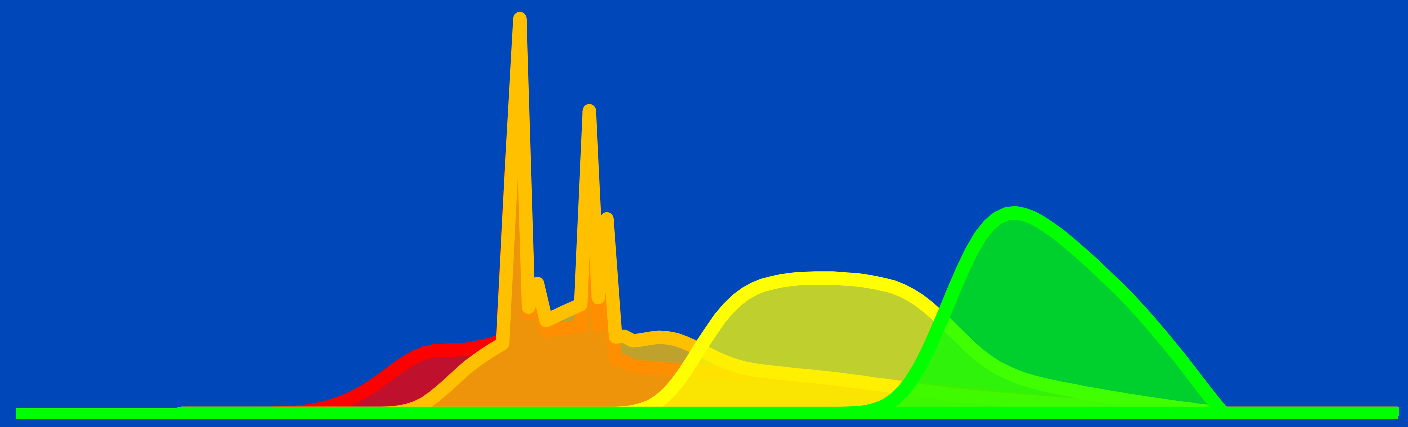

Spectra as seen after having passed a 32 cm water layer.

Decomposition Increases Noise

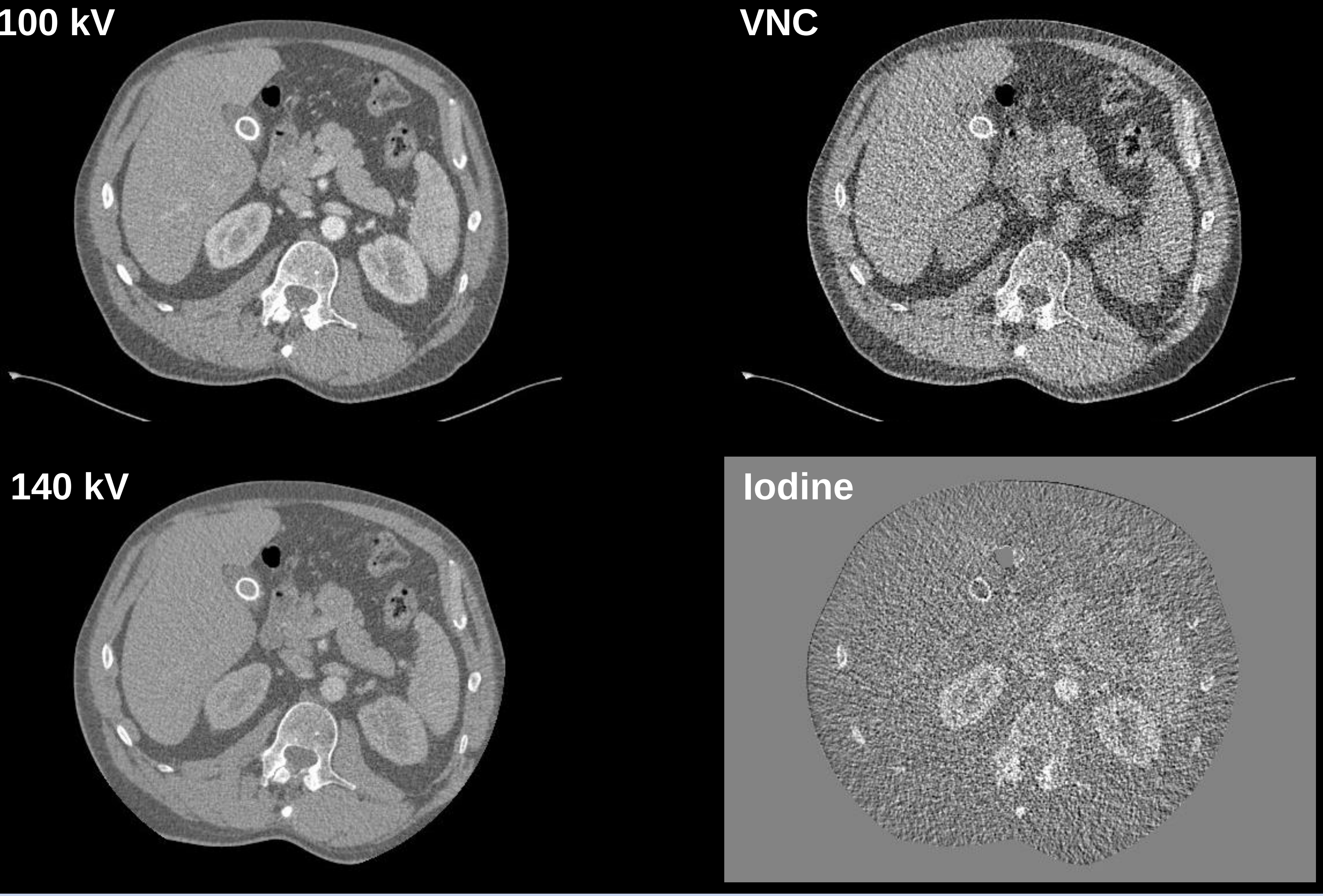

C = 0 HU, W = 700 HU

Denoising is Mandatory!

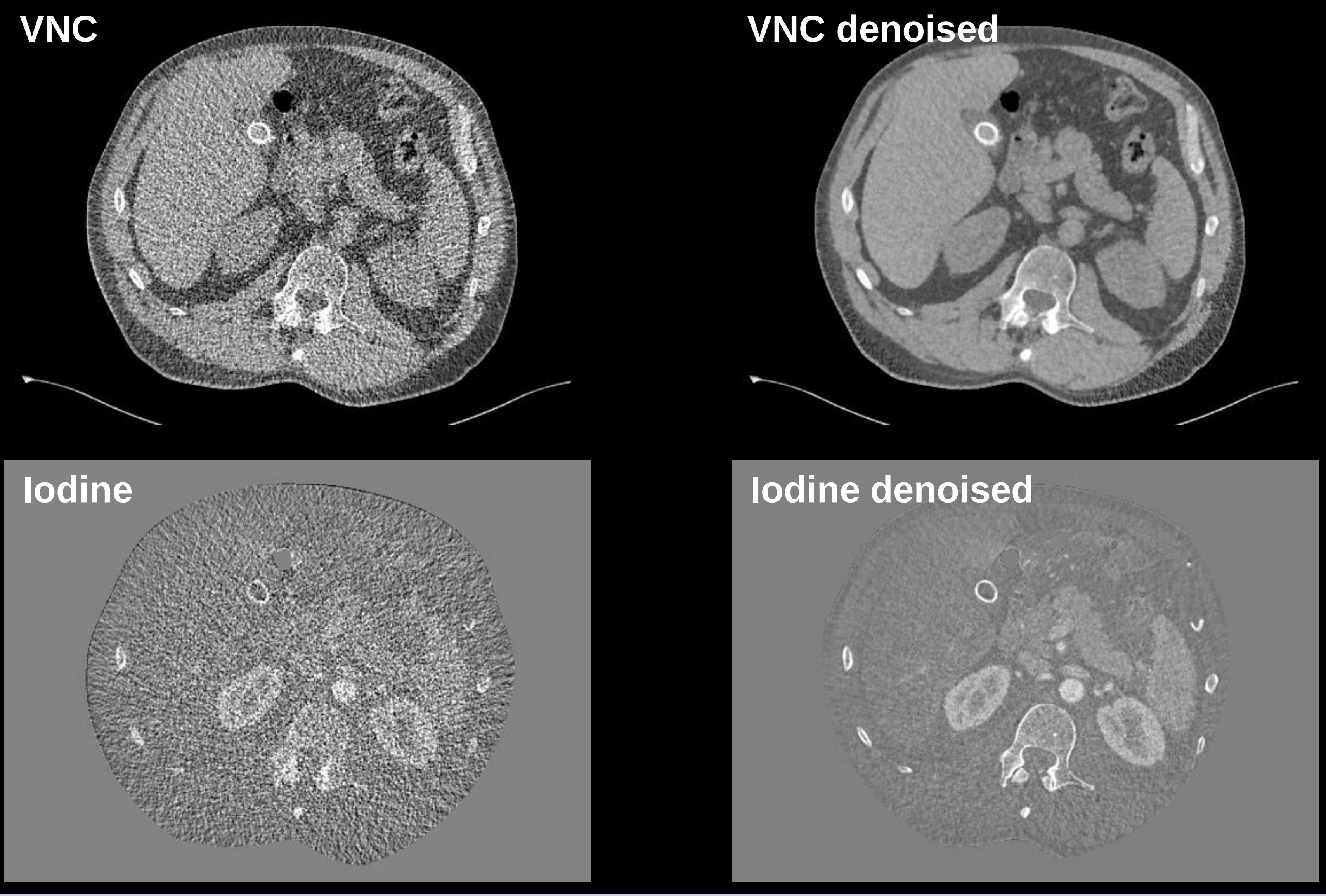

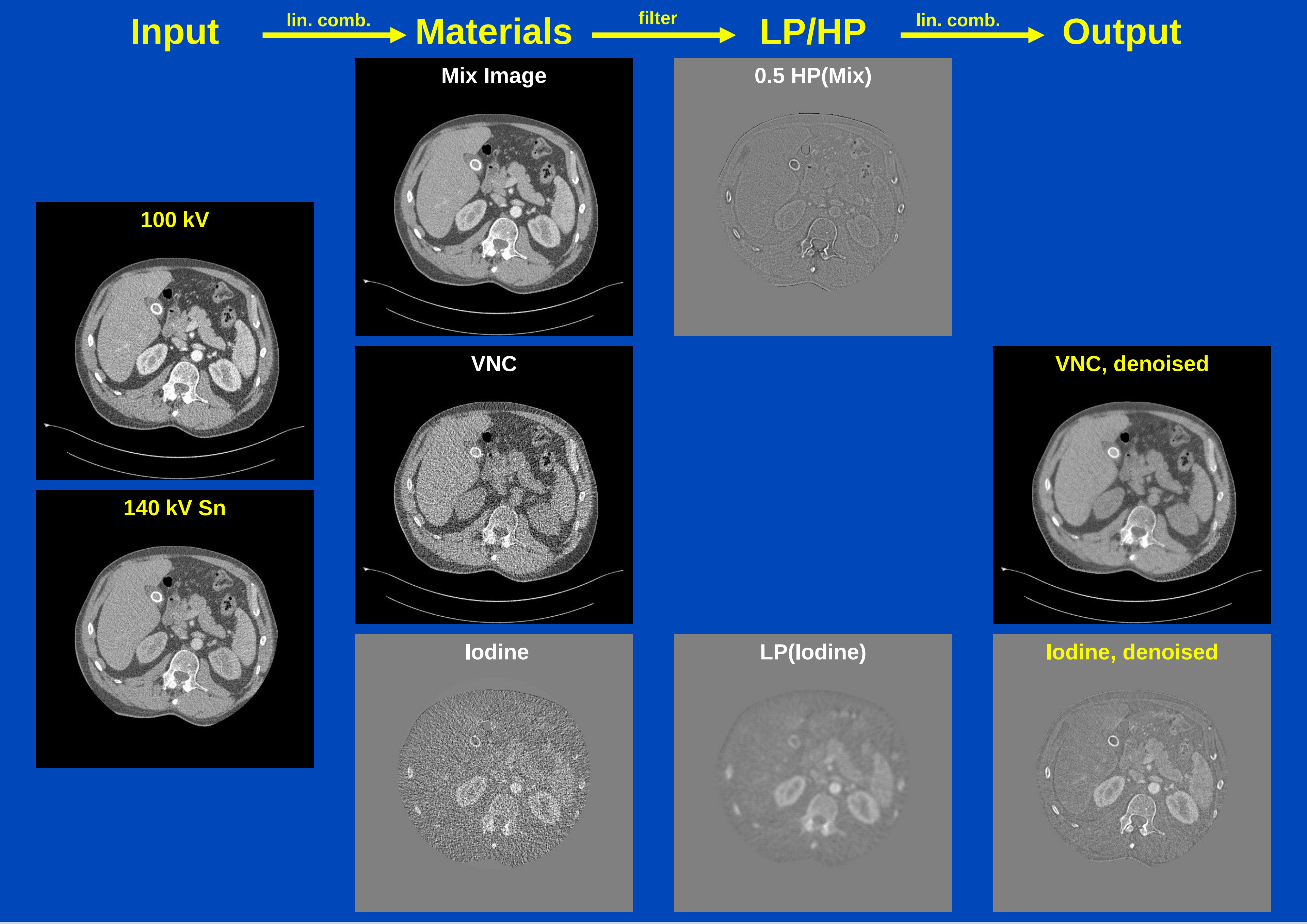

C = 0 HU, *W* = 500 HU for the low, high and VNC images. *C* = 0 mg/mL, *W* = 27.6 mg/mL for the iodine images.

Questions?

Photon Counting CT

Indirect Conversion (Today)

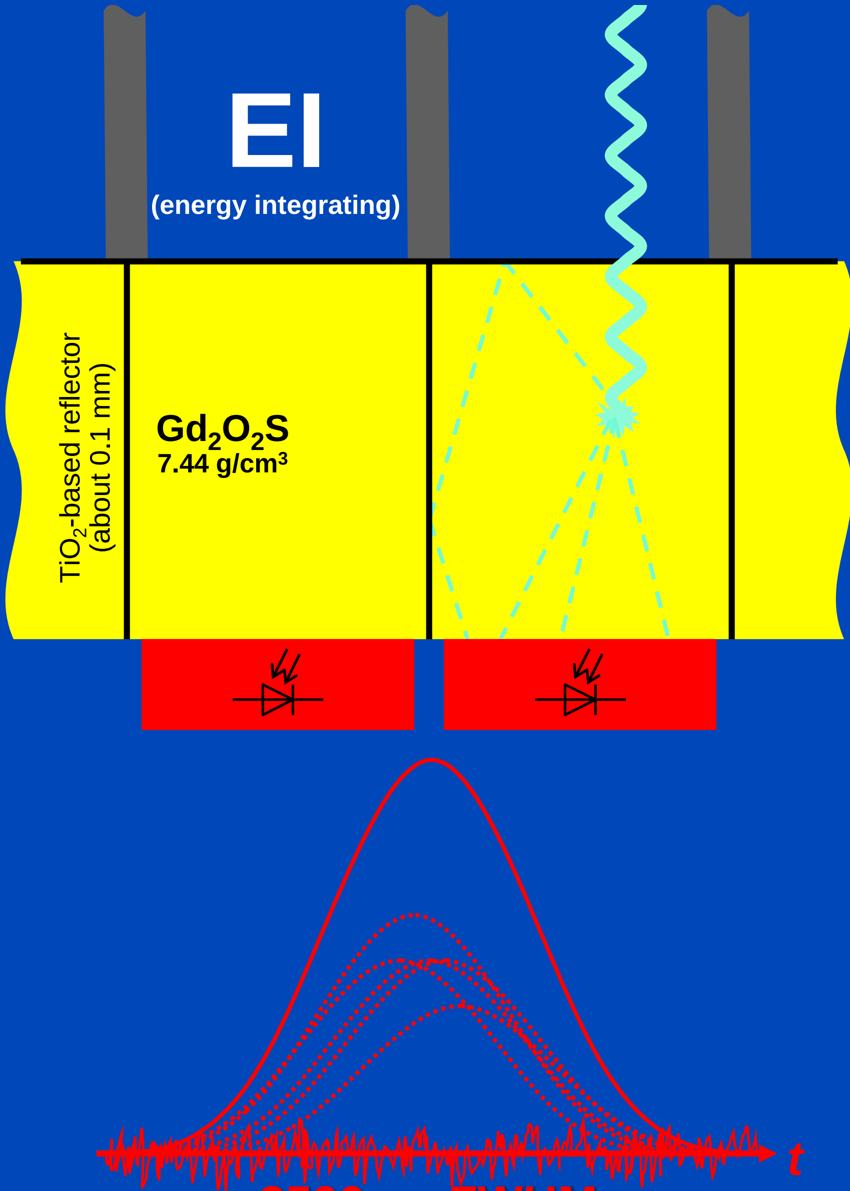

2500 ns FWHM

i.e. max O(40·10³) cps

Direct Conversion (Future)

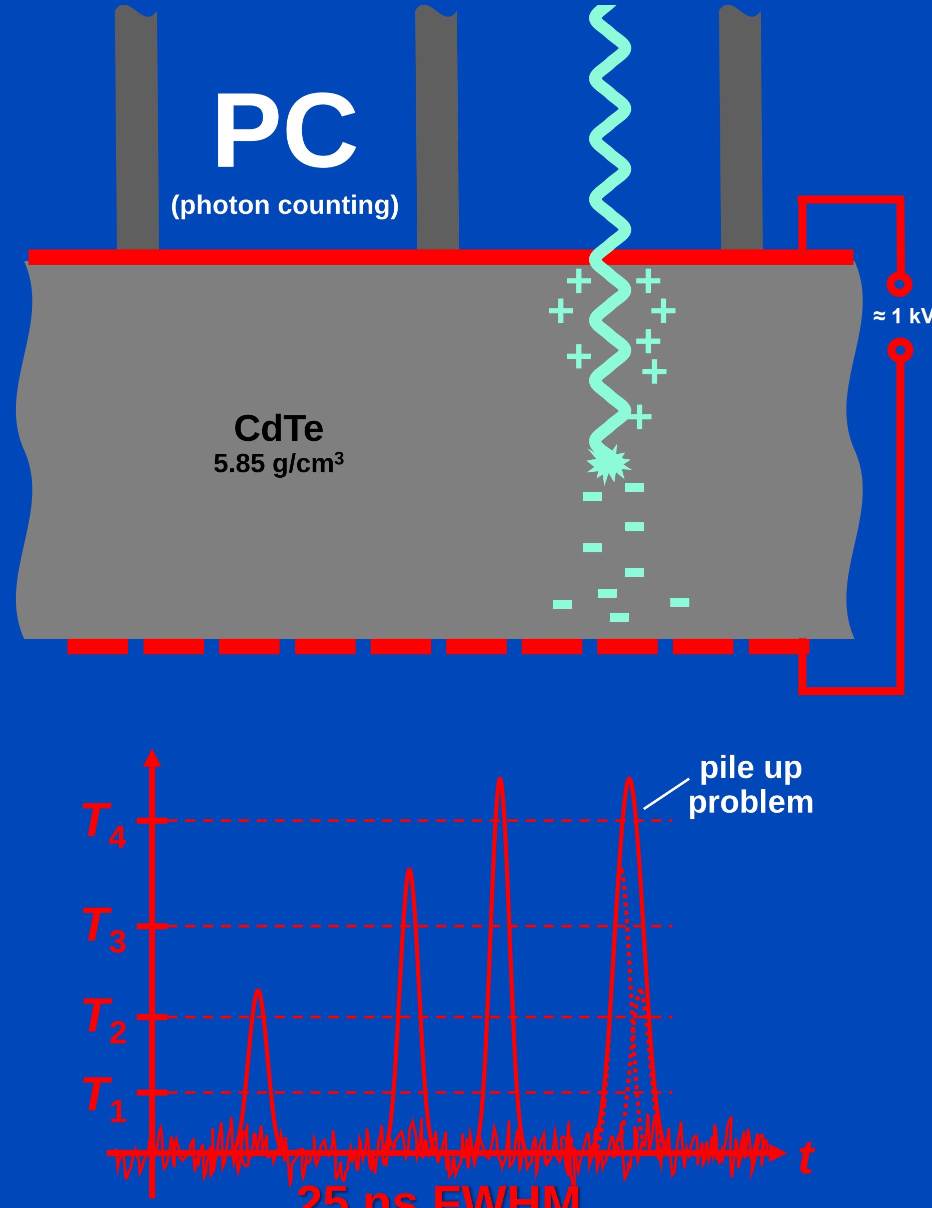

25 ns FWHM

i.e. max O(40·10⁶) cps

Requirements for CT: up to 10^9 x-ray photon counts per second per mm². Hence, photon counting only achievable for direct converters.

Dark Image of Photon Counter Shows Background Radiation

18 frames, 5 min integration time per frame

Energy Integrating (Dexela) | Photon Counting (Dectris Santis)

Events per Frame

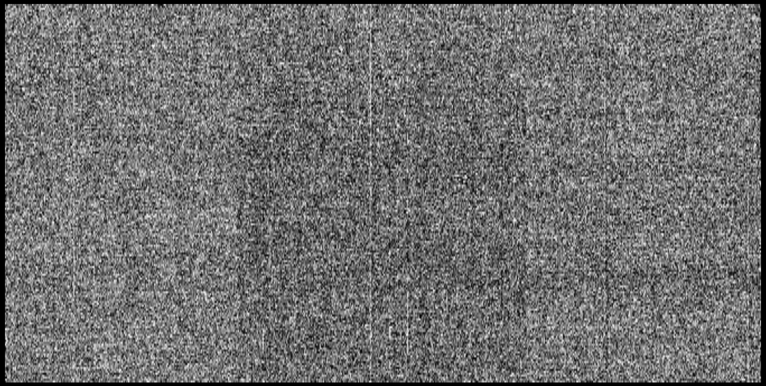

C/W = 0 a.u./70 a.u.

C/W = 1 cnts/2 cnts

Accumulated Signal

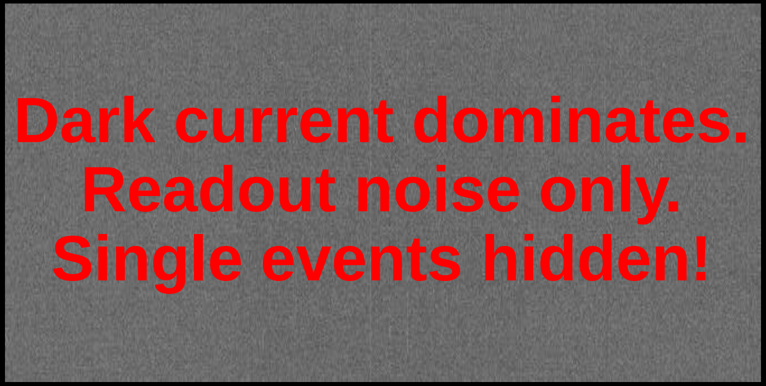

C/W = 30 a.u./450 a.u.

No dark current.
No readout noise.
Single events visible!

C/W = 3 cnts/8 cnts

Energy-Selective Detectors: Improved Spectroscopy, Reduced Dose?

Ideally, bin spectra do not overlap, …

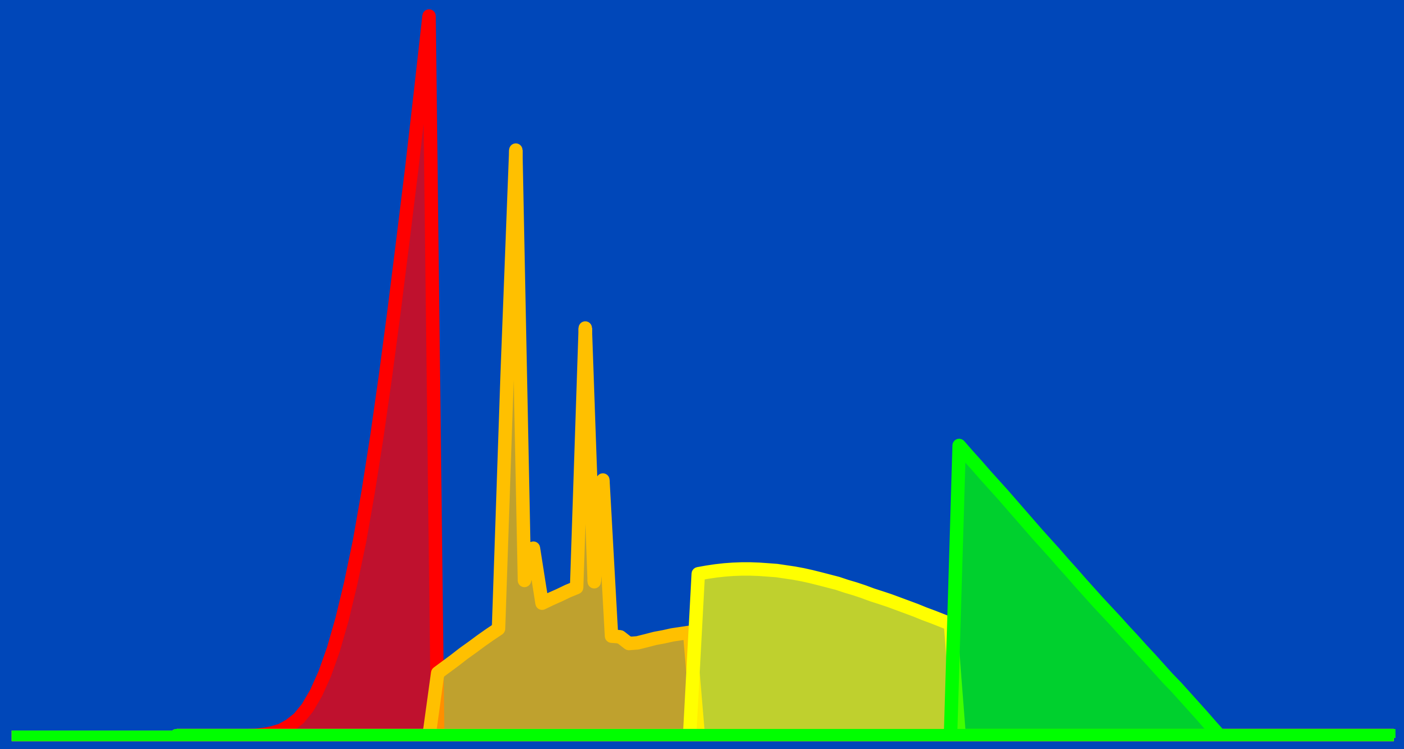

Spectra as seen after having passed a 32 cm water layer.

Energy-Selective Detectors: Improved Spectroscopy, Reduced Dose?

… realistically, however they do!

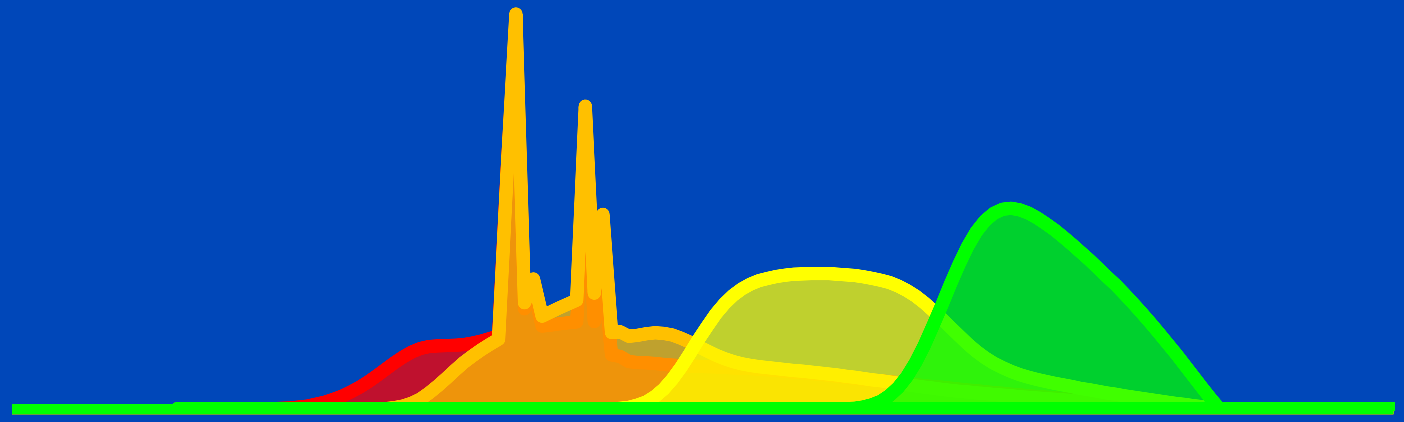

Spectra as seen after having passed a 32 cm water layer.

Bin Images

Bin 1 | Bin 2 | Bin 3 | Bin 4

[25,45] keV | [45,75] keV | [75,90] keV | [90,140] keV

C = 900 HU, W = 3500 HU

Diagnostic CT (Conventional Detector) of a Low Contrast Phantom

Photon Counting Detector CT of a Low Contrast Phantom

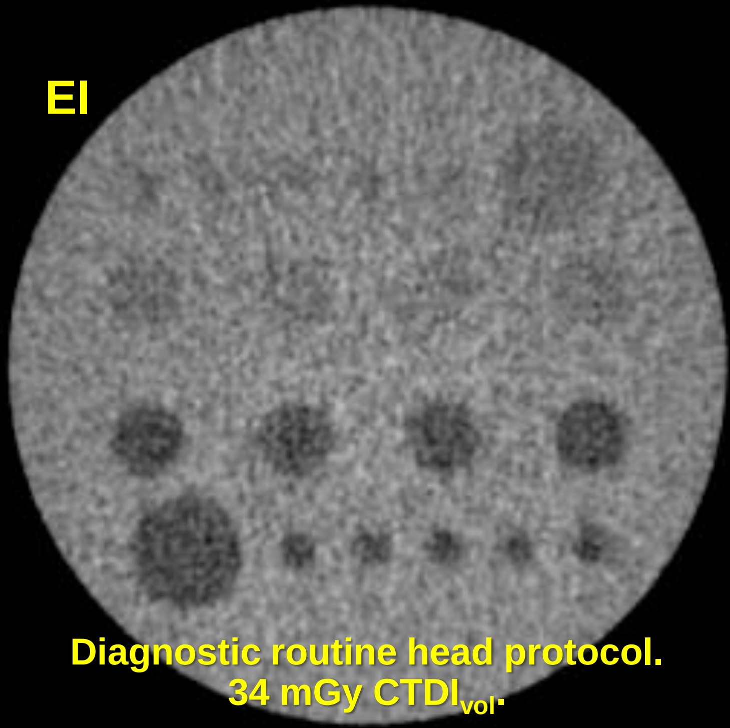

Diagnostic routine head protocol.
34 mGy CTDI_{vol}.

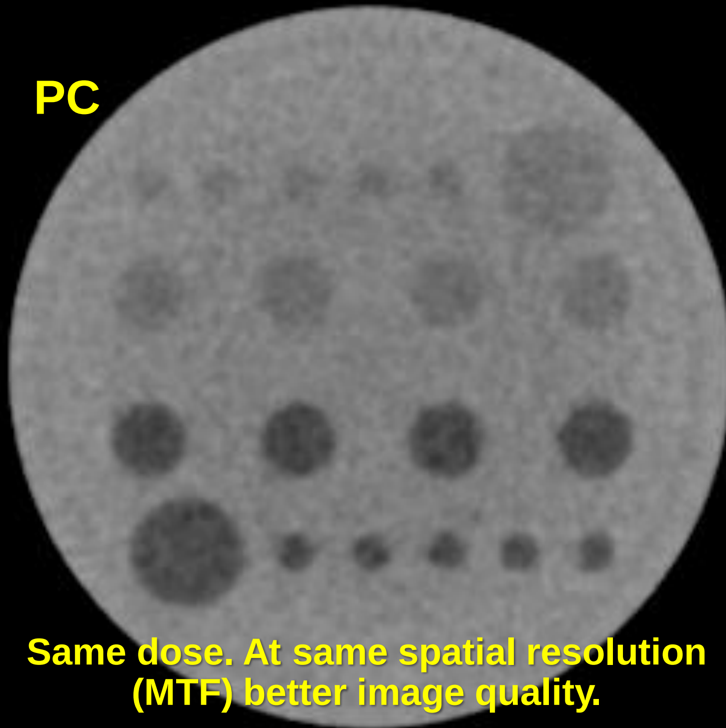

Same dose. At same spatial resolution (MTF) better image quality.

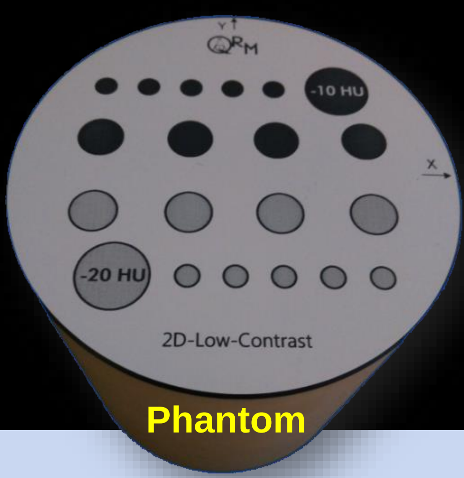

Phantom

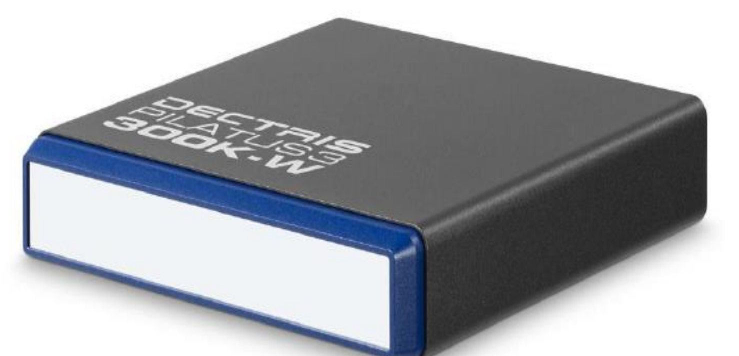

Photon Counting Detector

C = 0 HU, W = 80 HU


SIEMENS
SOMATOM CounT
@ dkfz.

Siemens CounT CT System

Gantry from a clinical dual source scanner

A: conventional CT detector (50.0 cm FOV)

B: Photon counting detector (27.5 cm FOV)

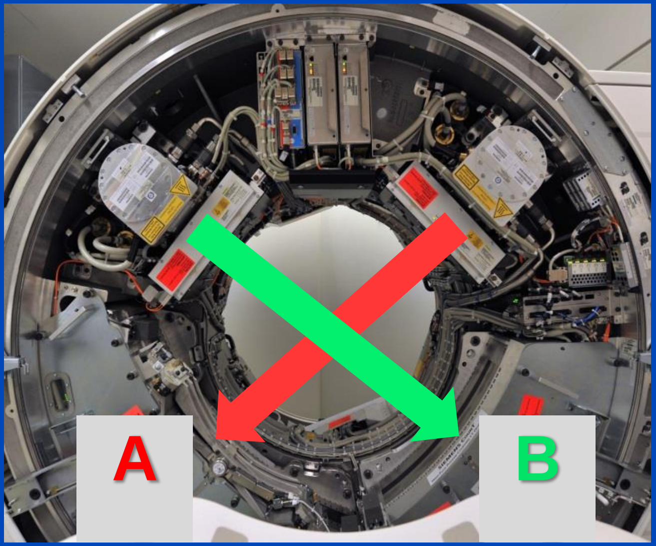

Readout Modes of the CounT

PC-UHR Mode	PC-Macro Mode	EI detector
0.25 mm pixel size	0.50 mm pixel size	0.60 mm pixel size

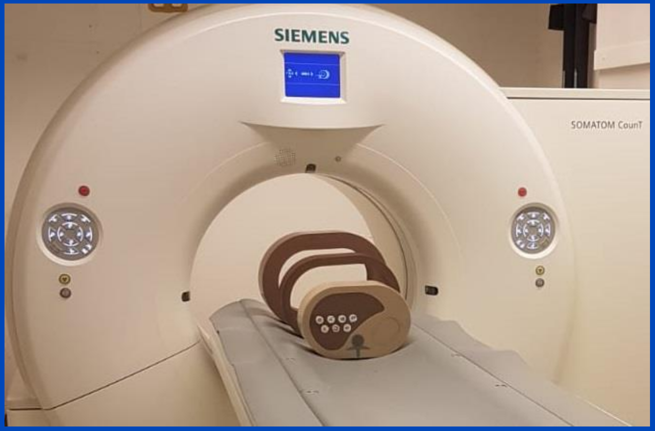

Readout Modes of the Siemens CounT

Macro Mode
0.9 × 1.1 mm focus
2 readouts
16 mm z-coverage

12	12	12	12
12	12	12	12
12	12	12	12
12	12	12	12

Chess Mode
0.9 × 1.1 mm focus
4 readouts
16 mm z-coverage

12	34	12	34
34	12	34	12
12	34	12	34
34	12	34	12

Sharp Mode
0.9 × 1.1 mm focus
5 readouts
12 mm z-coverage

1	1	1	1
1	1	1	1
1	1	1	1
1	1	1	1

2	2	2	2
2	2	2	2
2	2	2	2
2	2	2	2

UHR Mode
0.7 × 0.7 mm focus
8 readouts
8 mm z-coverage

12	12	12	12
12	12	12	12
12	12	12	12
12	12	12	12

1.6 mm CdTe sensor. No FFS on detector B (photon counting detector). 4×4 subpixels of 225 µm size = 0.9 mm pixels (0.5 mm at isocenter). An additional 225 µm gap (e.g. for anti scatter grid) yields a pixel pitch of 1.125 mm.The whole detector consists of 128×1920 subpixels = 32×480 macro pixels.

This photon-counting whole-body CT prototype, installed at the Mayo Clinic, at the NIH and at the DKFZ is a DSCT system. However, it is restricted to run in single source mode. The second source is used for data completion and for comparisons with EI detectors.

Detector Pixel Force vs. CounT Plus[1]

Force
920 × 96 detector pixels
pixel size 0.56 × 0.6 mm at iso
57.6 mm z-coverage

CounT+ (Macro)
1376 × 144 macro pixels
pixel size 0.3 × 0.4 mm at iso
57.6 mm z-coverage

CounT+ (UHR)
2752 × 120 pixels
pixel size 0.15 × 0.2 mm at iso
24 mm z-coverage

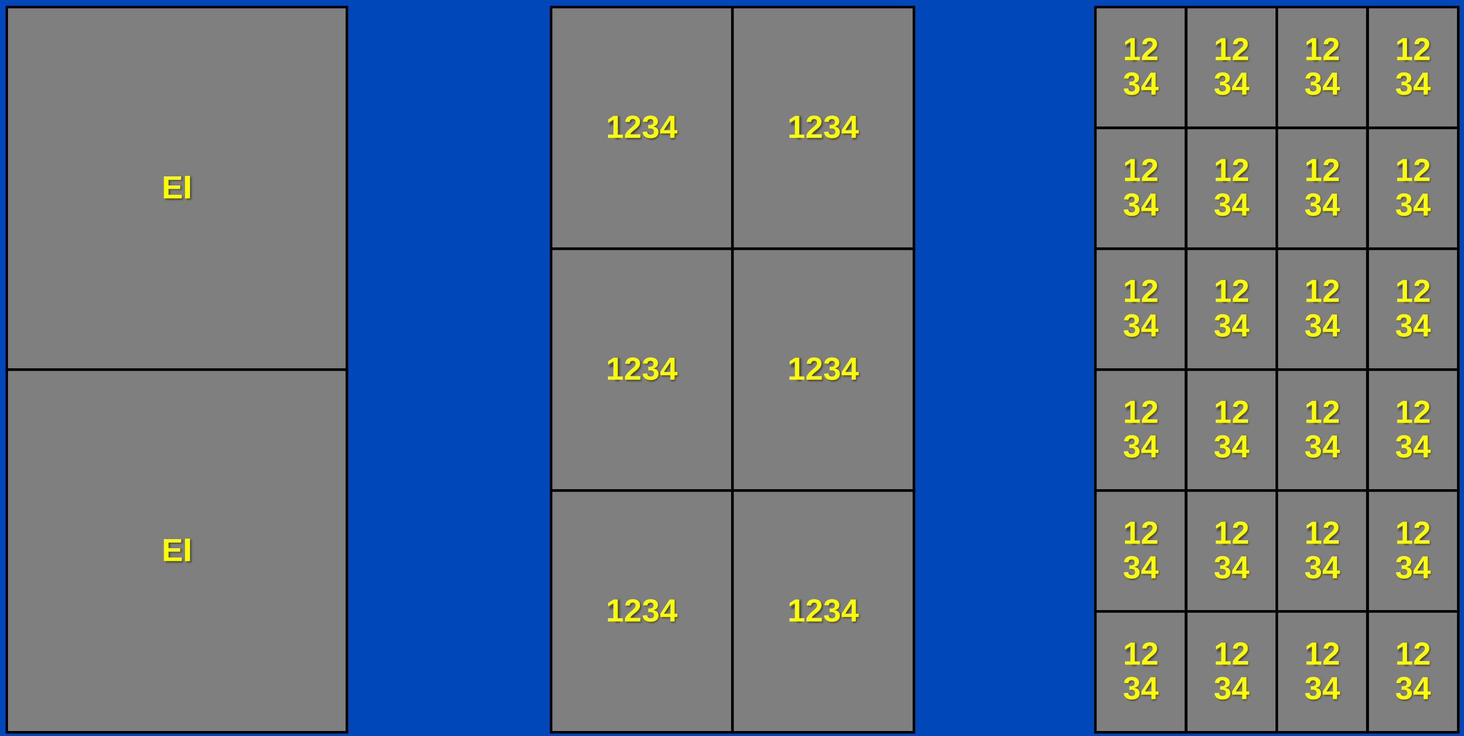

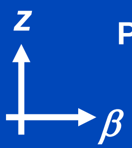

Pixel arrangement (2×1, 3×2, 6×4) drawn such that approximately the same area is covered in all three cases.

Focus sizes of Vectron tube: 0.4×0.5 mm, 0.6×0.7 mm, 0.8×1.1 mm

[1]J. Ferda et al. Computed tomography with a full FOV photon-counting detector in a clinical setting, the first experience. European Journal of Radiology 137:109614, 2021

Questions?

Advantages of Photon Counting CT

- No reflective gaps between detector pixels
  - Higher geometrical efficiency
  - Less dose
- No electronic noise
  - Less dose for infants
  - Less noise for obese patients
- Counting
  - Swank factor = 1 = maximal
  - “Iodine effect“ due to higher weights on low energies
- Energy bin weighting
  - Lower dose/noise
  - Improved iodine CNR
- Smaller pixels (to avoid pileup)
  - Higher spatial resolution
  - “Small pixel effect” i.e. lower dose/noise at conventional resolution
- Spectral information on demand
  - Dual Energy CT (DECT)
  - Multi Energy CT (MECT)

No Electronic Noise!

- Photon counting detectors have no electronic noise.
- Extreme low dose situations will benefit
  - Pediadric scans at even lower dose
  - Obese patients with less noise
  - …

Energy Integrating (Dexela)

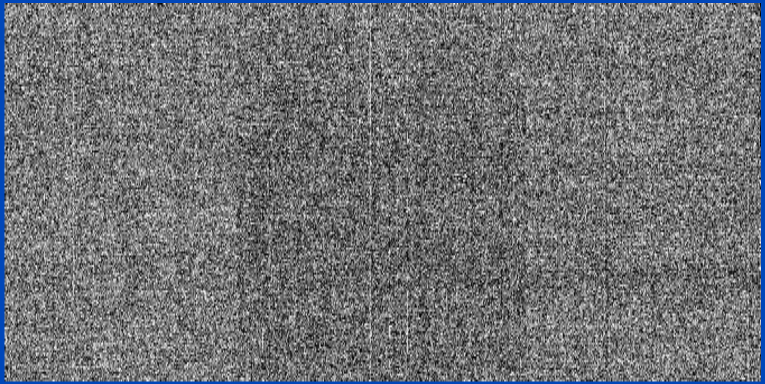

Photon Counting (Dectris Santis)

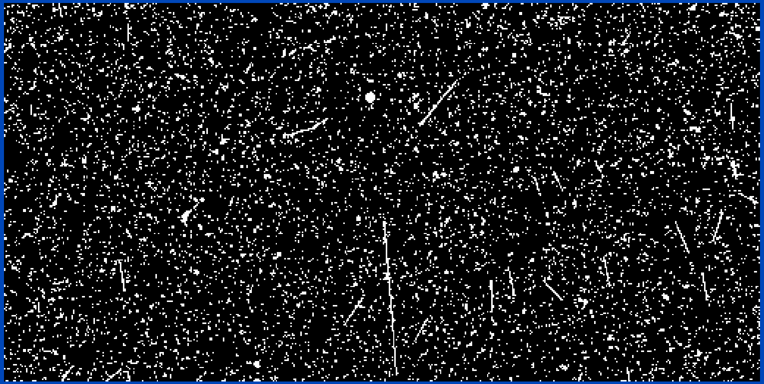

Expected Value and Variance

- **Transmitted number of photons *N*:**

$$N(E) = N_0(E)e^{-p\psi(E)}$$

- **Poisson distribution:** $\mathrm{E}N(E) = \mathrm{Var}N(E)$
- **Detected signal *S* with sensitivity *s*(*E*):**

$$S = \int dE\, s(E)N(E)$$

- **Expected value and variance of the signal *S*:**

$$\mathrm{E}S = \int dE\, s(E)\mathrm{E}N(E) \text{ and } \mathrm{Var}S = \int dE\, s^2(E)\mathrm{E}N(E)$$

- **Detector sensitivity: PC** $s(E) = 1$**, but EI** $s(E) \propto E$ **!**

Energy Integrating
(Detected Spectra at 100 kV and 140 kV)

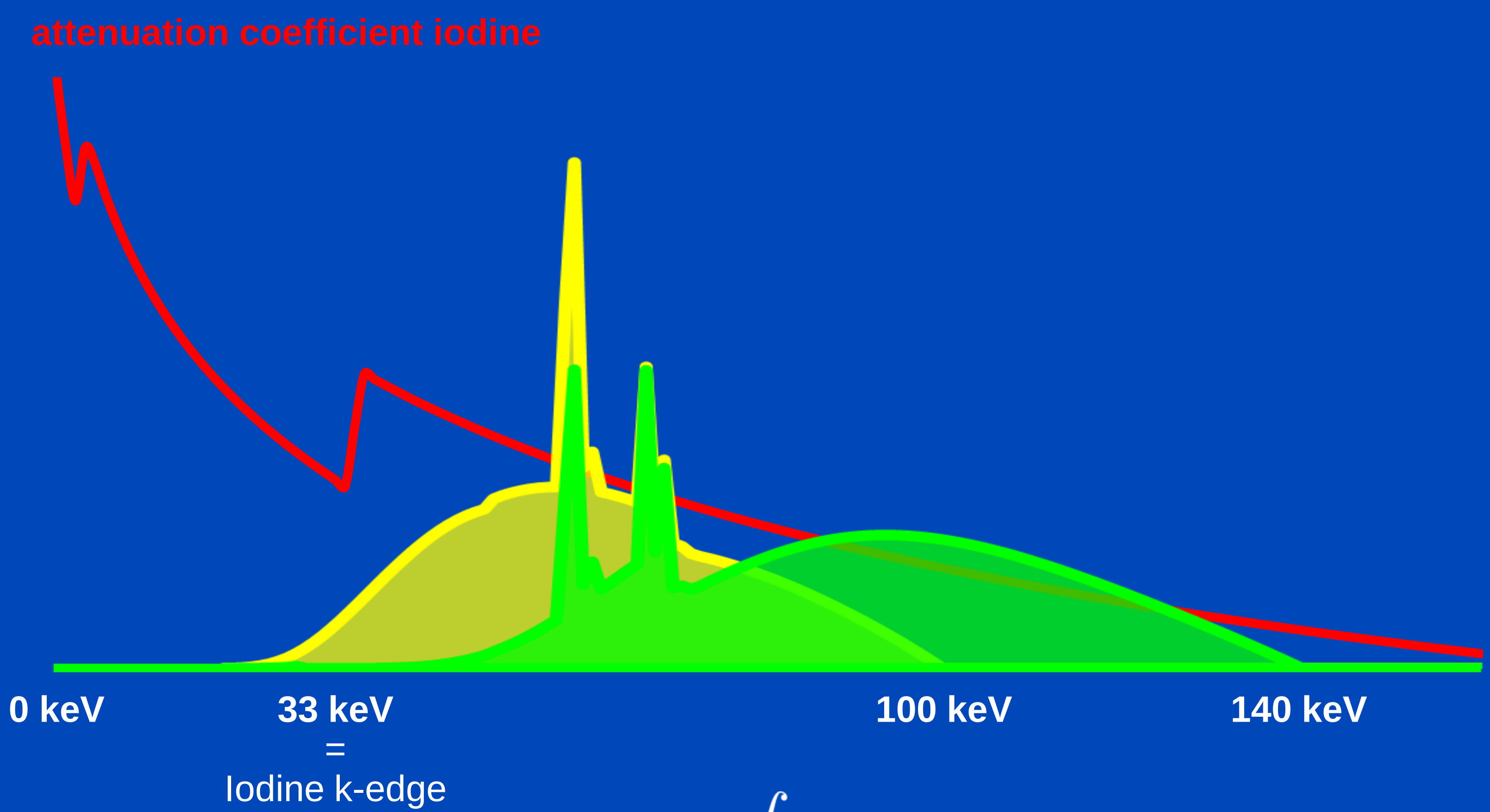

$$\mathrm{Signal}_{\mathrm{EI}} = \int dE\, E\;\; N(E)$$

Photon Counting
(Detected Spectra at 100 kV and 140 kV)

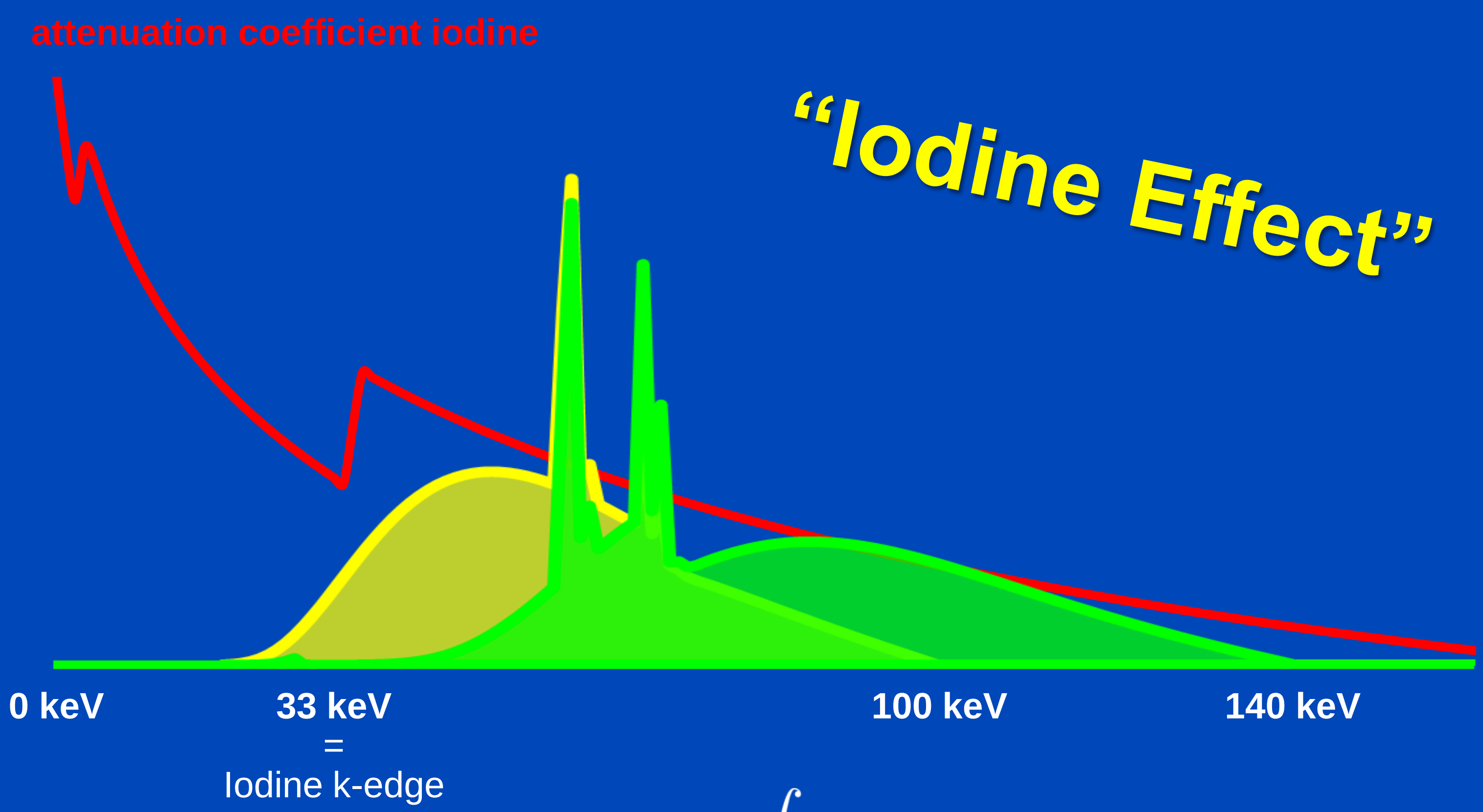

$$\mathrm{Signal}_{\mathrm{PC}} = \int dE\, 1\ N(E)$$

Spectra as seen after having passed a 32 cm water layer.

Swank Factor

- The Swank factor measures the relative SNR^2, and thus the relative dose efficiency between photon counting (PC) and energy integrating (EI).
- PC always has the highest SNR.

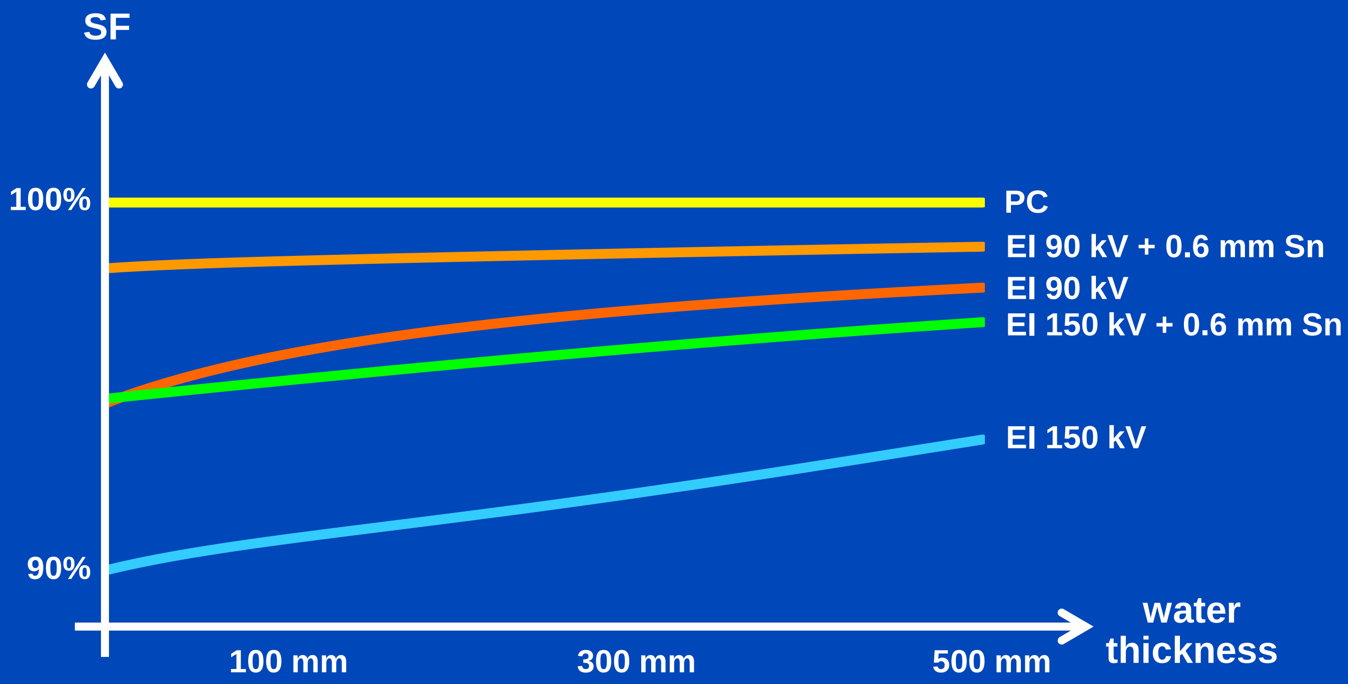

$$\mathrm{SF} = \frac{\mathrm{SNR}^2_{\mathrm{EI}}}{\mathrm{SNR}^2_{\mathrm{PC}}} = \frac{\left(\int dE\, E N(E)\right)^2}{\left(\int dE\, N(E)\right)\left(\int dE\, E^2 N(E)\right)} \leq 1$$

due to Schwarz' inequality

Swank Factor

- The procedure of "guessing" that a constant sensitivity $s(E)$ yields the optimal SNR is rather heuristic.
- More correctly, one would have asked for a sensitivity $s(E)$ that maximizes

$$\mathrm{SNR} = \frac{\mathrm{E}S}{\sqrt{\mathrm{Var}S}}$$

- Formulate this as minimizing Var S for E S given:

$$\int dE \left(s^2(E) + \lambda s(E)\right) \mathrm{E}I(E)$$

- Variational calculus shows that the minimum occurs at $2\,s(E) + \lambda = 0$ which implies

$$s(E) = const.$$

Photon Counting used to Maximize CNR

- With PC energy bin sinograms can be weighted individually, i.e. by a weighted summation
- To optimize the CNR the optimal bin weighting factor w_b is given by (weighting after log):

$$w_b \propto \frac{C_b}{V_b}$$

- The resulting CNR is

$$\mathrm{CNR}^2 = \frac{\left(\sum_b w_b C_b\right)^2}{\sum_b w_b^2 V_b}$$

- At the optimum this evaluates to

$$\mathrm{CNR}^2 = \sum_{b=1}^{B} \mathrm{CNR}_b^2$$

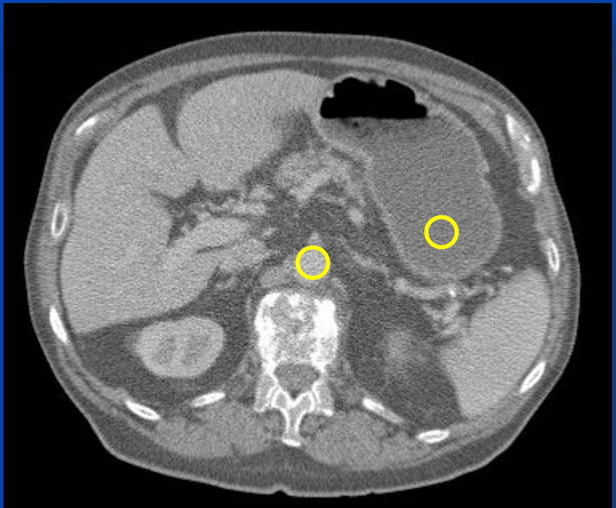

The two ROIs are used to measure the CNR.

Energy Integrating vs. Photon Counting
with 1 bin from 20 to 140 keV

Energy Integrating

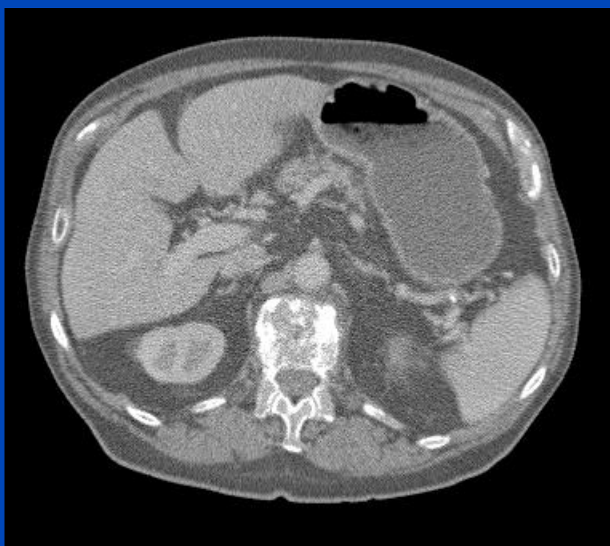

PC minus EI

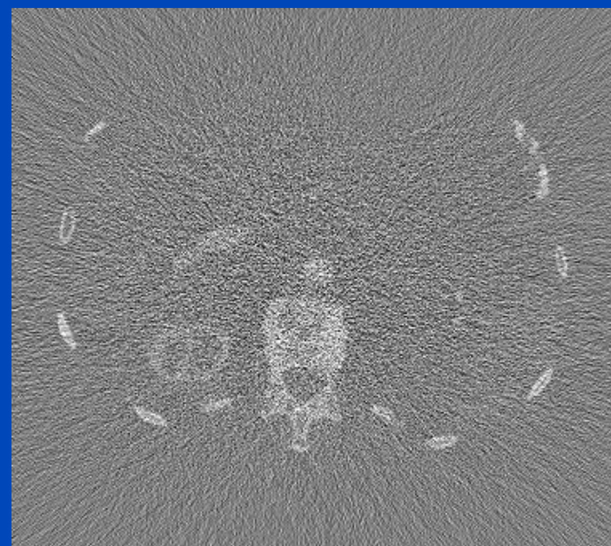

Photon Counting

CNR = 2.11

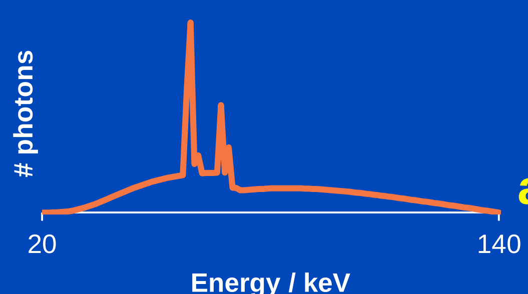

40% CNR improvement or 49% dose reduction achievable due to improved Swank factor and more weight on low energies (iodine contrast benefits).

CNR = 2.95

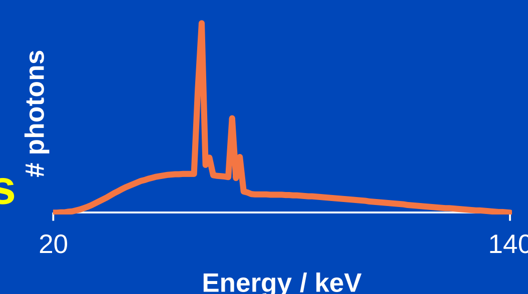

Images: *C* = 0 HU, *W* = 700 HU, difference image: *C* = 0 HU, *W* = 350 HU, bins start at 20 keV

Energy Integrating vs. Photon Counting
with 4 bins from 20 to 140 keV

Energy Integrating

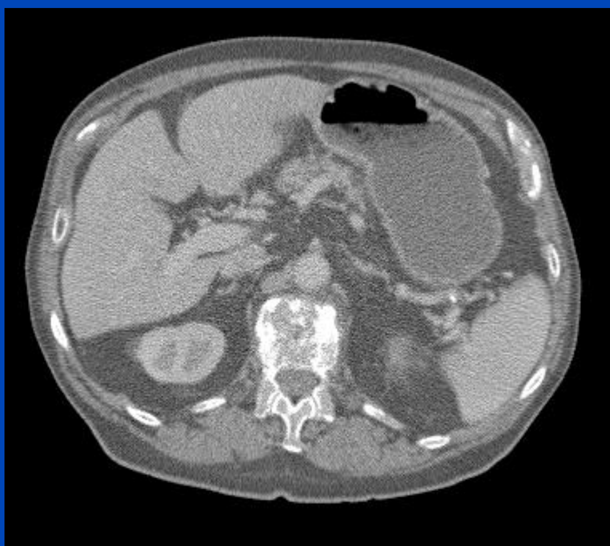

CNR = 2.11

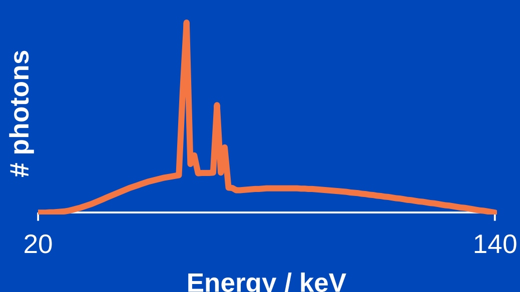

PC minus EI

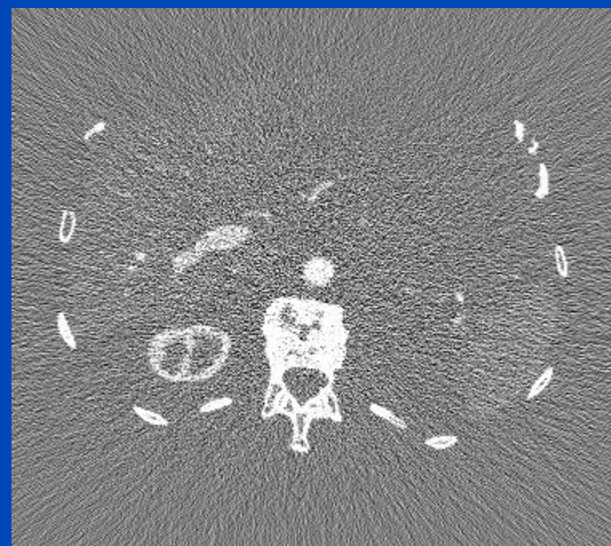

Photon Counting

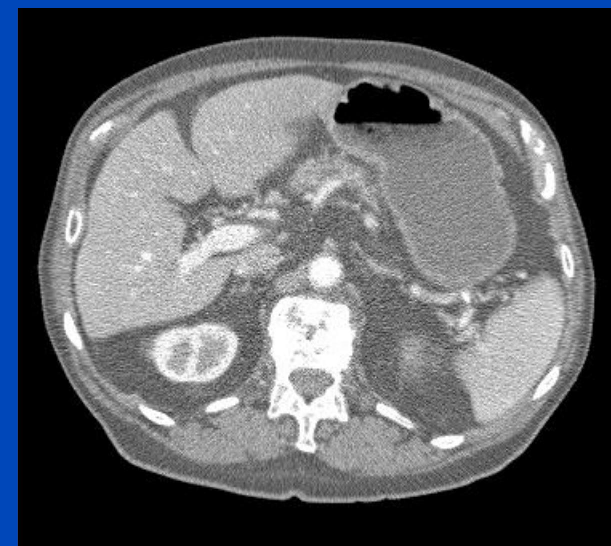

CNR = 4.19

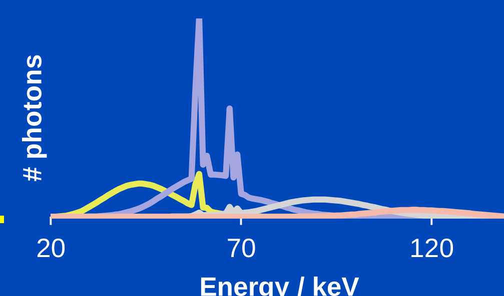

99% CNR improvement or 75% dose reduction achievable due to improved Swank factor and optimized energy weighting.

Images: *C* = 0 HU, *W* = 700 HU, difference image: *C* = 0 HU, *W* = 350 HU, bins start at 20 keV

Material-Selective vs. CNR Optimizing

- f_{LH} = low/high energy or bin image, background at 0 HU
- C_{LH} = contrast in low/high energy or bin image
- V_{LH} = variance in low/high energy or bin image
- **Material-selective image:** $f_\mathrm{L} - f_\mathrm{H}$ (e.g. iodine map)

$$\mathrm{CNR}^2_\mathrm{mat} = \frac{(C_\mathrm{L} - C_\mathrm{H})^2}{V_\mathrm{L} + V_\mathrm{H}}$$

- **Optimum CNR image:** $(1-\alpha) f_\mathrm{L} + \alpha f_\mathrm{H}$

$$\alpha_\mathrm{opt} = \frac{C_\mathrm{H} V_\mathrm{L}}{C_\mathrm{H} V_\mathrm{L} + C_\mathrm{L} V_\mathrm{H}} \qquad \mathrm{CNR}^2_\mathrm{opt} = \frac{C_\mathrm{L}^2}{V_\mathrm{L}} + \frac{C_\mathrm{H}^2}{V_\mathrm{H}}$$

- **Optimum is optimal:**

$$\mathrm{CNR}^2_\mathrm{opt} = \mathrm{CNR}^2_\mathrm{mat} + \frac{(C_\mathrm{L} V_\mathrm{H} + C_\mathrm{H} V_\mathrm{L})^2}{V_\mathrm{L} V_\mathrm{H} (V_\mathrm{L} + V_\mathrm{H})}$$

Iodine CNRD Assessment

- Images are acquired at different tube voltages:
  - 80 kV at 4.40 mGy ($CTDI_{vol\ 32\ cm}$) using 200 mAs_{eff}
  - 100 kV at 9.20 mGy ($CTDI_{vol\ 32\ cm}$) using 200 mAs_{eff}
  - 120 kV at 15.03 mGy ($CTDI_{vol\ 32\ cm}$) using 200 mAs_{eff}
  - 140 kV at 21.76 mGy ($CTDI_{vol\ 32\ cm}$) using 200 mAs_{eff}
- Pitch in all acquisitions was 0.6.
- Collimation for EI (32×0.6 mm) and PC (32×0.5 mm) was matched as close as possible, i.e. geometric efficiency is 80% vs. 82%
- Reconstruction is performed with matched spatial resolution using a D40f kernel onto a grid with a voxel spacing of 0.54 mm and a slice thickness of 1.2 mm.
- The thresholds were fixed at 20 keV and 50 keV, resulting in two bins: [20 keV, 50 keV] and [50 keV, *eU*].

Iodine CNRD Assessment

Reconstruction Examples @ 80 kV

Small (200 × 300 mm)

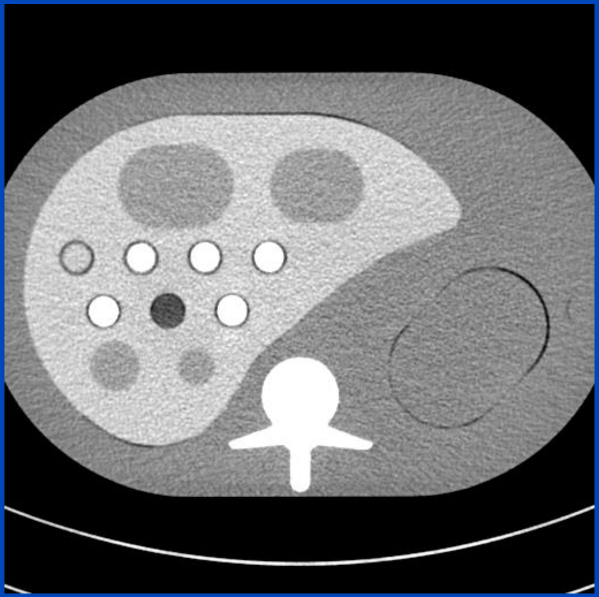

Medium (250 × 350 mm)

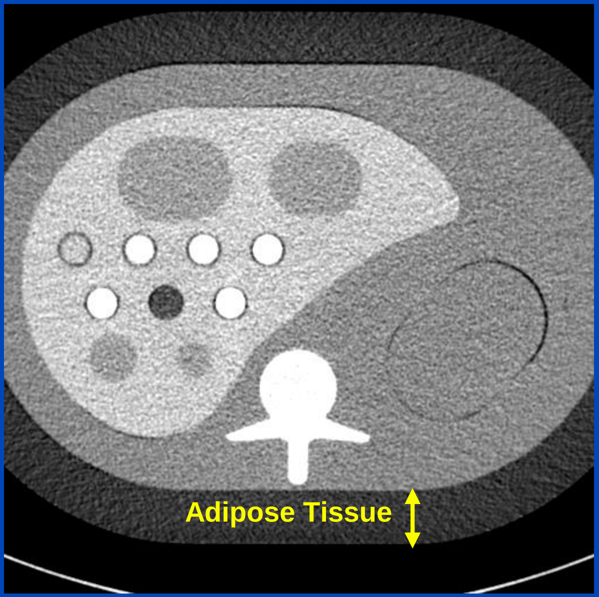

Large (300 × 400 mm)

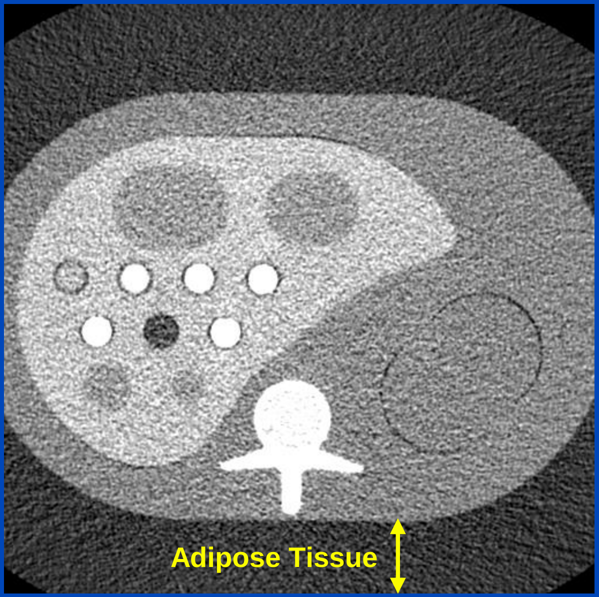

C/W=0 HU/400HU

Iodine CNRD Assessment

Regions of Interest

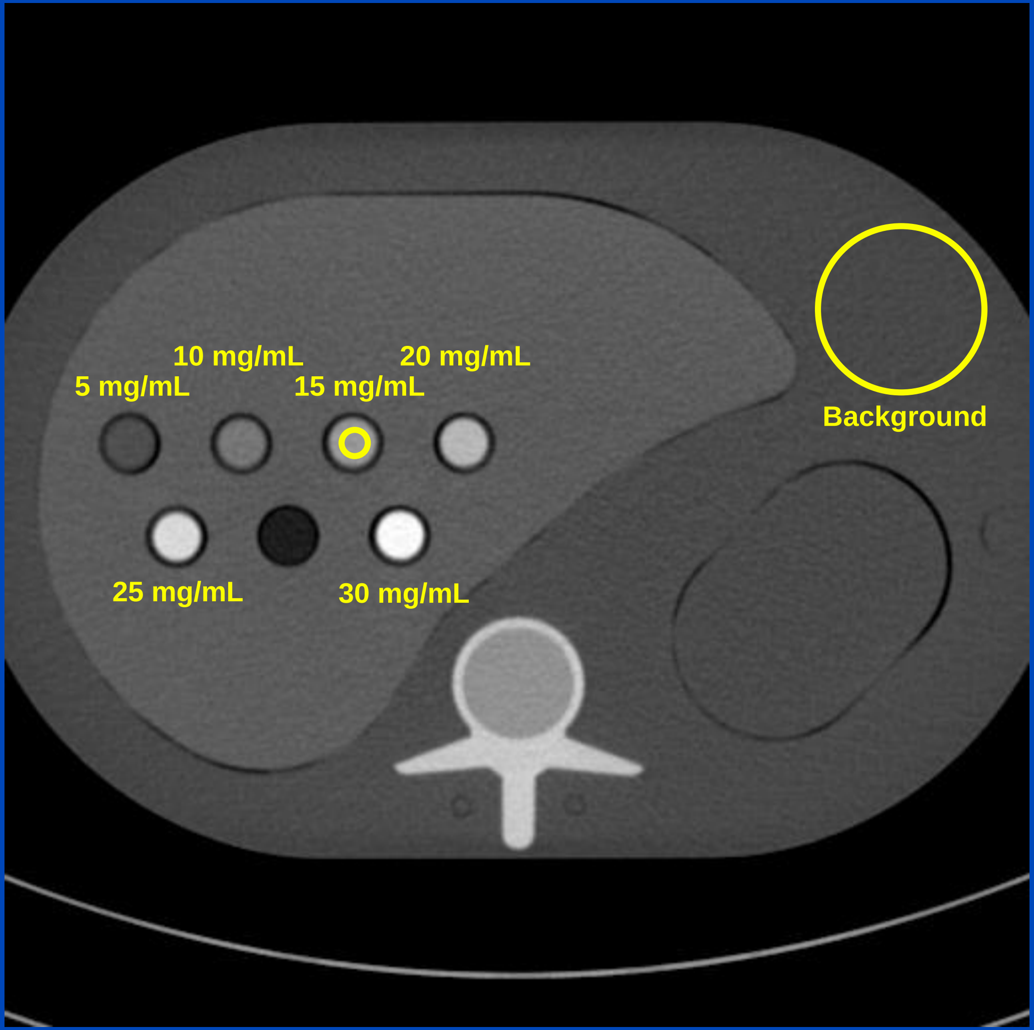

C/W=180 HU/600HU

Results

CNRD – Small Phantom

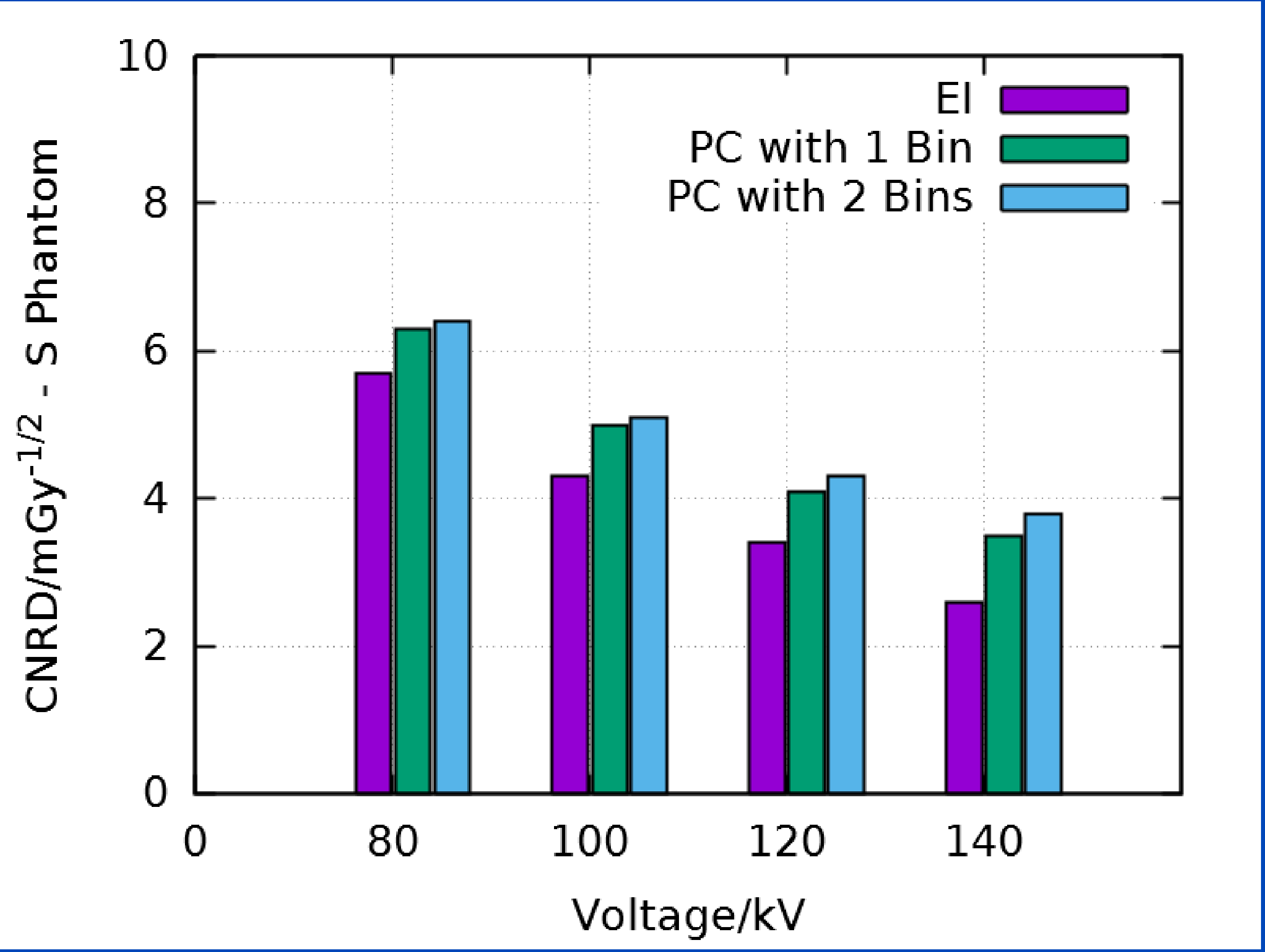

Results

CNRD – Medium Phantom

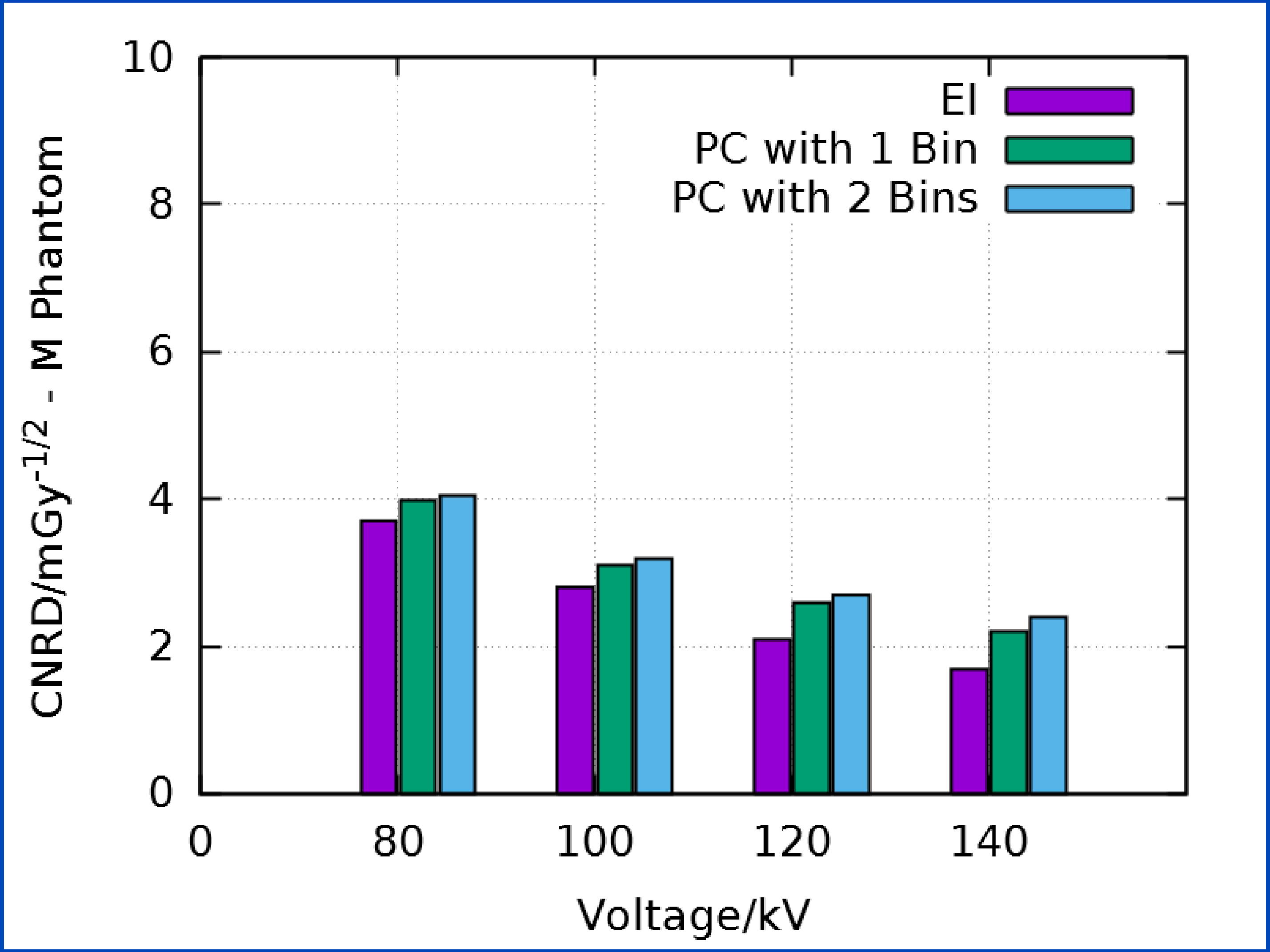

Results

CNRD – Large Phantom

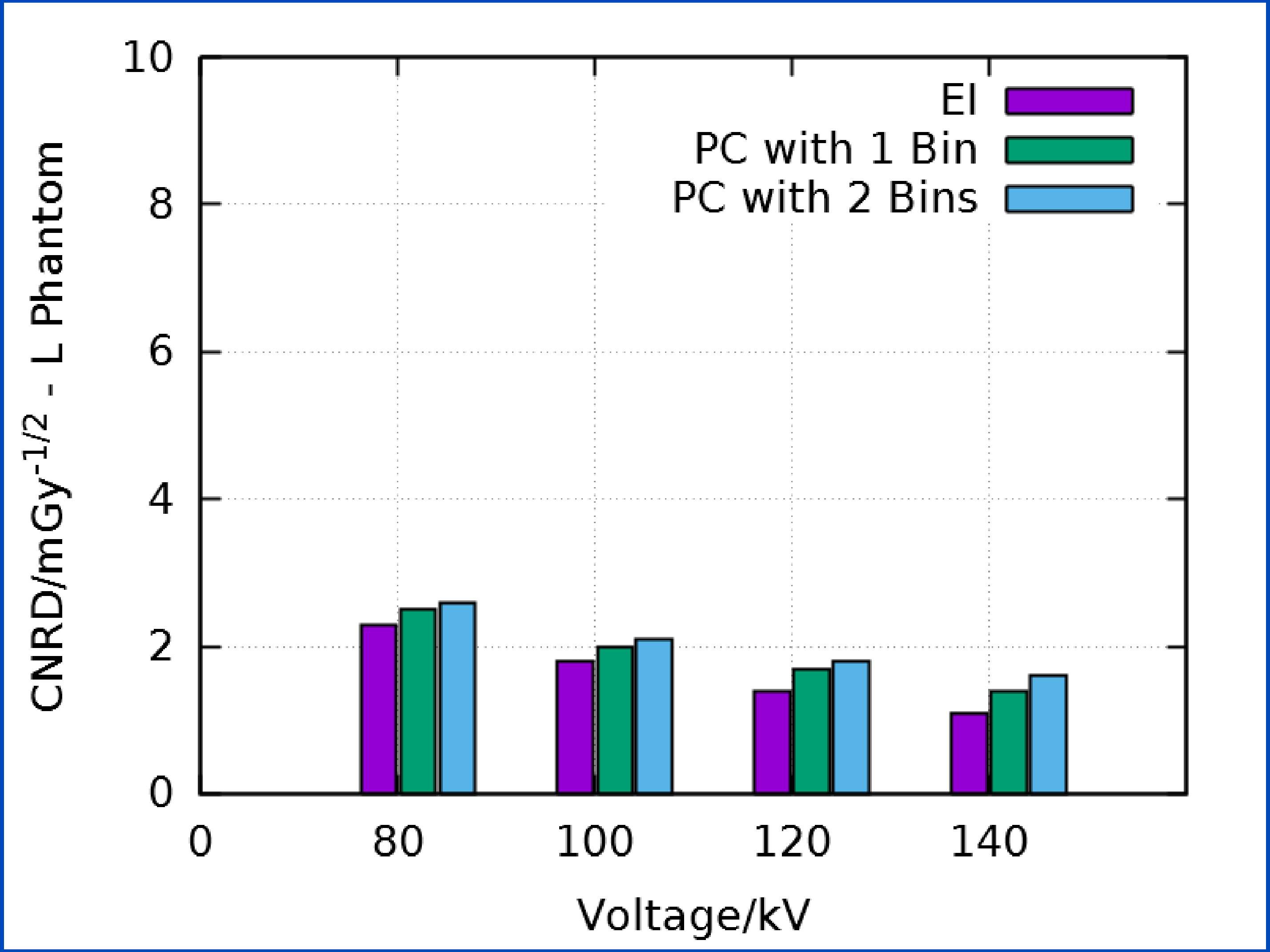

PC with 1 Bin vs. EI

Potential Dose Reduction

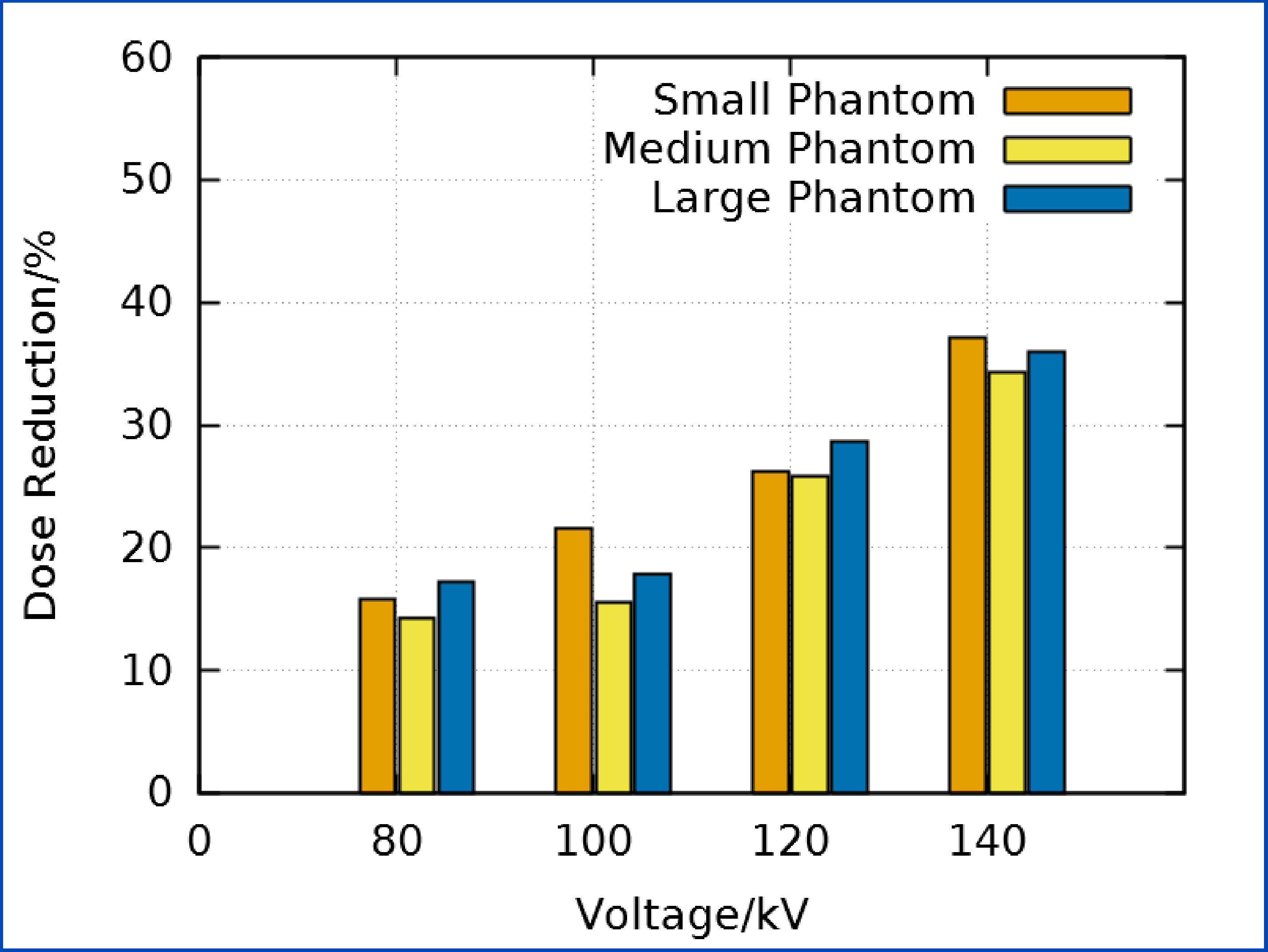

PC with 2 Bins vs. EI

Potential Dose Reduction

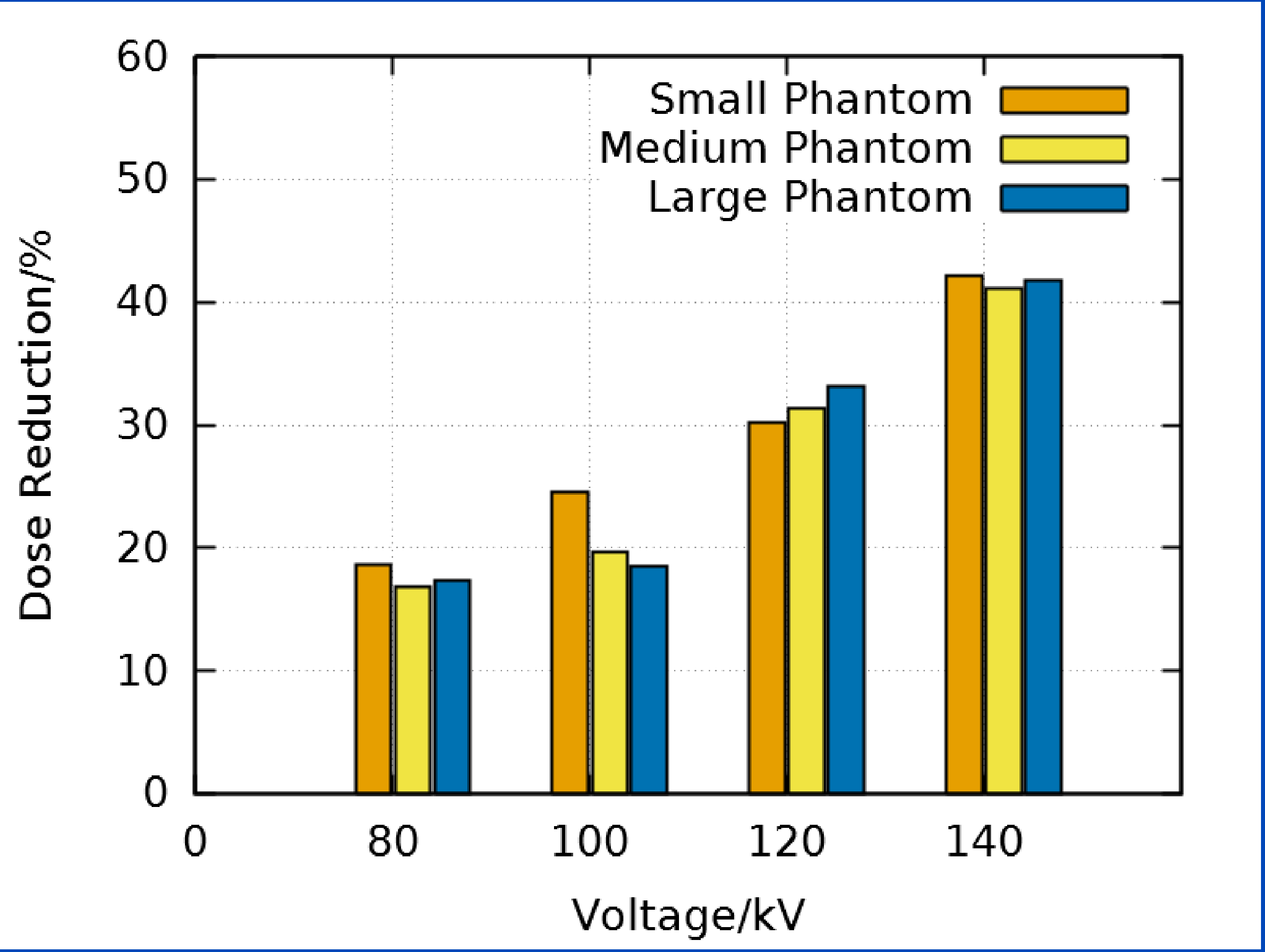

Spatial Resolution

- Small electrodes are necessary to avoid pile-up.
- High bias voltages (around 300 V) limit charge diffusion and thus blurring in the non-structured semiconductor layer.
- Thus, higher spatial resolution is achievable.

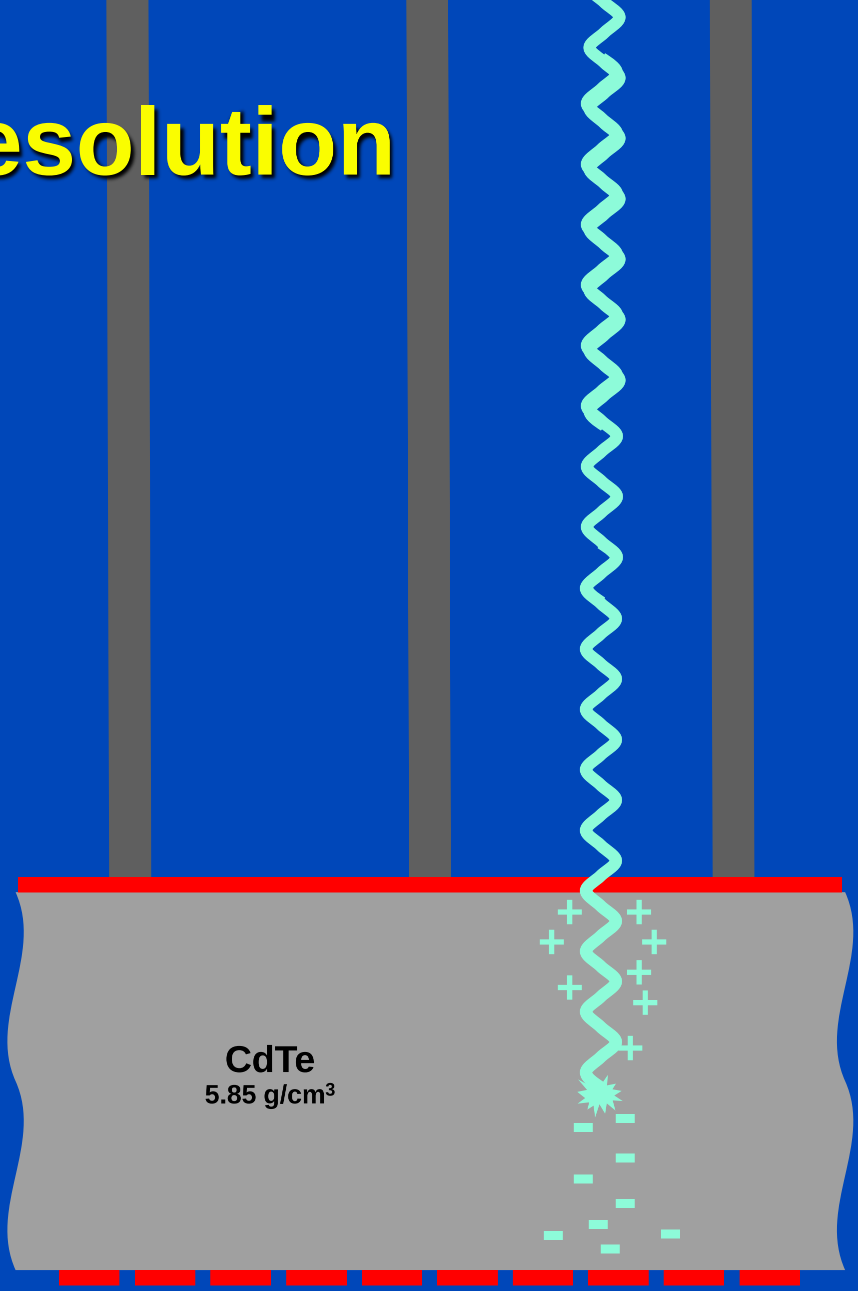

Ultra-High Resolution on Demand

Energy Integrating CT
(Somatom Flash)

Photon Counting CT
(Somatom CounT in UHR-Mode)

MAYO
CLINIC

Courtesy of Cynthia McCollough, Mayo Clinic, Rochester, USA.

CounT Detector Pixel Size EI vs. PC

EI
0.6 mm pixel size

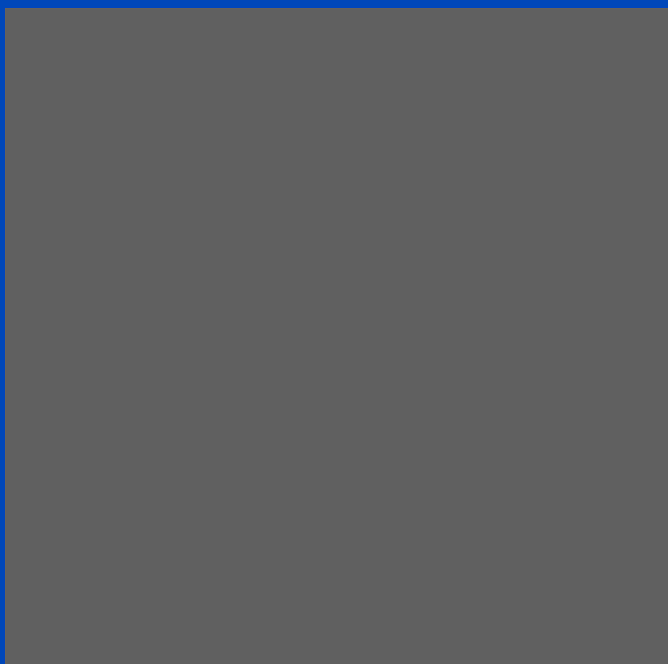

PC Macro or Chess Mode
0.5 mm pixel size

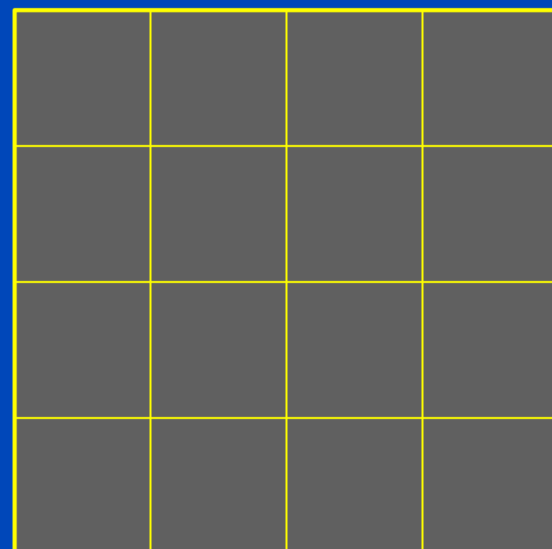

PC UHR Mode
0.25 mm pixel size

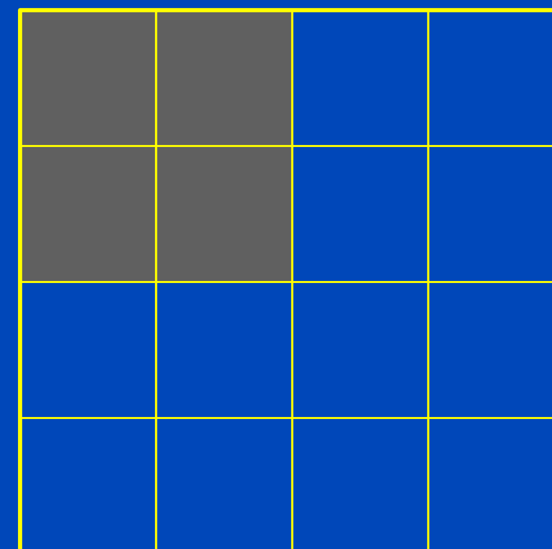

PC-UHR
B70f
512×512
0.54 mm pixels
1.00 mm slices

PC-UHR
U70f
1024×1024
0.27 mm pixels
1.00 mm slices

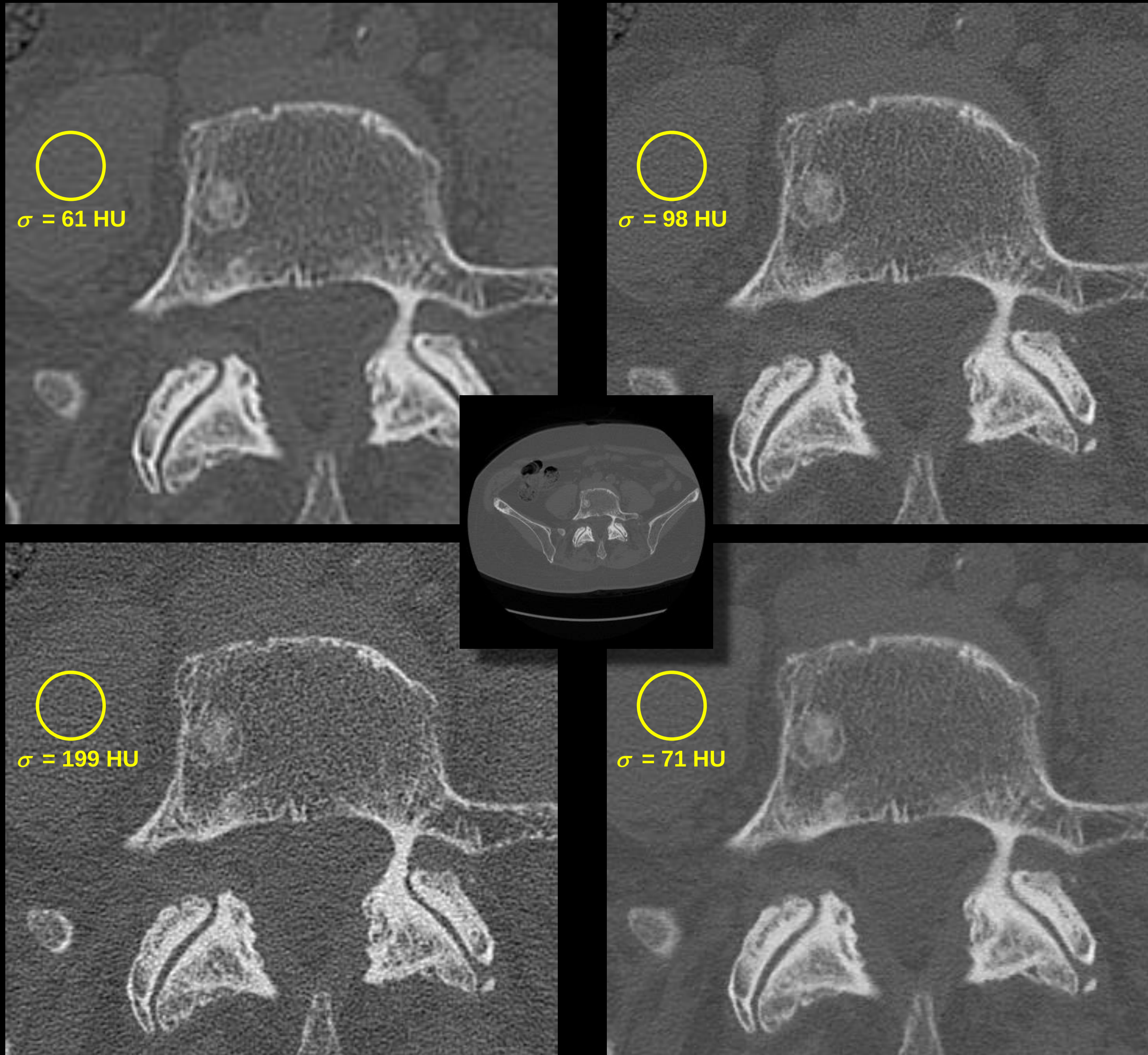

PC-UHR
U70f
1024×1024
0.27 mm pixels
0.25 mm slices

PC-UHR
V70f strength 3
1024×1024
0.27 mm pixels
0.25 mm slices

Osteoblastic bone metastasis in a patient with breast cancer. $\mathrm{CTDI_{vol}}$ = 24.17 mGy, C = 500 HU, W = 3000 HU
Images courtesy of the Division of Radiology of the German Cancer Research Center (DKFZ)

System Model

- Object *f*(*x*)
- Presampling function *s*(*x*), normalized to unit area
- Algorithm *a*(*x*), normalized to unit area
- Image *g*(*x*) with

$$g(x) = f(x) * s(x) * a(x) = f(x) * \mathrm{PSF}(x)$$

- Example:

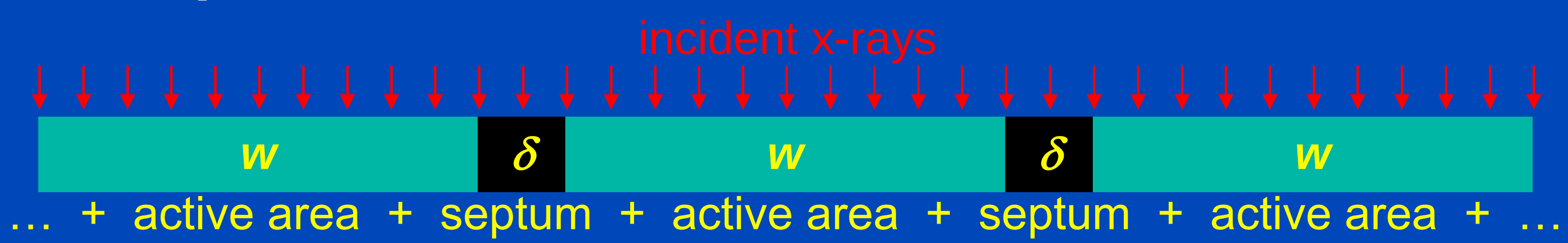

$$s(x) = \mathrm{II}_d^*(x)$$

w = detector pixel width
δ = dead space between pixels

Kachelrieß, Kalender. Med. Phys. 32(5):1321-1334, May 2005

To Bin or not to Bin?
(the continuous view)

This nice phrase was coined by Norbert Pelc.

- We have $\mathrm{PSF}(x) = s(x) * a(x)$ and $\mathrm{MTF}(u) = S(u)A(u)$.
- From Rayleigh‘s theorem we find noise is

$$\sigma^2 = \int dx\, a^2(x) = \int du\, A^2(u) = \int du\, \frac{\mathrm{MTF}^2(u)}{S^2(u)}$$

- Compare Small (A) with la[illegible] pixels:

Avoid binning, if possible!

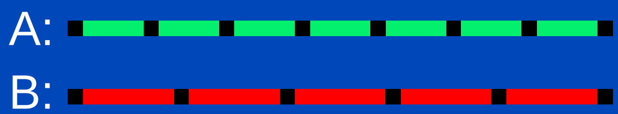

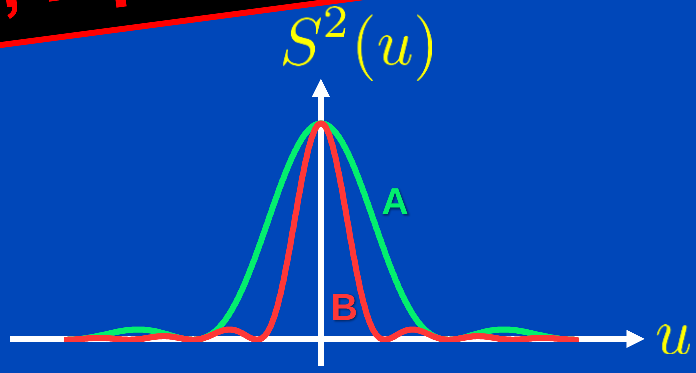

- We have $S_\mathrm{A}(u) > S_\mathrm{B}(u)$ and thus $\sigma_\mathrm{A}^2 < \sigma_\mathrm{B}^2$.
- This means that a desired PSF/MTF is often best achieved with smaller detectors.

Kachelrieß, Kalender. Med. Phys. 32(5):1321-1334, May 2005
Baek, Pineda, and Pelc. PMB 58:1433-1446, 2013

The “Small Pixel Effect”

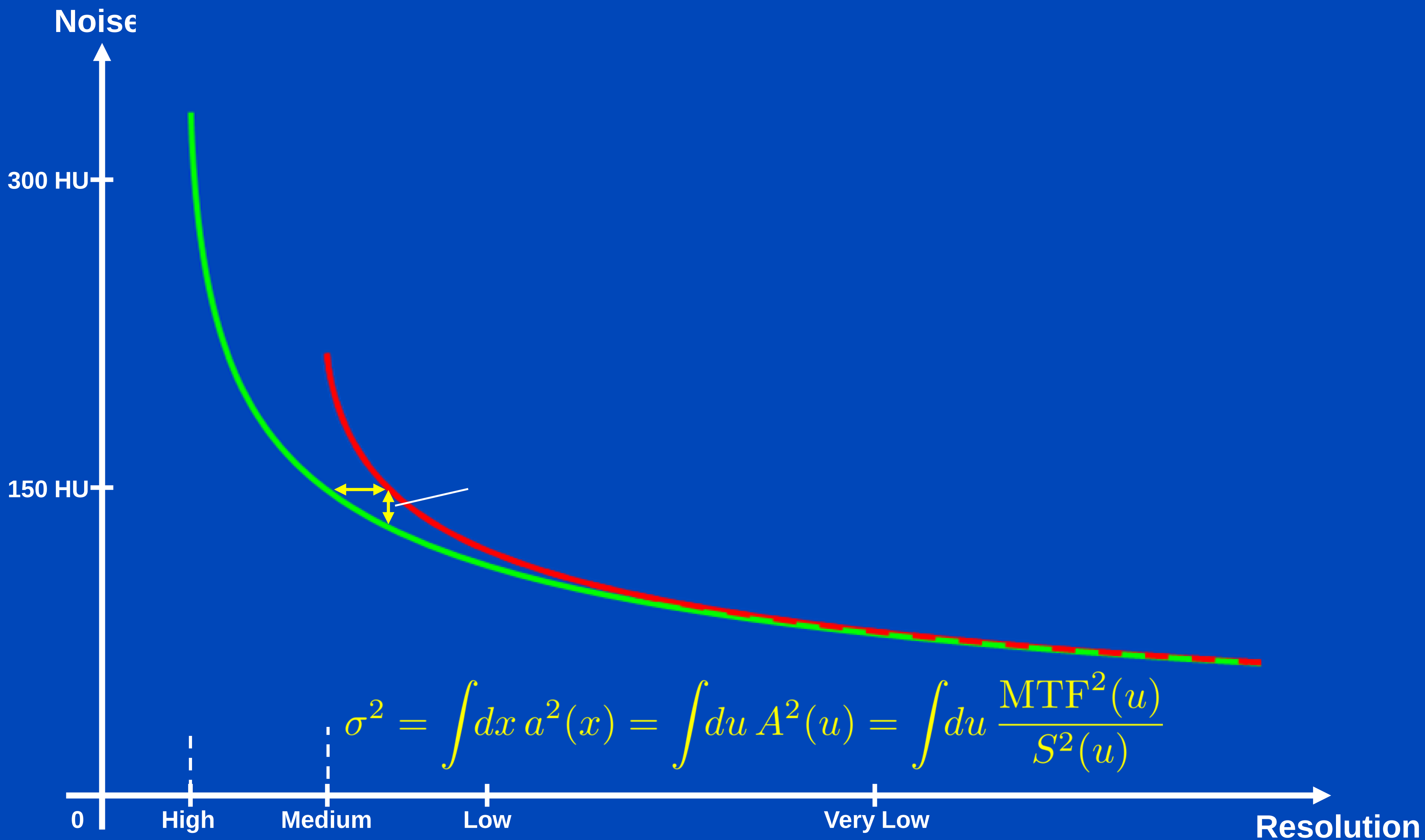

$$\sigma^2 = \int dx\, a^2(x) = \int du\, A^2(u) = \int du\, \frac{\mathrm{MTF}^2(u)}{S^2(u)}$$

Questions?

To Bin or not to Bin?
(the discrete view, LI)

- Let detector B be the 2-binned version of detector A:

$$B_{2n} = \tfrac{1}{2}(A_{2n} + A_{2n+1}) \qquad \mathrm{Var}B = \tfrac{1}{2}\mathrm{Var}A$$

- Assume LI to be used to find in-between pixel values. Wlog we may then consider B to be upsampled with mid-point interpolati… …r A:

$$\hat{B} \ldots \ldots)$$

- To o… …etector we n…

$$a = \tfrac{1}{2}\left(1,\ 1\right) * \tfrac{1}{4}\left(1,\ 2,\ 1\right) = \tfrac{1}{8}\left(1,\ 3,\ 3,\ 1\right)$$

- Noise propagation yields 20% more noise (variance) for the binned detector:

$$\mathrm{Var}\hat{A} = \tfrac{20}{64}\mathrm{Var}A = \tfrac{5}{16}\mathrm{Var}A$$

$$\mathrm{Var}\hat{B} = \tfrac{3}{8}\mathrm{Var}A = \tfrac{6}{5}\mathrm{Var}\hat{A} = 1.2\,\mathrm{Var}\hat{A}$$

20% more noise variance may be compensated by 20% more x-ray dose. Any alternative? Yes:

Avoid binning, if possible!

In 2D binning implies 44% more noise variance or dose. Again, the answer is: „not to bin“.

To Bin or not to Bin?
(the discrete view, NN)

- **Let detector B be the 2-binned version of detector A:**

$$B_{2n} = \tfrac{1}{2}(A_{2n} + A_{2n+1}) \qquad \mathrm{Var}B = \tfrac{1}{2}\mathrm{Var}A$$

- **Let us now do an upsampling of the detector B such that each of B´s pixels becomes two pixels with the same value and with the pixel size of detector A:**

$$\hat{\boldsymbol{B}} = \left(\ldots,\ B_2,\ B_2,\ B_4,\ B_4,\ B_6,\ B_6,\ \ldots\right)$$

- **To obtain the same PSF/MTF with the unbinned detector we need to convolve A with**

$$\boldsymbol{a} = \tfrac{1}{4}\left(1,\ 2,\ 1\right)$$

- **Noise propagation yields 30% more noise (variance) for the binned detector:**

$$\mathrm{Var}\hat{A} = \tfrac{6}{16}\mathrm{Var}A = \tfrac{3}{8}\mathrm{Var}A$$

$$\mathrm{Var}\hat{B} = \tfrac{1}{2}\mathrm{Var}A = \tfrac{4}{3}\mathrm{Var}\hat{A} = 1.3\,\mathrm{Var}\hat{A}$$

CounT Std | CounT HighRes

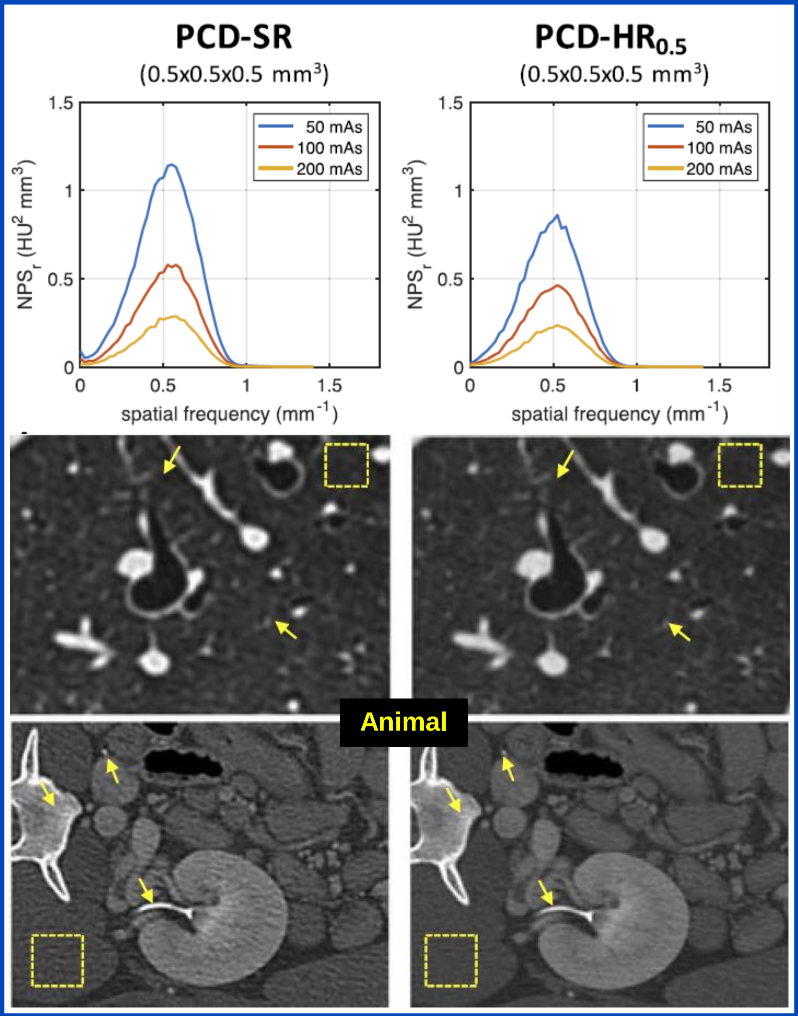

"However, when comparing with standard resolution data at same in-plane resolution and slice thickness, the PCD 0.25 mm detector mode showed **19% less image noise** in phantom, animal, and human scans."

CounT Std | CounT HighRes

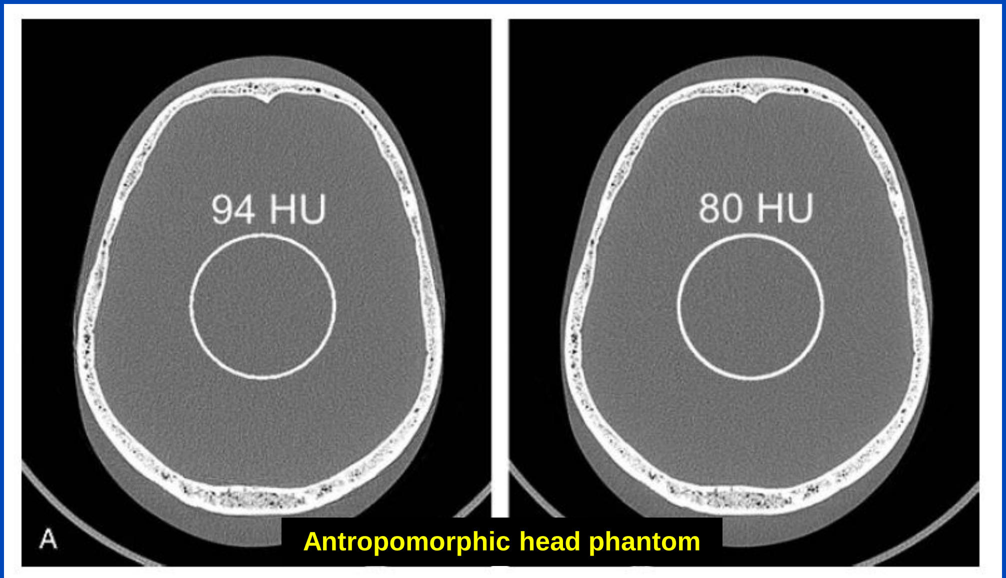

A **15% noise reduction** (from 94 HU to 80 HU) was observed (same spatial resolution and dose). This corresponds to a dose reduction of 28%.

Pourmorteza et al. Dose Efficiency of Quarter-Millimeter Photon-Counting Computed Tomography: First-in-Human Results. Invest. Radiol. 53(6), 2018.

Leng et al. 150 µm Spatial Resolution Using Photon-Counting Detector Computed Tomography Technology. Invest. Radiol. 53(11), 2018

All images reconstructed with 1024^2 matrix and 0.15 mm slice increment.
C = 1000 HU
W = 3500 HU

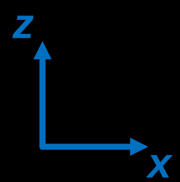

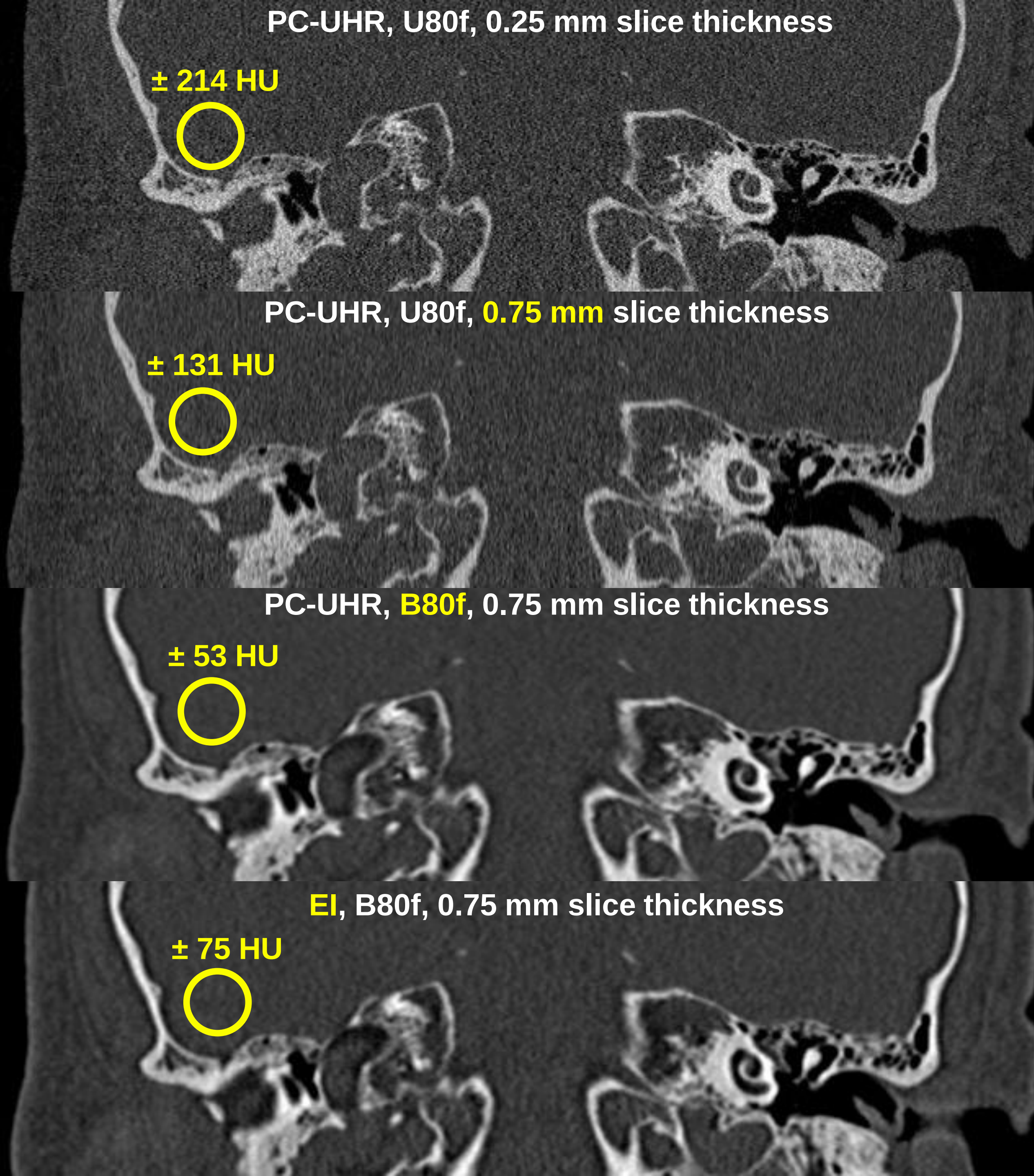

10% MTF: 19.1 lp/cm
10% MTF:17.2 lp/cm
xy FWHM: 0.48 mm
z FWHM: 0.40 mm
$CTDI_{vol}$: 16.0 mGy

10% MTF: 19.1 lp/cm
10% MTF:17.2 lp/cm
xy FWHM: 0.48 mm
z FWHM: 0.67 mm
$CTDI_{vol}$: 16.0 mGy

10% MTF: 9.3 lp/cm
10% MTF:10.5 lp/cm
xy FWHM: 0.71 mm
z FWHM: 0.67 mm
$CTDI_{vol}$: 16.0 mGy

10% MTF: 9.3 lp/cm
10% MTF:10.5 lp/cm
xy FWHM: 0.71 mm
z FWHM: 0.67 mm
$CTDI_{vol}$: 16.0 mGy

Data courtesy of the Institute of Forensic Medicine of the University of Heidelberg and of the Division of Radiology of the German Cancer Research Center (DKFZ)

dkfz.

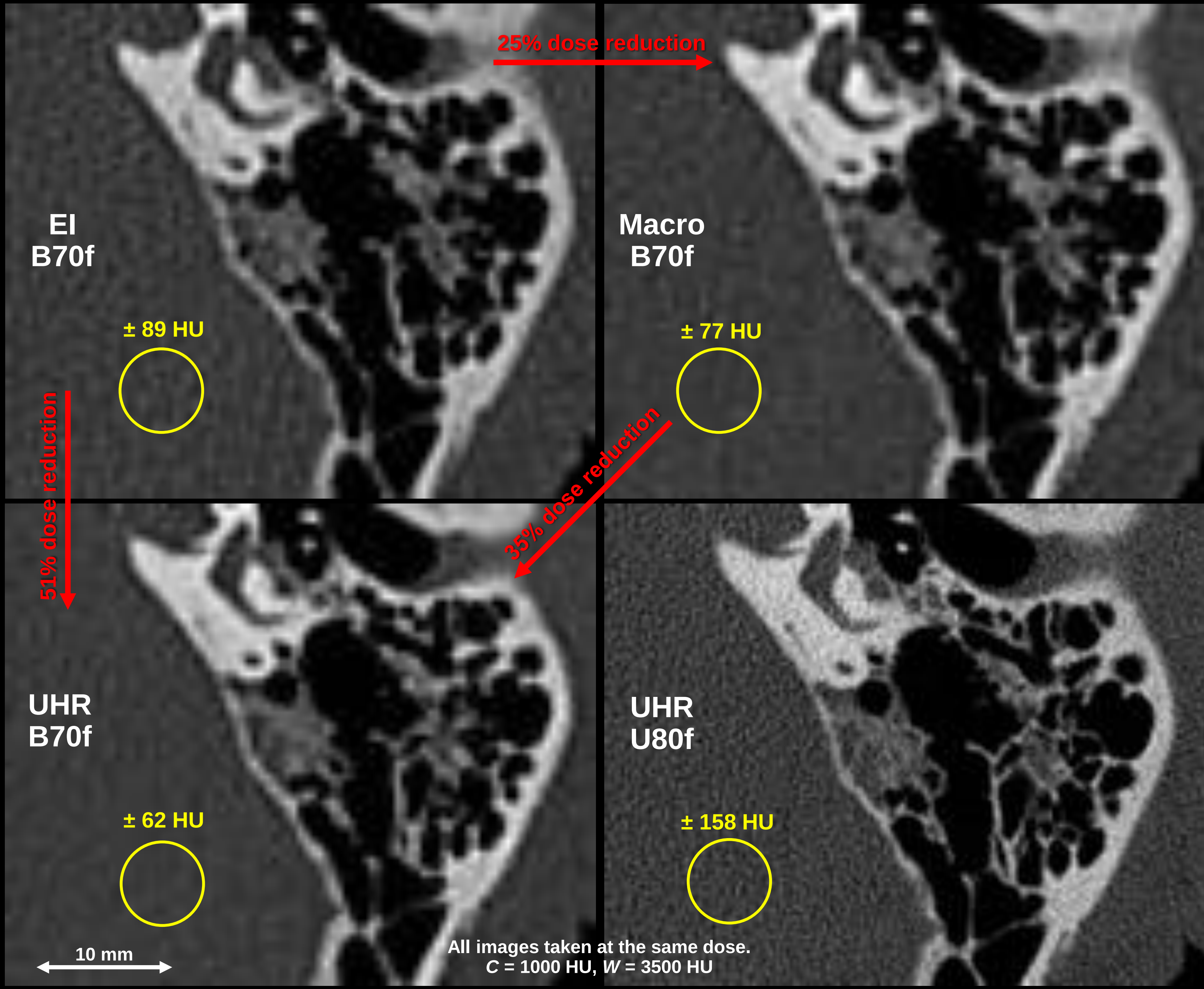

25% dose reduction
EI B70f
± 89 HU
Macro B70f
± 77 HU
51% dose reduction
35% dose reduction
UHR B70f
± 62 HU
UHR U80f
± 158 HU
10 mm
All images taken at the same dose.
C = 1000 HU, W = 3500 HU

Acquisitions at same noise

EI, B70f

UHR, B70f

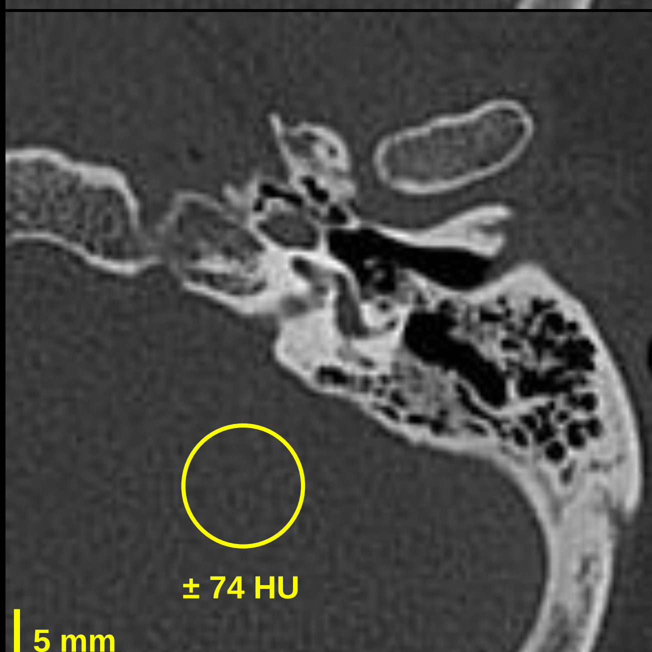

C = 1000 HU
W = 3500 HU

Acquisition with EI:

- **Tube voltage of 120 kV**
- **Tube current of 350 mAs**
- **Resulting dose of $\mathrm{CTDI}_{\mathrm{vol\ 32\ cm}}$ = 26.4 mGy**

Acquisition with UHR:

- **Tube voltage of 120 kV**
- **Tube current of 200 mAs**
- **Resulting dose of $\mathrm{CTDI}_{\mathrm{vol\ 32\ cm}}$ = 16.1 mGy**

This is a 39% reduction of dose!

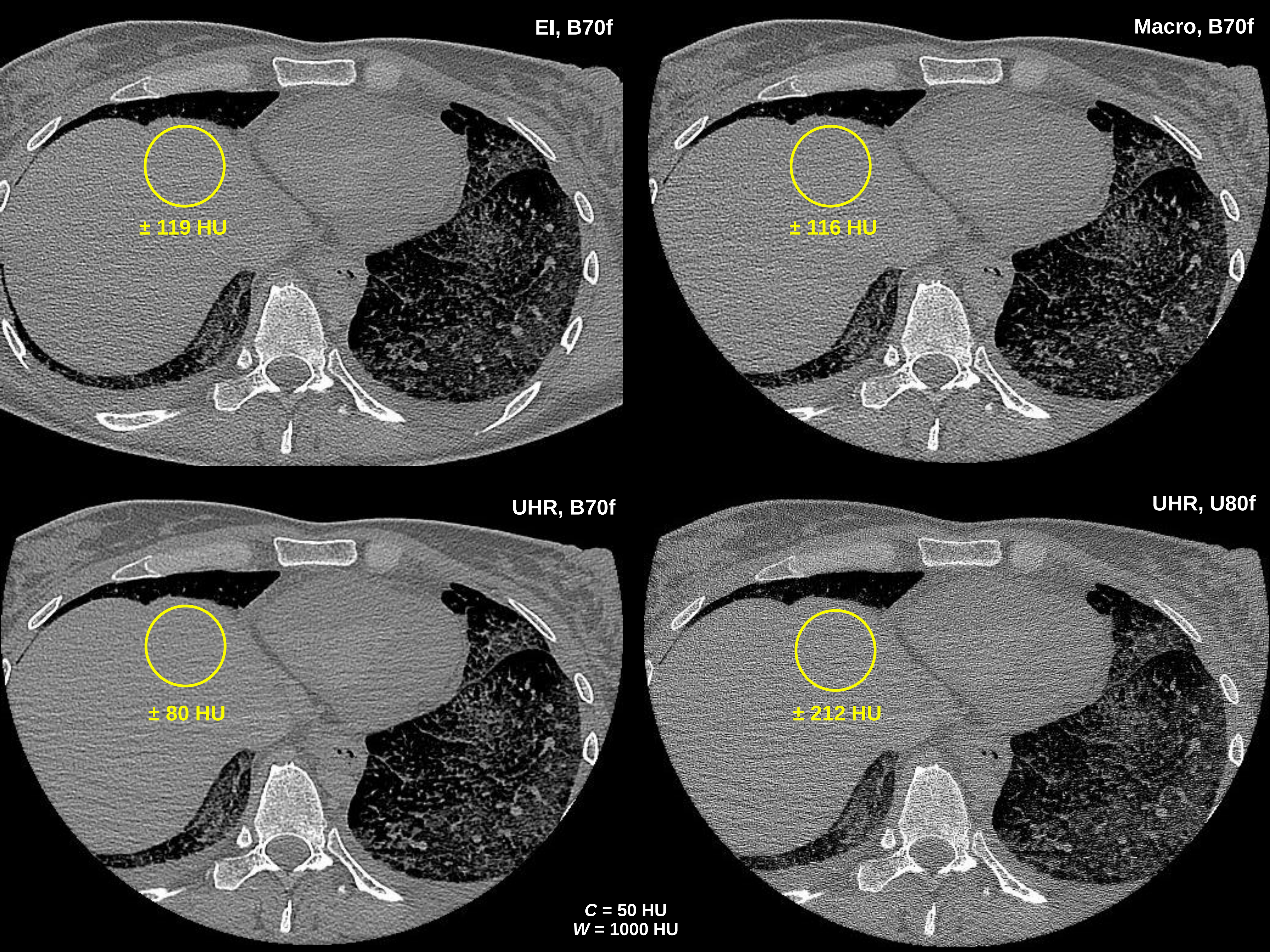
EI, B70f
± 119 HU
Macro, B70f
± 116 HU
UHR, B70f
± 80 HU
UHR, U80f
± 212 HU
C = 50 HU
W = 1000 HU

L. Klein, C. Amato, S. Heinze, M. Uhrig, H.-P. Schlemmer, M. Kachelrieß, and S. Sawall. **Effects of Detector Sampling on Noise Reduction in a Clinical Photon Counting Whole-Body CT**. Investigative Radiology, vol. 55(2):111-119, February 2020.

Energy Integrating Detector (B70f)

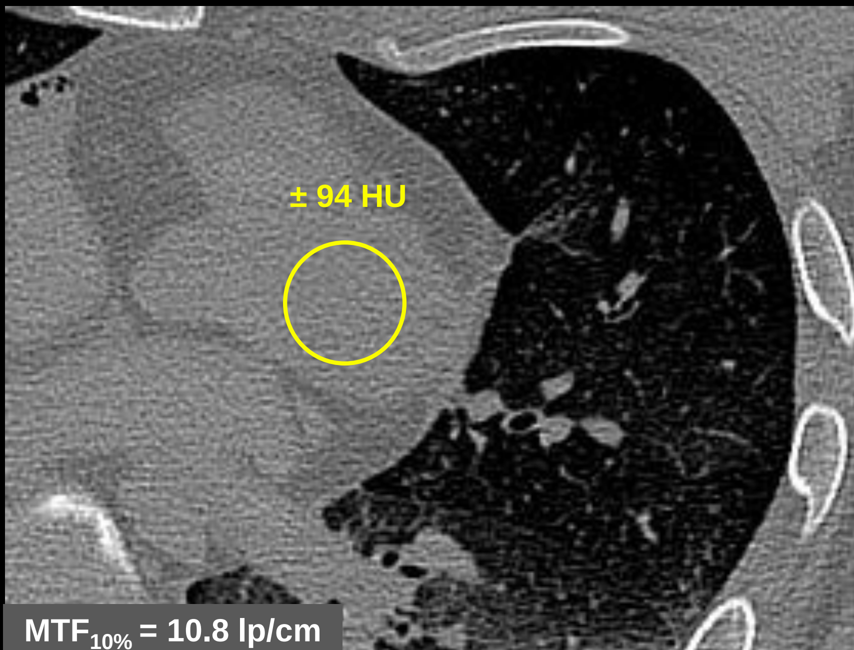

Acquisition with EI:

- Tube voltage of 120 kV
- Tube current of 300 mAs
- Resulting dose of $CTDI_{vol\ 32\ cm}$ = 22.6 mGy

Photon Counting Detector (B70f)

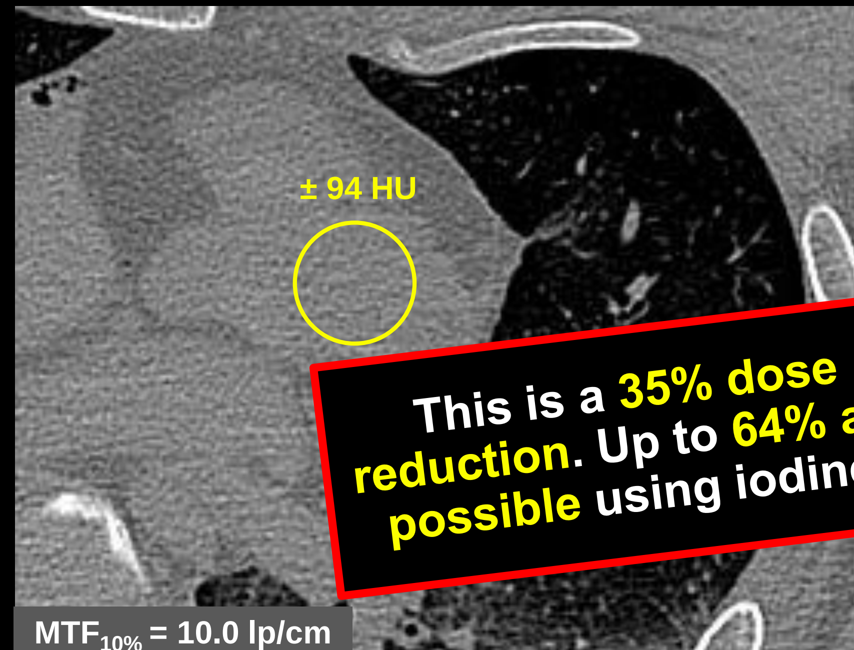

This is a 35% dose reduction. Up to 64% are possible using iodine.

Acquisition with UHR:

- Tube voltage of 120 kV
- Tube current of 180 mAs
- Resulting dose of $CTDI_{vol\ 32\ cm}$ = 14.6 mGy

C = 50 HU, *W* = 1500 HU

S. Heinze, M. Uhrig, L. Klein, S. Dorn, C. Amato, J. Maier, H.-P. Schlemmer, M. Kachelrieß, S. Sawall, and K. Yen. **Photonenzählende Computertomographie – Mögliche Anwendungen in der forensischen Bildgebung**. 98. Internationale Jahrestagung der Deutschen Gesellschaft für Rechtsmedizin, September 2019.

Energy Integrating Detector (B70f)

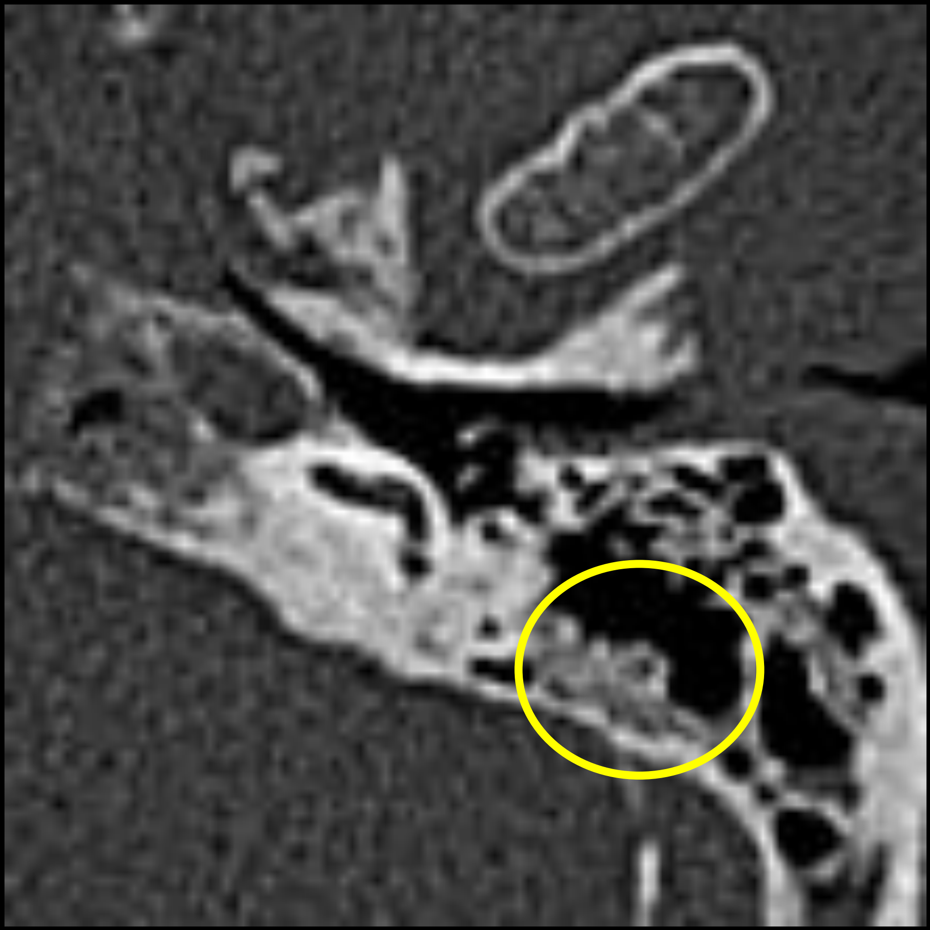

Photon Counting Detector (U80f)

***C* = 500 HU, *W* = 2000 HU**

E. Wehrse, L. Klein, M. Kachelrieß, H.-P. Schlemmer, C. H. Ziener, M. Wennmann, S. Delorme, M. Uhrig, and S. Sawall. **First Experience in Man with an Ultra-High Resolution Whole-Body Photon-Counting CT for Oncologic Imaging**. ECR 2020.

Energy Integrating Detector **Photon Counting Detector**

***C* = 500 HU, *W* = 3000 HU**

X-Ray Dose Reduction of B70f

PC vs. PC
("small pixel effect only")

UHR vs. Macro	80 kV	100 kV	120 kV	140 kV
S	**23%** ± 12%	**34%** ± 10%	**35%** ± 11%	**25%** ± 10%
M	**32%** ± 10%	**32%** ± 8%	**35%** ± 8%	**34%** ± 9%
L	**35%** ± 10%	**29%** ± 15%	**27%** ± 9%	**31%** ± 11%

PC vs. EI
("small pixel effect"
and "iodine effect")

UHR vs. EI	80 kV	100 kV	120 kV	140 kV
S	**33%** ± 9%	**52%** ± 5%	**57%** ± 7%	**57%** ± 6%
M	**41%** ± 8%	**47%** ± 7%	**60%** ± 6%	**62%** ± 4%
L	**48%** ± 8%	**43%** ± 10%	**54%** ± 6%	**63%** ± 5%

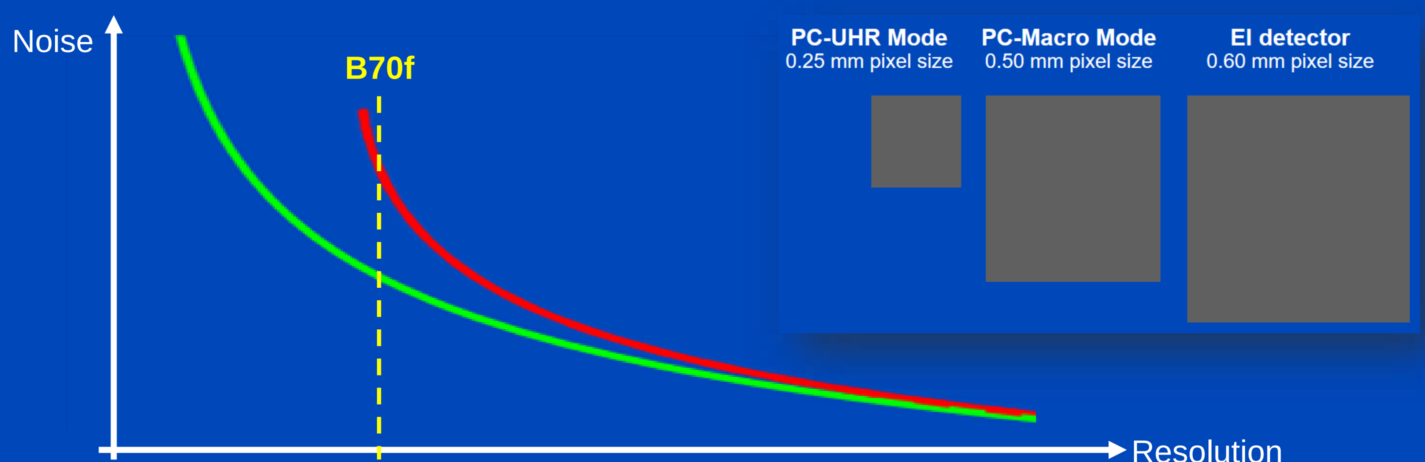

X-Ray Dose Reduction of D40f

PC vs. PC
(“small pixel effect only”)

UHR vs. Macro	80 kV	100 kV	120 kV	140 kV
S	**5%** ± 16%	**12%** ± 17%	**17%** ± 17%	**9%** ± 15%
M	**11%** ± 14%	**9%** ± 12%	**16%** ± 16%	**13%** ± 13%
L	**11%** ± 14%	**6%** ± 17%	**6%** ± 17%	**4%** ± 17%

PC vs. EI
(“small pixel effect” and “iodine effect”)

UHR vs. EI	80 kV	100 kV	120 kV	140 kV
S	**10%** ± 11%	**28%** ± 11%	**36%** ± 12%	**38%** ± 12%
M	**15%** ± 12%	**23%** ± 12%	**40%** ± 10%	**43%** ± 9%
L	**24%** ± 14%	**17%** ± 11%	**33%** ± 12%	**43%** ± 9%

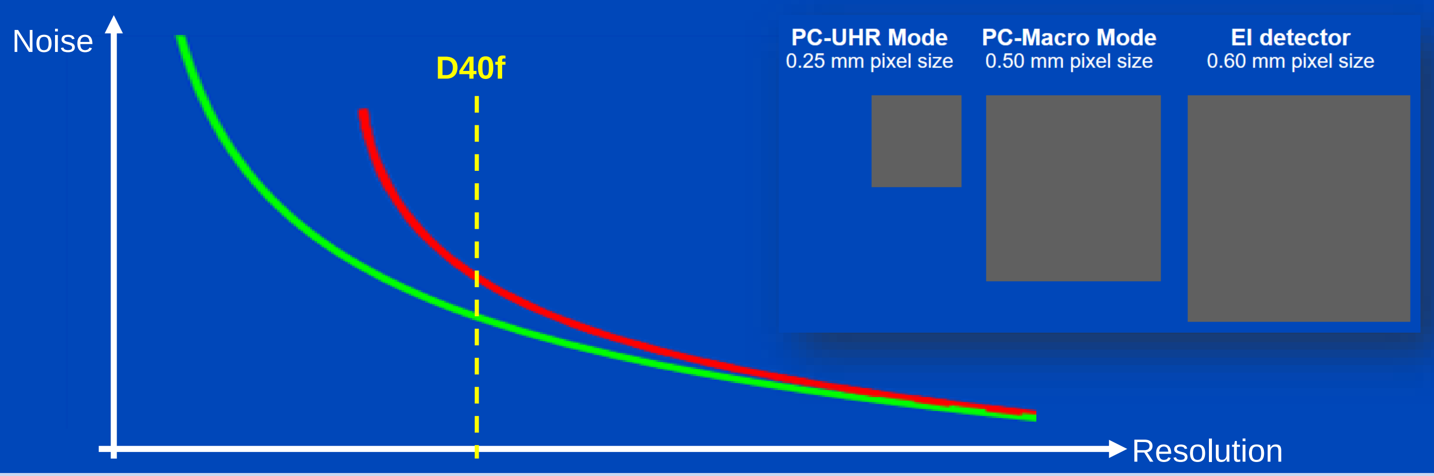

dkfz.

Patient with prostate carcinoma

EI CT (University Hospital Heidelberg)

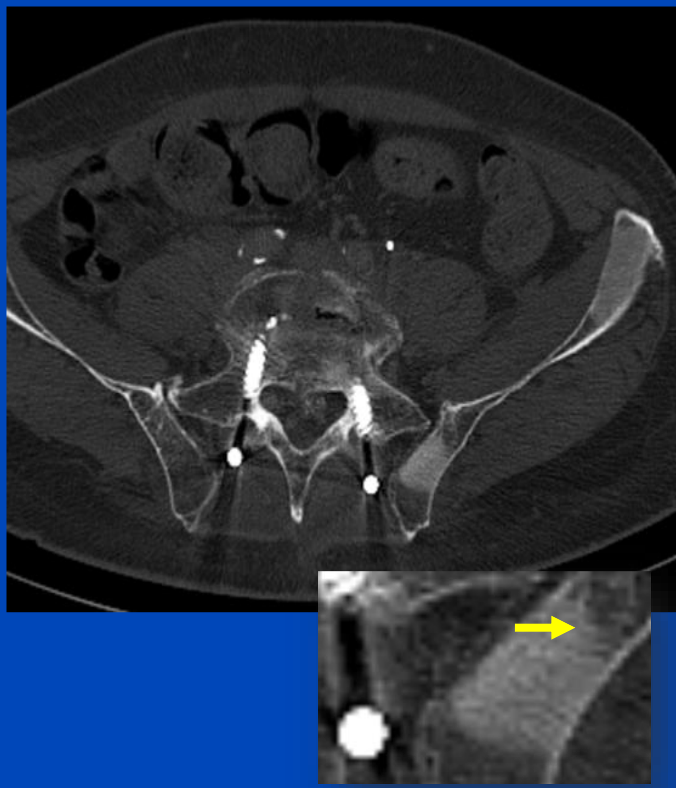

PC CT (DKFZ)

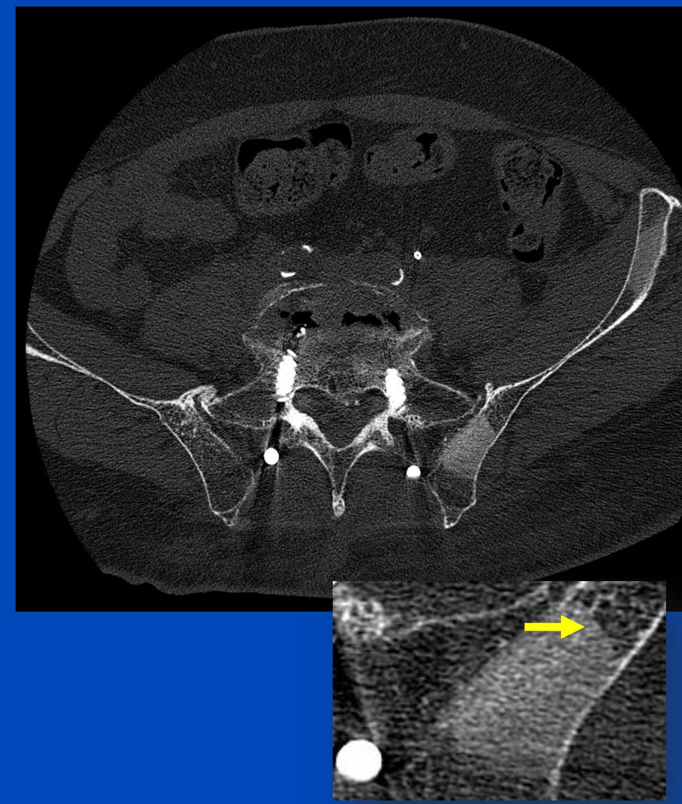

59 years old patient with osteoblastic metastases of prostate cancer in the left iliac bone.

EI CT: Progress was diagnosed due to suspicious morphology (infiltration of bone marrow?) of these metastases.

PC CT: Metastases show clear margins → non-active sclerotic lesions.

MR (not shown): Image quality is severely affected by metal and motion artifacts.

More than Dual Energy?

- Ways to remove the spectral overlap?
- Lower noise, less dose?
- Improve contrast-to-noise ratio at unit dose?
- Distinguish more than three materials?

$$\mu(E) = \cancel{\eta(E)} + \tau(E) + \sigma(E) + \cancel{\kappa(E)}$$

Rayleigh Photo Compton Pair

$$\tau(E) \propto \rho \frac{Z^3}{E^3}$$

$$\sigma(E) \propto \rho \frac{Z}{A} f(E)$$

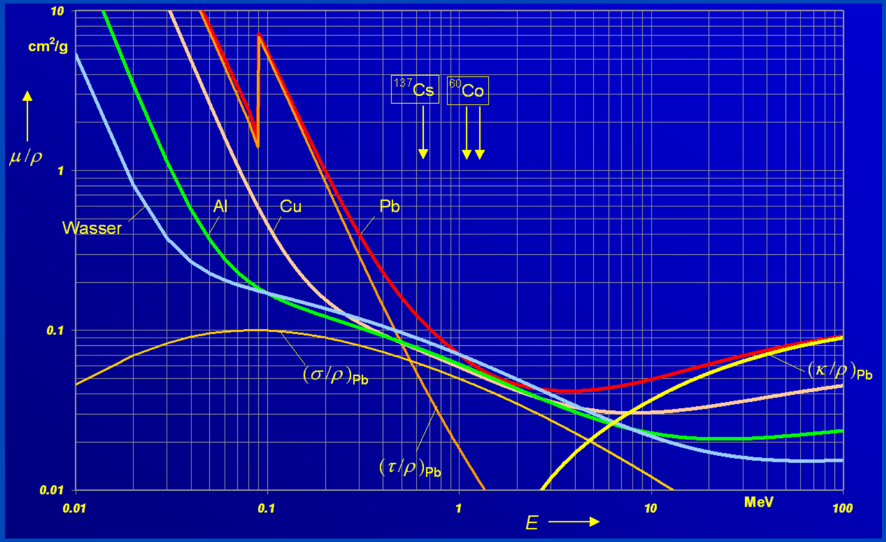

K-Edges: More than Dual Energy CT?

$$\mu(\boldsymbol{r}, E) = f_1(\boldsymbol{r})\psi_1(E) + f_2(\boldsymbol{r})\psi_2(E) + \cancel{f_3(\boldsymbol{r})\psi_3(E)} + \dots$$

Apart from special applications, e.g.
Iodine k-edge imaging of the breast

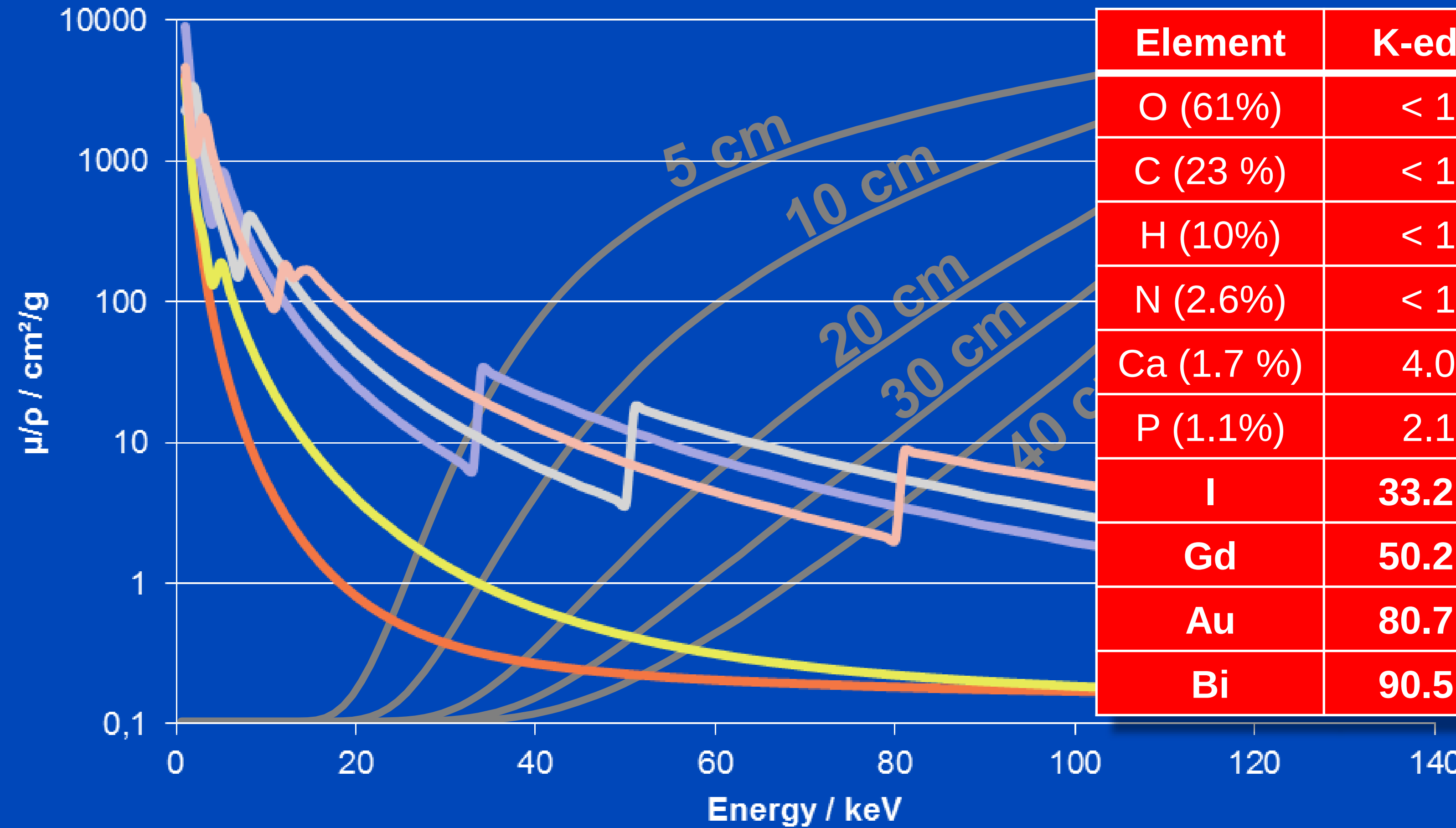

Element	K-edge
O (61%)	< 1 keV
C (23 %)	< 1 keV
H (10%)	< 1 keV
N (2.6%)	< 1 keV
Ca (1.7 %)	4.0 keV
P (1.1%)	2.1 keV
I	**33.2 keV**
Gd	**50.2 keV**
Au	**80.7 keV**
Bi	**90.5 keV**

Gray curves: 120 kV water transmission on a non-logarithmic ordinate individually normalized to 1 at 140 keV.

MECT

Ca-Gd-I Decomposition

Chess pattern mode
140 kV, 20/35/50/65 keV
C = 0 HU, W = 1200 HU

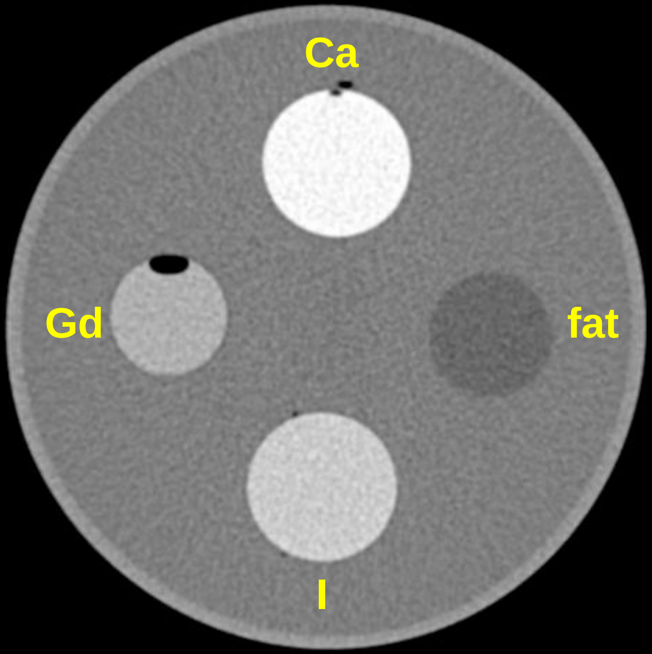

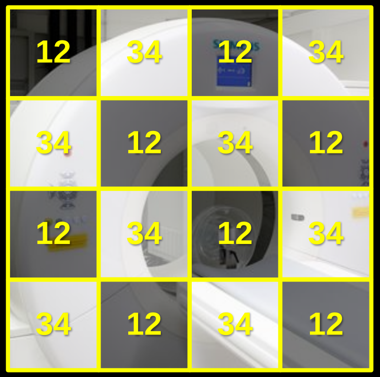

Calcium image

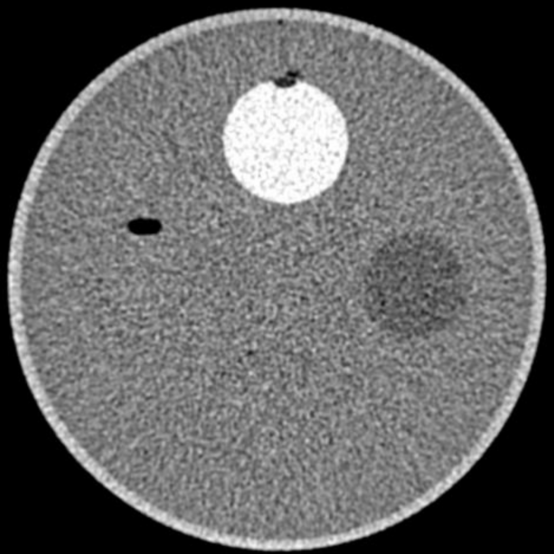

Gadolinium image

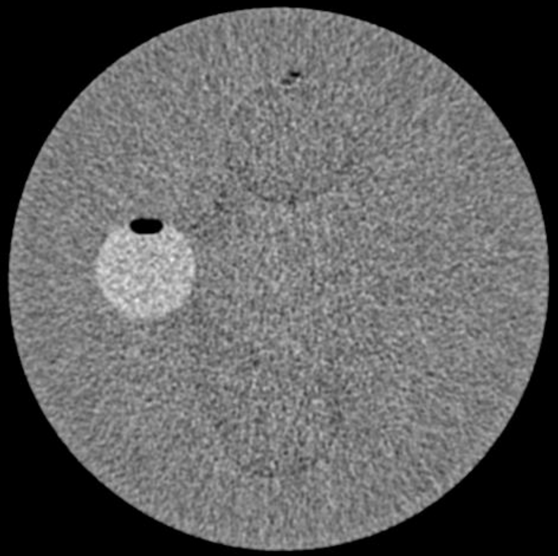

Iodine image

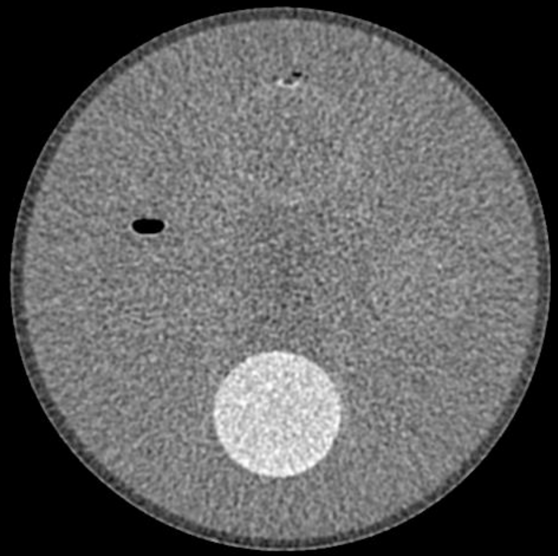

Courtesy of Siemens Healthcare

MIP of low threshold images (20 keV)

Coronal Sagittal

Scan 1

Scan 2

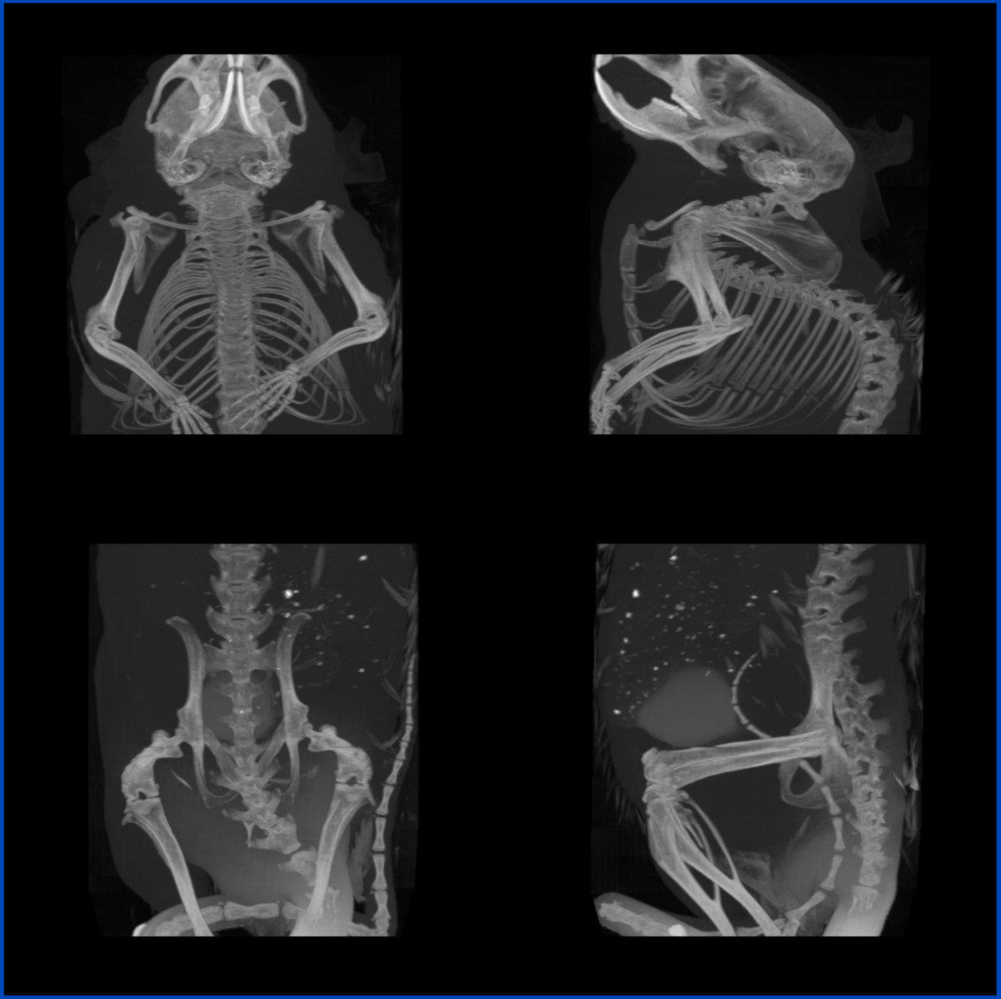

Scan at 60 kV of the late phase of iodine based contrast agent (iodine in the bladder). Part of the contrast agent was injected outside of the vessel (enhancement in the tail).

MIP of iodine and bone

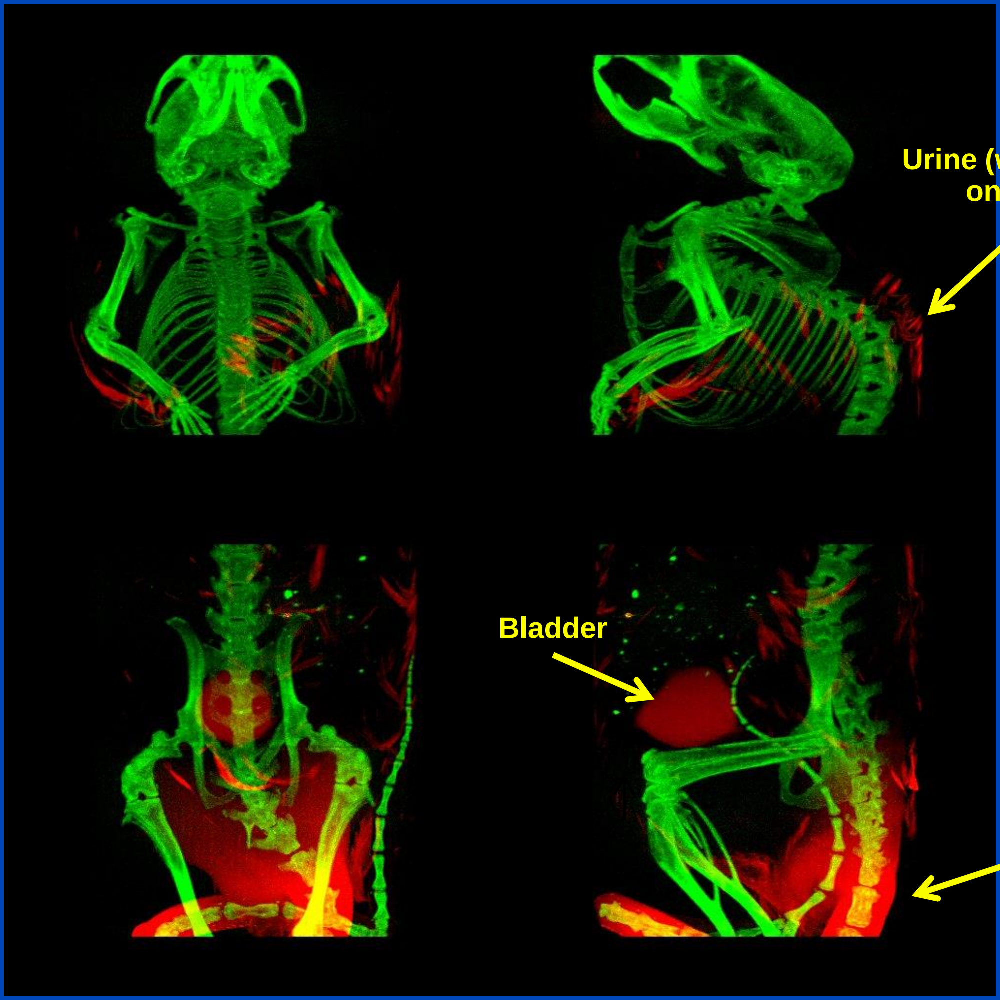

Energy thresholds at 20 and 32 keV.
Iodine k-edge at 33 keV.

Possibility to unambiguously differentiate iodine and bone.

Potential Advantages of PCCT

- Everything retrospectively on demand
  - Spatial resolution
  - Spectral information
  - Virtual tube voltage setting
- Higher spatial resolution due to
  - smaller pixels
  - lower cross-talk between pixels
- Lower dose/noise due to
  - energy bin weighting
  - no electronic noise
  - Swank factor = 1
  - smaller pixels
- Spectral information on demand
  - single energy
  - dual energy
  - multiple energy
  - virtual monochromatic
  - K-edge imaging
  - …

Thank You!

This presentation will soon be available at www.dkfz.de/ct.

Job opportunities through DKFZ’s international PhD or Postdoctoral Fellowship programs (marc.kachelriess@dkfz.de).

Parts of the reconstruction software were provided by RayConStruct® GmbH, Nürnberg, Germany.